# Pyrolysis of Waste Plastics into Fuels

A thesis

Submitted in fulfilment

Of the requirements for the Degree of

Doctor of Philosophy in

Chemical and Process Engineering

By

Feng Gao

University of Canterbury

2010

# Summary

Waste plastic disposal and excessive use of fossil fuels have caused environment concerns in the world. Both plastics and petroleum derived fuels are hydrocarbons that contain the elements of carbon and hydrogen. The difference between them is that plastic molecules have longer carbon chains than those in LPG, petrol, and diesel fuels. Therefore, it is possible to convert waste plastic into fuels.

The main objectives of this study were to understand and optimize the processes of plastic pyrolysis for maximizing the diesel range products, and to design a continuous pyrolysis apparatus as a semi-scale commercial plant. Pyrolysis of polyethylene (PE), polypropylene (PP), and polystyrene (PS) has been investigated both theoretically and experimentally in a lab-scale pyrolysis reactor. The key factors have been investigated and identified. The cracking temperature for PE and PP in the pyrolysis is at 450 ºC, but that of PS is lower, at 320 ºC. High reaction temperature and heating rate can significantly promote the production of light hydrocarbons. Long residence time also favours the yield of the light hydrocarbon products. The effects of other factors like type of reactor, catalyst, pressure and reflux rate have also been investigated in the literature review.

From the literature review, the pyrolysis reaction consists of three progressive steps: initiation, propagation, and termination. Initiation reaction cracks the large polymer molecules into free radicals. The free radicals and the molecular species can be further cracked into smaller radicals and molecules during the propagation reactions. β-scission is the dominant reaction in the PE propagation reactions. At last, the radicals will combine together into stable molecules, which are termination reactions. There are three types of cracking of the polymers: random cracking, chain strip cracking, and end chain cracking. The major cracking on the polymer molecular backbone is random cracking. Some cracking occurs at the ends of the molecules or the free radicals, which is end chain cracking. Some polymers have reactive functional side group on their molecular

backbones. The functional groups will break off the backbone, which is chain strip cracking. Chain strip cracking is the dominant cracking reaction during polystyrene pyrolysis. The reaction kinetics was investigated in this study. The activation energy and the energy requirement for the pyrolysis are dependent on the reaction process and the distribution of the final products. Following the equations from other literatures, the theoretical energy requirement for pyrolyze 1kg PE is 1.047 MJ. The estimated calorific value of the products is about 43.3 MJ/kg. Therefore, the energy profit is very high for this process.

The PE pyrolysis products are mainly 1-alkenes, n-alkanes, and α, ω-dialkenes ranging from $C_1$ to $C_{45+}$. The 1-alkenes and the n-alkanes were identified with a special method developed in this research. It was found that secondary cracking process has a significant influence on the distribution of the product. This process converts heavy hydrocarbons into gas or light liquid product and significantly reduces 1-alkenes and α, ω-dialkenes. This secondary process can be controlled by adjusting the reflux rate of the primary product. The product of PE pyrolysis with maximized diesel range output consist of 18.3% non-condensable gases, 81.7% w/w liquid product, and less than 1% pure carbon under high reflux rate process. Some zeolite catalysts were tested to reduce the heavy molecular weight wax. It was found that NKC-5 (ZSM-5) was the most effective catalyst among zeolites tested. The proportion of the non-condensable gases was promoted from 17% w/w to 58% w/w by adding 10% w/w NKC-5 into the PE feedstock.

The products of PP pyrolysis are mainly methyl- oligomers. The reflux effect on the product from pyrolysis of PP is not as great as that on PE. The PP pyrolysis product with high reflux rate consists of 15.7% non-condensable gases, 84.2% condensed liquid product, and less than 0.25% char. Cyclohexane is the dominant component, 21%w/w in the liquid product. 44%v/v of the non-condensable gases is propene.

In the pyrolysis product of PS, there are 4% non-condensable gases, 93% liquid, and 3% char. Styrene accounts for 68.59%w/w in the PS liquid pyrolysis products due to the chain strip reactions. There was 19% v/v hydrogen in the gas product, which did not exist in the PE pyrolysis gas product. The composition of the char is almost pure carbon, which is similar to that from PE pyrolysis.

The mixture of virgin and post-consumer PE, PP and PS have also been investigated to identify the feedstock interaction and the effect of the contamination on the product. The interaction promotes the production of non-condensable gases. However, the effect of the interaction on the distribution of total product is not significant. Contamination of paper labels on the post-consumer plastics may result in higher solid residue in the product but no significant effect on the product was found in this study.

Based on the achievements, a continuous semi-scale reactor has been designed and constructed at maximum capacity of 27.11kg/hr in this research. From the experiments of pyrolysis of both virgin PE and post-consumer PE on this semi-scale pyrolysis reactor, it was found that the major components are 1-alkenes, n-alkanes, and α, ω-dialkenes. The distribution of the condensed products of PE pyrolysis from the semi-scale reactor is the same as that of the products from low reflux rate process with the lab-scale reactor. However, the proportion of non-condensable gases is much higher than that from pyrolysis in the lab-scale tests with low reflux rate because the semi-scale plant has higher reaction temperature and heating rate. Lower proportion of unsaturated hydrocarbons was found in the condensed product from the post-consumer PE pyrolysis than in the virgin PE product because of the contamination on the post-consumer PE. The actual energy consumption for cracking and vaporizing PE into fuels is 1.328 MJ/kg which is less than 3% of the calorific value of the pyrolysis products. Therefore, the pyrolysis technology has very high energy profit, 42.3 MJ/kg PE, and is environmental-friendly. The oil produced has very high quality and close to the commercial petroleum derived liquid fuels. The experience of design and operation of the semi-scale plant will be helpful for building a commercial scale plant in the future.

# Acknowledgement

Without the support, assistance, and motivation provided by those around me, this study would have never been accomplished.

In particular, I would like to thank my supervisor Professor Pang for his help and guidance during the period of research. Prof. Pang provided significant comments and financial support on defining the topic and proceeding with the research. His assistance in editing was very greatly appreciated. His enthusiastic nature always encourages me. I have gained much about this study from his rigorous attitude.

I must thank CAPE department of Canterbury University and Green Fuel Technologies Ltd. for providing the opportunity to investigate the pyrolysis technology of waste plastic into fuels and their financial and technical assistance.

I need to thank Dr. Chris Williamson for his valuable advice. I would also like to acknowledge the technical staffs in the department, Bob Gordon and David Brown for teaching me the experimental techniques and how to use the analysis devices. Their valuable suggestions, discussions, and endless enthusiasm were much appreciated.

And thanks especially to my parents, Xiangyun Gong, Xiaochen Zhu, Yanhua Lu, and Qi Li, and all my friends who kept me encouraged throughout the five years of research and thesis writing.

# Table of Content

# Table of Figure

# Table of Table

# COMMON ABBREVIATIONS USED

| | |
|---|---|
| SPI | Society of Plastic Industry |
| PE | Polyethylene |
| HDPE | High density polyethylene |
| LDPE | Low density polyethylene |
| PP | Polypropylene |
| PS | Polystyrene |
| PVC | Polyvinyl Chloride |
| PET | Polyethylene Terephthalate |
| GC | Gas chromatography |
| MS | Mass spectrometry |
| TGA | Thermo gravimetric analysis |
| LPG | Liquefied petroleum gases |
| MW | Molecular weight |
| Micro-GC | Micro gas chromatography |
| SEM | Scanning electron microscope |
| EDS | Energy-dispersive x-ray spectrometer |
| ZAF | a standardless method for SEM-EDS |
| Norm% | Normalized percentage |
| ZSM | Zeolite Socony Mobil |

# 1.Introduction

## *1.1. Background*

Plastic is a high molecular weight material that was invented by Alexander Parkes in 1862. [1] Plastics are also called polymers. The term polymer means a molecule made up by repetition of simple unit. For example, the structure of polystyrene can be written in a form as shown in Figure 1-1 or in Figure 1-2.

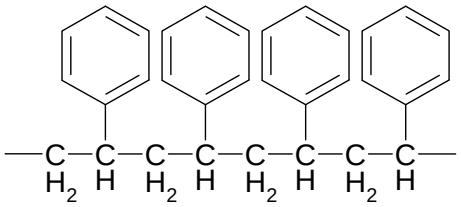

**Figure 1-1 Common expression of polystyrene molecular structure**

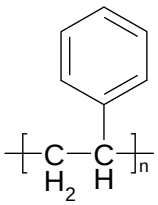

**Figure 1-2 A simplified expression of polystyrene molecular structure**

The repeating unit of the polymer is in the brackets with a subscript, n, to represent the number of the unit in this polymer molecule. [2]

Plastic is one of the most commonly used materials in daily life which can be classified in many ways such as based on its chemical structure, synthesis process, density, and other properties. In order to assist recycling of the waste plastic, Society of Plastic

Industry (SPI) defined a resin identification code system that divides plastics into the following seven groups based on the chemical structure and applications [3]:

PET (Polyethylene Terephthalate)

HDPE (High Density Polyethylene)

PVC (Polyvinyl Chloride)

LDPE (Low Density Polyethylene)

PP (Polypropylene)

PS (Polystyrene)

Other

The above seven types of plastics are marked on various plastic products as follows [3]:


**Figure 1-3 Marks of the seven types of plastics on various plastic products [3]**

Due to the convenience to manufacturing and use, the world plastic production has been increasing since it was firstly commercially manufactured, from 1.5 million tons in 1950 to 260 million tons in 2007 as shown in Figure 1-4. [4] One of the major concerns for extensive use of the plastics is the disposal of the waste plastic. In addition, the plastics are produced from non-sustainable oil or coal, and thus it is a non-sustainable product. There were 30.7 million tons of waste plastic generated in the U.S. in 2007, which accounts for 12.1% of the total municipal solid wastes. [5] In U.K., 4.9 million tons of plastics were consumed in 2007. [6] Europe consumes about 25% of the global plastic production, which is equivalent to 60 million tons per year. [4]

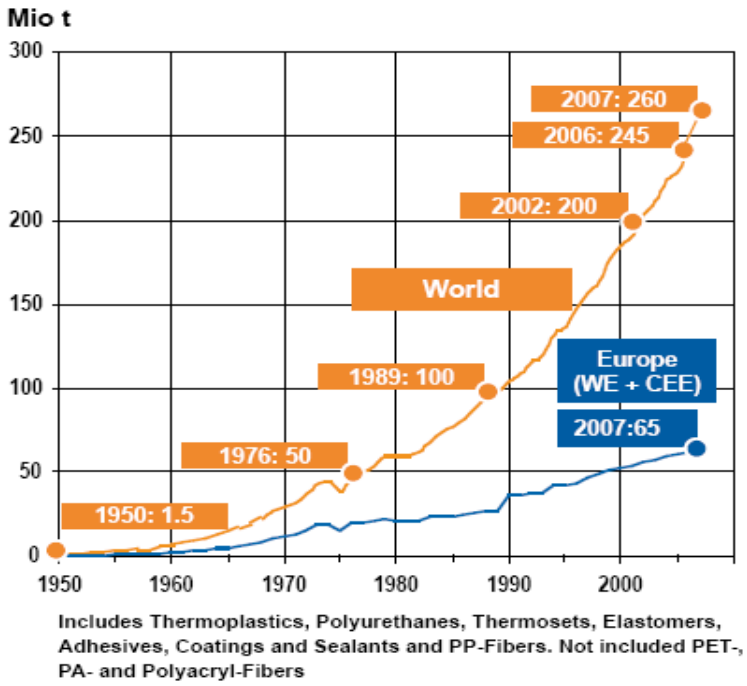


**Figure 1-4** Plastic production in the world and in Europe from 1950 to 2007 [4]

In New Zealand, 262,904 tonnes of virgin plastics were imported for processing in 2004 and at least 71.3% (187,451 tonnes) of the plastic products were consumed domestically with the remaining being exported. [7] The type and the quantity of the imported plastics were given in Table 1-1. It was found that over 30% of manufactured plastics were LDPE and 20% were HDPE.

Most cities in New Zealand have plastic collection and recycling systems, however, only 13.5% of these post-consumed plastics (35,442 tonnes) were recovered in 2004 as shown in Table 1-2. The majority of the recovered plastics were PE that accounted for 60% in total recovered plastics, including 35% for LDPE and 25% for HDPE. In Table 1-2, the proportions of PET and HDPE in the recycled plastics are relatively higher than those in the imported plastic materials because these two types of plastics are identified and separated in recycling of the municipal solid waste (MSW) in New Zealand. On the contrary, PVC is widely used in construction that has a longer lifespan than other packaging plastics, and there is no public recycling system for PVC. Therefore, the proportion of the recovered PVC is relatively low.

**Table 1-1** Breakdown of the total manufactured and proportion of packaging plastic types (2004) [7]

| Material type | Imported (ton) | Proportion in total (%) | Used for Packaging (ton) |
|---|---|---|---|
| PET | 22,433 | 9 | 16,802 |
| HDPE | 52,587 | 20 | 21,508 |
| PVC | 39,202 | 15 | 1,372 |
| LDPE | 79,513 | 30 | 61,543 |
| PP | 32,402 | 12 | 16,233 |
| PS | 21,065 | 8 | 11,788 |
| Other | 15,702 | 6 | 8,715 |
| Total | 262,904 | 100 | 137,961 |

**Table 1-2** **Tonnages of each type of recovered plastic in NZ in 2004 [7]**

| Recovered plastic type | Quantity (ton) | Proportion (%) |
|---|---|---|
| PET | 8,016 | 23 |
| HDPE | 8,932 | 25 |
| PVC | 2,412 | 7 |
| LDPE | 12,444 | 35 |
| PP | 1,415 | 4 |
| PS | 635 | 2 |
| Other | 1,588 | 4 |
| Total | 35,442 | 100 |

The total manufactured plastic products in New Zealand are either exported or consumed domestically. The latter would eventually be recovered or disposed at the landfill. In Christchurch city, 15% of the landfill wastes were plastics on average and more detailed data are given in Table 1-3. [8] Due to high durability, plastics will not be decomposed in decades under natural landfill conditions. As land resource is limited for island countries, New Zealanders started to use degradable plastics or other "green" materials, which are relatively high cost but certainly reduce the volume of the landfill requirement. Christchurch City Council also started a new collection system in 2009 to collect and separate all plastics.

**Table 1-3 Estimated annual mass and percentage of main components in the MSW, surveyed in Christchurch for the period from 1 July 2003 to 30 June 2004 [8]**

| Material | Quantity (ton) | Percentage (%) |
|---|---|---|
| Paper | 52,225 | 21.5 |
| Plastic | 36,386 | 15 |
| Kitchen | 38,315 | 15.8 |
| Green | 27,975 | 11.5 |
| Wood | 23,875 | 9.8 |
| Textiles & rubber | 20,784 | 8.6 |
| Rubble | 16,946 | 7 |
| Soil | 7,306 | 3 |
| Metal | 8,577 | 3.5 |
| Glass | 5,096 | 2.1 |
| Sanitary | 4,019 | 1.7 |
| Potentially hazardous | 1,553 | 0.6 |
| Total | 243,054 | 100 |

With heavy consumption of fossil energy and fuels, the world will be faced with shortage of energy and environmental concerns in the near future if no other solutions are to be found. On the other hand, renewable energy sources and waste streams can be processed for production of energy and fuels. Pyrolysis of waste plastic is an economical method to solve waste plastic problem and to produce quality liquid fuel which can have similar properties to the commonly used petroleum fuels.

## 1.2. Economic value to the community

The technology helps to save land resources by utilizing waste plastics to generate valuable energy. Currently, a majority of the waste plastic is land filled and it is not sustainable because waste plastic takes very long time to decay. **[4]** However, it seems that New Zealand has no other choices but continues to do so in the foreseeable future. New Zealand is an island country and given its limited land resources, the society as a whole has to pay increasing attention to the environmental sustainability for the next generations.

The world's annual consumption of plastic which was five million tones in the 1950's has skyrocketed to a global production of 245 million tones in 2008 and waste plastic generation is rapidly increasing. Plastic waste is the third largest contributor to municipal and industrial waste systems after food and paper. Christchurch produced 243054 tons of municipal refuse between July 2003 and Jun 2004 of which 15% was plastic waste. PE, PS and PP account for over 70% of this plastic waste according to the Christchurch City Council. [8] Therefore, significant amount of energy can be produced with this technology. This could be an alternative energy resource for substituting fossil fuels. The New Zealand government could reduce the reliance on the imported oils. The community may also reduce the reliance on the hydrolic power generation.

The fuels produced from this process do not contain sulphur content because there is no sulphur in the waste plastic feedstock. This is an advantage compared with the classic fossil fuels such as diesel because sulphur content in the fuels could form $SO_2$ after combustion. $SO_2$ is a pollutant causing severe air pollutions, which affects people health and damages the concrete structure.

Therefore, this technology is environmental friendly and has significant positive impact on the local government and community.

## 1.3. The pyrolysis of Plastic Materials

Pyrolysis is a thermal cracking reaction of the large molecular weight polymer carbon chains under an oxygen free environment and produces small molecular weight molecules. [9-12] Traditional treatments for post-consumed plastics were landfills or incineration. However, landfill of the post-consumed plastics has potential problems because of limited land resource and high durability of plastics. Incomplete incineration may generate poisonous substances and causes serious health problems. Other methods like gasification and bioconversion are mainly used for organic materials. [13]

HDPE, LDPE, PP and PS are all hydrocarbons consisting entirely of carbon and hydrogen, which are similar to hydrocarbon fuels such as liquefied petroleum gas (LPG), petrol and diesel. [14-16] Plastics are derived from petroleum and have calorific values in a similar range as those of LPG, petrol and diesel as given in **Table1-4**. [14]

Table1-4 Comparison of energy density of plastics and different types of fuels **[14]**

| Material | Calorific value (MJ/kg) |
|---|---|
| Polyethylene | 46.3 |
| Polypropylene | 46.4 |
| Polystyrene | 41.4 |
| Polyvinyl chloride | 18.0 |
| Coal | 24.3 |
| Liquefied petroleum gas | 46.1 |
| Petrol | 44.0 |
| Kerosene | 43.4 |
| Diesel | 43.0 |
| Light fuel oil | 41.9 |
| Heavy fuel oil | 41.1 |

Some commercial plastic pyrolysis plants have been in operation in which all types of post-consumed plastics accepted need to be treated using hydrochloride scrubber which is for PVC cracking and is not preferable in the fuel product because chloride is not desirable in the fuels. [17-18] Those plants are sophisticated and not suitable for relatively small scale production.[17] In these plants, catalysts are also used to improve the quality of pyrolysis products in many existing equipments. Those equipments with catalysts have some weakness in terms of long material resistance time, undesired contact between plastics and catalysts, required high heat transfer rate, and cost of the catalysts. [19]

In order to understand and optimise the pyrolysis of waste plastic and to investigate the impacts of different types of the plastics, extensive research has been conducted in the past decade. Kaminsky, Scheirs and their colleagues [17, 20-23] investigated the effects of reaction conditions on the pyrolysis product. Williams studied the products from pyrolysis of different individual and mixed plastics. [10-11, 24-27] Aguado *et.al.* investigated the effect of catalysts on the pyrolysis reactions. [28-32] In these studies, the lab-scale pyrolysis reactors were either batch type or semi-batch type rather than continuous type. Most studies focused on the effects of operation temperature, heating rate, and catalysts on the product yield. However, there are few researches in the literature review investigating the cracking process of the pyrolysis products during the pyrolysis which is believed to be complex. In addition, the final products are also very complicated. There could be over a hundred of components in the hydrocarbon products including paraffin, olefin and their isomers. Normally, the PONA system, which is an abbreviation for paraffin, olefin, naphthene and aromatic compounds, is used to describe those petroleum hydrocarbons. [17] Paraffins are saturated hydrocarbons with straight or branched carbon chain, which are also called “alkane”. Olefins have similar chain as paraffins, but they have one or more multiple bonds between carbon atoms in their chains. Naphthenes are saturated hydrocarbons like paraffins but their chains merge to a ring in their structure. Aromatics contain a benzene ring in the structure. Another common way to describe the hydrocarbons is based on the carbon numbers in their molecule structure. It is particularly applied to petroleum fuels. The complex pyrolysis products may also be grouped as petroleum gases, petrol, kerosene, diesel and

wax. The above fuels contain hydrocarbon group with different carbon chain lengths as given in Table1-5. [33] There are also other ways to describe the hydrocarbons such as boiling range, phase of products at room temperature etc.

Table1-5 Hydrocarbon range in commercial fuels

| Fuels | LPG | Petrol | Kerosene | Diesel* | Heavy Fuel oil |
|---|---|---|---|---|---|
| Hydrocarbons | $C_3$ to $C_4$ | $C_4$ to $C_{12}$ | $C_{12}$ to $C_{15}$ | $C_{12}$ to $C_{24}$ | $C_{12}$ to $C_{70}$ |

## 1.4. Objectives of the Investigation

The main objectives of this study were to understand and optimize the processes of plastic pyrolysis for maximizing the oil products, and to design a continuous pyrolysis apparatus as a semi-scale commercial plant. The materials to be tested in this study are HDPE, LDPE, PP and PS which account for 70% of the plastics used in packaging. PVC and PET are not studied due to health concerns.

This study was divided into three stages following an extensive literature review on plastic pyrolysis. The first stage of the study focused on understanding of the thermal cracking process and identifying key factors that affect the pyrolysis process and the quality of the plastic pyrolysis products. From the literature review, reaction temperature was the most important factor that influenced the whole process, however, this study have also investigated the secondary cracking process and other significant factors such as temperature, heating rate, type of plastic, catalysts, interaction between different plastics, pyrolysis process, etc.. The effects of secondary cracking were investigated. This work has not been found in other researches.

The second stage of the study was to optimize the operation conditions and the reactor design to produce high quality liquid fuel (diesel) from the pyrolysis of LDPE. Chemical analyses on the products were performed in this stage using gas chromatography (GC) and mass spectrometry (MS). Char content was also analysed by using electron microscope.

In the final stage, a continuous pyrolysis apparatus were designed and manufactured based on the results and the information collected from the work performed during the first two stages. The aim of this continuous apparatus was to convert LDPE and mixture of PE, PP and PS into gas and liquid fuels with maximizing the diesel range product. The apparatus consists of a feeding section, a pyrolysis reactor, and a separation section, which separated diesel, wax, petrol and non-condensable gases.

# 2. Literature Review on Plastic Pyrolysis

## *2.1. Factors affecting Plastic pyrolysis*

The major factors influencing the plastic pyrolysis process and pyrolysis product molecular distribution include chemical composition of the feedstock, cracking temperature and heating rate, operation pressure, reactor type, residence time and application of catalyst. These factors are summarized in this section as follows.

### 2.1.1. Chemical composition of feedstock

The pyrolysis products are directly related to the chemical composition and chemical structure of the plastics to be pyrolyzed. In addition, the chemical composition of the feedstock also affects the pyrolysis processes. In reality, waste plastics are possibly contaminated before recycling which could also have effects on the pyrolysis process and products.

As mentioned in Chapter 1, PE, PP and PS are most commonly used polymeric hydrocarbons and were selected as the investigated materials in this study. Polyethylene is formed from ethylene through chain polymerization which is shown in Formula 2-1. [2]

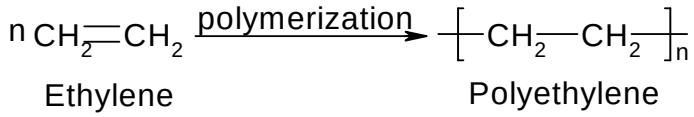


**Formula 2-1 Polymerization of ethylene to polyethylene**

Plastics can be classified, according to structural shape of polymer molecules, as linear, branched, or cross-linked in Figure 2-1. The units in linear polymer are linked only to two others, one to each ends. The polymer is termed branched when branches extend

beyond the main polymer chain randomly. Regularly repeating of side groups are considered to be part of the unit but not considered as branches. Based on the above description, polystyrene is called linear polymer although it contains functional groups as part of the monomer structure. In branched polymers, at least one of the monomers is connected to more than two functional groups due to the branching points produced from the polymerization process. The functional side group and the branch structure have significant effects on the pyrolysis product. For example, the dominant component in PS pyrolysis products is styrene that is the side group come off from PS carbon backbone. [12, 34-37]

There is a significant relationship between the density and the branching intensity of polymers. The PE with more branches has relatively lower density. This has been found in McMurry's study. [38] The branched polyethylene is also called low density polyethylene (LDPE), which is different from linear polyethylene that is called high density polyethylene (HDPE). [2]

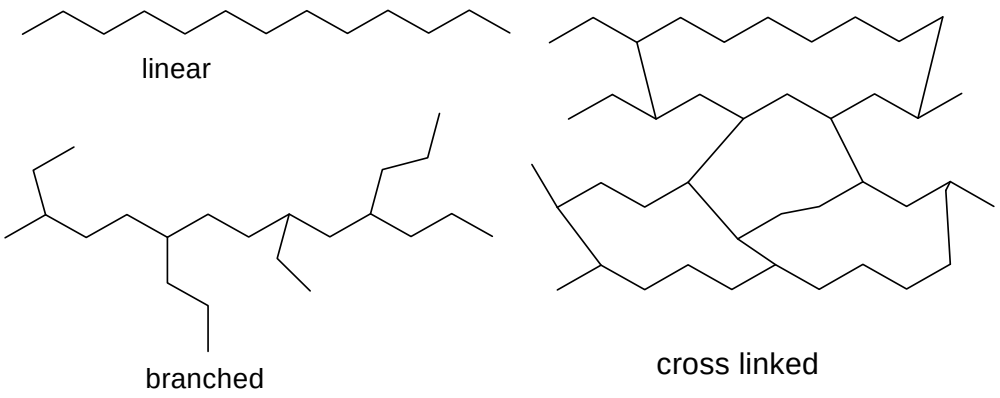


**Figure 2-1 Polymer structure, linear, branched and cross linked**

A cross linked polymer can be described as an interconnected branched polymer with all polymer chains are linked to form a large molecule. Thus, the cross linked polymer constitutes large molecule. Theoretically, the molecular weight of a cross linked polymer can be infinite. In reality, the molecular weight of a cross linked polymer will

be limited due to breaking down of the molecular inter-connections during the processing or the weight of the polymer sample. The cross linked polymer cannot be dissolved in solvents or be melted by heat because of their network structure. For example, PEX, a common abbreviate of cross-linked polyethylene, is widely used in oil and water piping. In pyrolysis process, cross linked polymer will crack rather than melt or evaporate. This is different from the reactions of linear or branched polymers in pyrolysis process.

### 2.1.2. Cracking temperature and heating rate

Temperature is one of the most important operating variable, since the temperature dominates the cracking reaction of the polymer materials. Not all of the polymer materials can be cracked by increasing the temperature. Van der Waals force is the force between the molecules, which attracts molecules together and prevents the collapse of molecules. When the vibration of molecules is great enough, the molecules will evaporate from the surface of the object. [39] However, the carbon chain will be broken if energy induced by van der Waals force along the polymer chains is greater than the enthalpy of the C-C bond in the chain. [40] This is the reason why high molecular weight polymer is decomposed rather than is boiled when it is heated. In theory, the temperature of thermal breaking the C-C bonds should be constant for a given type of plastic (polymer). However, this temperature has been found to differ in different studies. For example, the temperature when PP starts cracking was reported at 380 ºC in Ciliz *et al*.'s result but it is measured to be 650 ºC in Demirbas's result. [13, 41] Both of them used similar batch process reactor and thermo gravimetric analysis. According to the provided schemes, the most likely reason is the difference in the temperature measurement location where the temperature sensors were located. There was significant temperature gradient along the apparatus in which the melted plastic at the bottom of a fix-bed batch reactor had much lower temperature than that on the top surface of the reactor. It was also found that the space temperature in the pyrolyzer was strongly influenced by the product vapour. Different locations of the temperature sensors in different studies are believed to be one of the most important factors on the different cracking temperature reported. Karaduman *et al.* investigated the temperature profile along a tube heated by external furnace. [12] Large temperature variation was

observed between the ends and the centre of the tube. (Figure 2-2) Clearly, there was significant heat loss at both ends of the tube reactor.

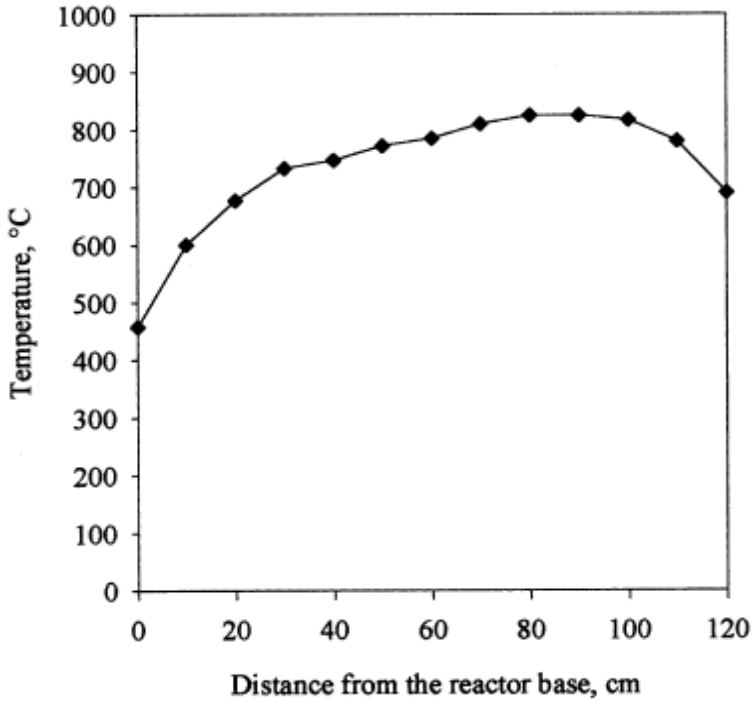


**Figure 2-2 Temperature profile along the tube reactor [12]**

The difference of the temperature on the surface in contact with the plastic and the temperature of the plastic close to the surface was measured by Karaduman, A., *et al.* for comparison, which is measured relatively minor and constant in this research study. Therefore, the temperature at the reaction surface is selected for monitoring the cracking temperature of plastics. In Shah *et al.*'s study, mixture of post-consumed plastics of PE, PP and PS was pyrolyzed in a fixed-bed batch reactor at different temperatures for one hour. [42] It was found that higher reaction temperature favours the gas production and production of heavy molecular weight products in the liquid. (Figure 2-3 and Figure 2-4) [42-43] Figure 2-3 shows the gas chromatography (GC) analysis results of the liquid products with the temperature on the curves indicating the cracking temperature. It is seen that the liquids produced at higher cracking temperatures have lower flash-off percentage at the same GC temperature during the analysis. This shows higher

proportion of heavy molecular weight components in the liquid. Similar conclusion was also found in other research using virgin plastics and fluidized-bed, semi-batch reactor. [10]

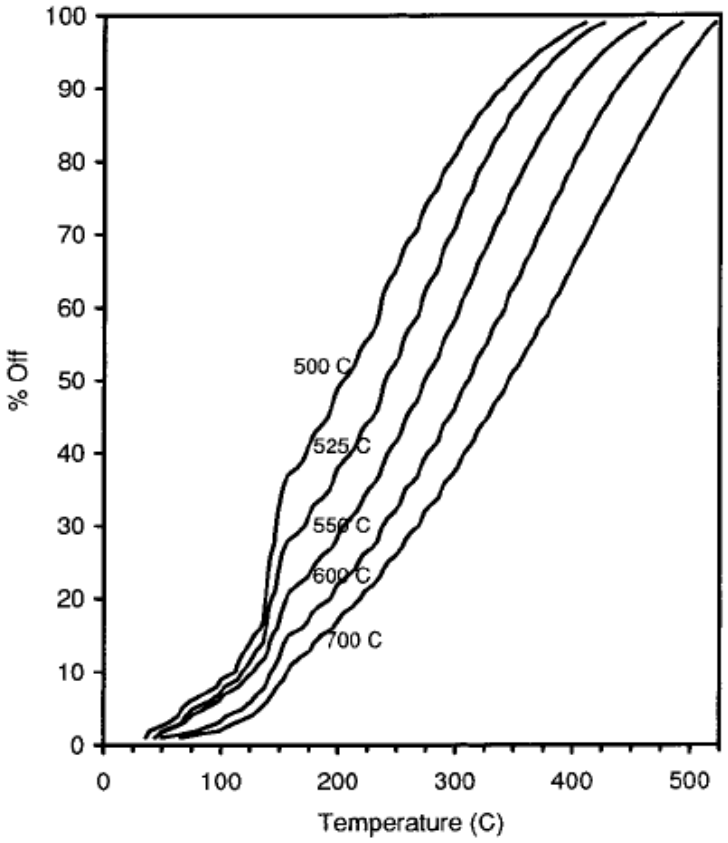


**Figure 2-3 GC analysis results of plastic pyrolysis liquid [42]**

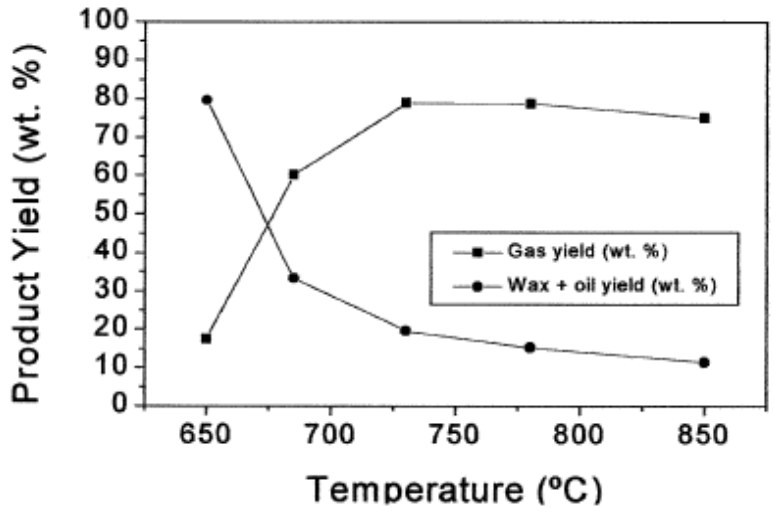


**Figure 2-4 Influence of temperature on product distribution [44]**

However, the overall gas proportion of gas product increased with increasing cracking temperature up to 730°C while the liquid product proportion decreased with the cracking temperature in the full range of temperature used. (Figure 2-4)

The other operating thermal dynamic parameter is heating rate. The term "heating rate" in this field means the increase of temperature per unit time. The influence of the heating rate on the plastic pyrolysis process and product distribution varies in different studies due to the differences in the pyrolysis reactor, operation conditions (temperature and pressure), and temperature measurement location. Normally, in a fast or flash pyrolysis, heating rate refers to the temperature change of the plastic from it dropped on the hot surface till decomposed and vaporized. The hot surface remains the temperature while the amount of plastic dropped on to it is relatively small. In this situation, the heating rate is very high, up to 10,000 K/s. [26, 45-47] This is hard to be measured precisely. Therefore, the surface temperature is normally applied as the reaction temperature indicator rather than heating rate in the flash and fast pyrolysis process. In a batch process, the plastic is normally heated from room temperature to the cracking temperature in several minutes. It is a slow pyrolysis process. Once the plastic feedstock is heated to the cracking temperature, the temperature remains relatively constant until all feedstock has been pyrolyzed. Therefore, heating rate is normally applied as the temperature indicator instead of reaction temperature in a slow pyrolysis process. It was found that heating rate usually varied from 10 to 100 ºC/minute in previous slow pyrolysis researches. [11, 24, 47-50] In Saha and Ghoshal's study on pyrolysis of Coca-Cola drink PET bottles, the influence of heating rate on the reaction process was investigated by using thermo gravimetric analysis (TGA) as shown in Figure 2-5. [51] In the figure, dAlpha/dT, defined as the rate of reaction ($K^{-1}$), is plotted as a function of absolute temperature for different heating rates from 10 to 25 K/min. It was found that higher heating rate promotes the rate of pyrolysis reactions. [24, 52-56]

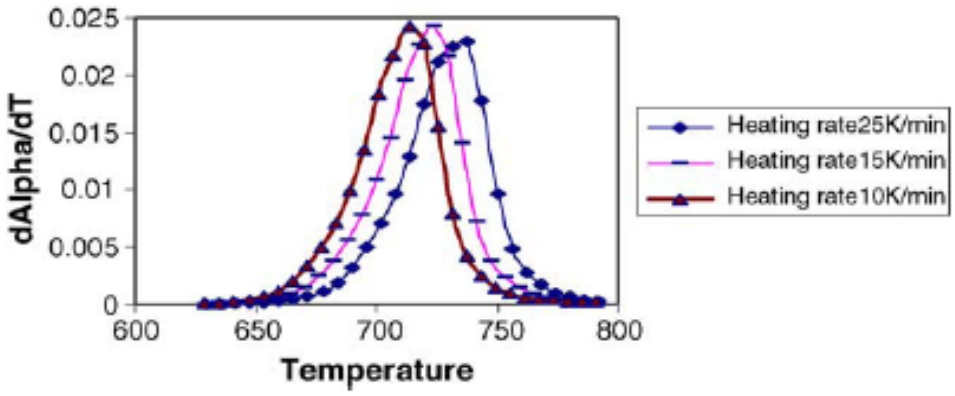


**Figure 2-5 Reaction rate as a function of temperature and heating rate in pyrolysis of Coca Cola soft drink PET bottle [51]**

### 2.1.3. Type of reactor

The reactor type for the plastic pyrolysis significantly influences on the heat transfer rate, mixing of plastics with pyrolysis products, residence time and the reflux level of the primary products. Reactors can be classified into batch, semi-batch and continuous or classified based on types of reactor bed.

Batch, semi-batch and continuous reactors

According to the feeding and product removal processes, the pyrolysis reactor is categorized into batch, semi-batch and continuous reactors. In the batch reactor, the materials are fed into the reactor in batches for pyrolysis either at the start of the process or after all of the fed materials are processed. In the continuous reactor, the feed materials are input from one part and the products are led out from the other part of the reactor. A semi-batch reactor removes the pyrolysis products continuously once they are generated but the feed materials are added initially before the pyrolysis process starts. Some semi-batch process uses inert carrier gas to help remove the pyrolysis products. Batch and semi-batch reactors are mainly applied on research, [24, 49-50, 57-60] and continuous reactor is mainly for industrial production such as Mitsui R21, Fuji, Toshiba, Veba Oel, PKA, etc. [17-18, 33, 61] Particular reactions and phenomenon such as

secondary pyrolysis may occur in semi-batch reactors and does not occur in batch reactors. [28]

Fixed bed, fluidized bed and screw kiln reactors

Based on the heat transfer methods and flow patterns of the feedstock and products, the pyrolysis reactors can be classified into fixed bed reactor, fluidized bed reactor and screw kiln reactor. In the fixed bed reactor, the pyrolysis occurs on a stationary bed which is easy to design and operate. However, the irregular sizes and shape of the feedstock plastics may cause feeding problems in continuous process and the low thermal conductivity of the plastics results in large temperature gradient in batch process devices. In some systems, the fixed bed reactors are only used as the secondary pyrolysis reactor because the products from the primary pyrolysis are mainly in liquid and gaseous phase which can be easily fed into the fixed bed. [62-64]

The fluidized bed reactor has been used in most commercial plants in which gaseous products or inert gas flow through an expanded bed of feedstock and other bed materials, forming bubbles or eddies. The advantages of fluidized bed reactor are the homogeneity of both temperature and composition. Heat and mass transfer rates are much higher than the fixed bed thus the low thermal conductivity in fluidized bed reactors is no longer a problem. In the fluidized bed reactor, the dimensions and the material of the bed material are the key parameters affecting the pyrolysis and products. Bed materials loss and separation from the gases are other issues which need consideration. [61]

In recent years, a new reaction system named screw kiln reactor has been widely applied for plastic processing. [27, 43-45] In this type of reactor, here is an extruder to screw the feedstock from a feeder in an oxygen free environment. The extruder is heated by external heat sources. Solid residues and pyrolysis products are separated and collected from the other end of the extruder. The high viscosity of plastics is not a

problem for the flow in screw kiln reactor because the flow is driven by the external motor. Melted plastic or even plastic solid particles can be fed into this reactor. The small diameter of the extruder and good mixing of the materials make the radial temperature gradient negligible. The process is relatively stable and does not use bed material as in the fluidised bed reactor. The feeding rate can be controlled by adjusting the rotation speed of the extruder, which also determines the residence time of plastics.

### 2.1.4. Residence time

The definition of residence time differs in various studies. In fast pyrolysis or continuous pyrolysis process, it refers to the contact time of the plastic on the hot surface throughout the reactor. However in slow pyrolysis and batch process, the residence time means the duration from the time when feedstock plastic start to be heated to the time when the products are removed. Longer residence time favours a further conversion of the primary products thus yielding more thermal stable products such as light molecular weight hydrocarbons, non-condensable petroleum gases. [31, 43, 59, 65] In a slow pyrolysis, long residence time encourages the carbonization process and produces more tar and char in the products. [66] The pyrolysis conditions, residence time and target products are given in Table 2-1.

**Table 2-1 Pyrolysis processes and target products [47]**

| Process | Heating rate | Residence time | Temperature (°C) | Target Products |
|---|---|---|---|---|
| Slow carbonization | Very low | Days | 450-600 | Charcoal |
| Slow pyrolysis | 10-100K/min | 10-60 min | 450-600 | Gas, oil, char |
| Fast pyrolysis | Up to 1000K/s | 0.5-5 s | 550-650 | Gas, oil, (char) |
| Flash pyrolysis | Up to 10000K/s | <1 s | 450-900 | Gas, oil, (char) |

Except for the batch pyrolysis reactor in a closed system, residence time is difficult to be controlled directly but can be adjusted by altering other operation parameters such as feeding rate, carrier gas flow rate and product discharge rate. Residence time was, then, calculated for these controllable operation parameters. [38, 46-47] Secondary pyrolysis cracking occurs when residence time is long enough, which enhances the yield of gaseous product. (Figure 2-6) [38, 46] Higher value of V/m represents longer residence time in Figure 2-6. The Y axis is the conversion of HDPE to gaseous product. [65, 67] There is a significant effect on the conversion when the residence time varies in a certain range during the non-catalyst thermal reaction.

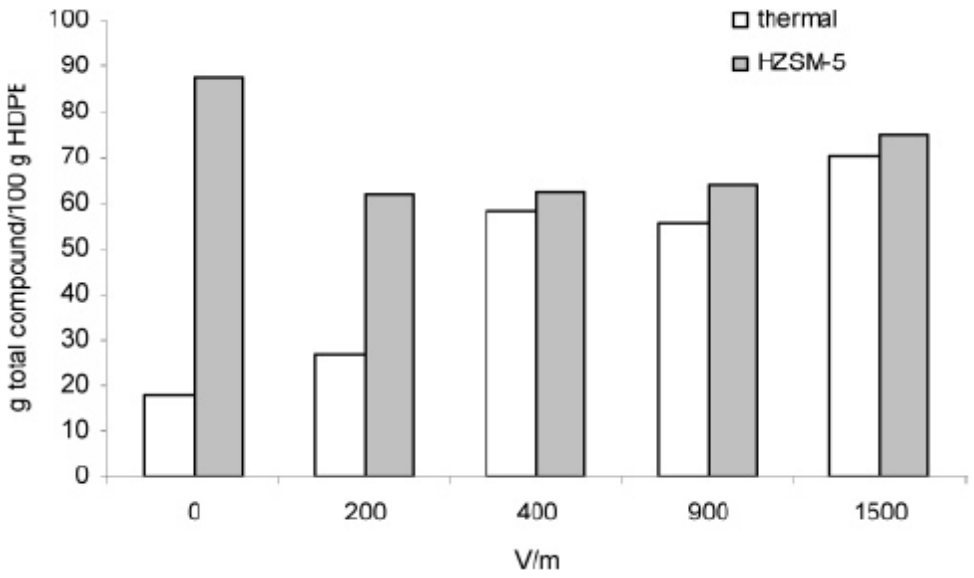


**Figure 2-6 Influence of residence time on the production of gaseous product (from HDPE thermal and catalytic cracking) [65, 67]**

### 2.1.5. Use of catalyst

Advantages of using catalyst

In order to optimize plastic pyrolysis reactions and modify the distribution of pyrolysis products, catalysts are widely used in research and industrial pyrolysis processes.

Petroleum fuels, such as LPG, petrol, kerosene, and diesel, are hydrocarbons from $C_1$ to $C_{24}$. The PE pyrolysis products are mainly straight hydrocarbons from $C_1$ up to $C_{80}$, which contain much more heavier molecular weight components [28] One of the main purposes of using catalysts is to shorten the carbon chain length of the pyrolysis products and thus to decrease the boiling point of the products. Catalysts are found to be mainly applied to PE pyrolysis because the primary product from other plastics, such as PP and PS, are mainly light hydrocarbons, with similar carbon chain length to the range of commercial fuels. The products from non-catalytic PE pyrolysis contain high proportion of 1-alkenes and dialkenes. [28, 68] Some catalysts are applied specifically to reduce the unsaturated hydrocarbons and promote the yield of aromatics and naphthenes. This can significantly increase the stability and cetane number of the oil products. Moreover, it is reported that activation energies ($E_a$) measured in the PE pyrolysis with catalysts (such as HZSM-5, HY, and MCM-41) were much lower than those when no catalyst was added. [69]

Catalyst classification

Homogeneous and heterogeneous catalysts have been studied for the catalytic cracking of plastics. Homogeneous catalysts used for polyolefin pyrolysis have mostly been classical Lewis acids such as $AlCl_3$.[32] Generally, heterogeneous catalysts are preferred due to their easy separation and recovery from the reacting medium. Heterogeneous catalysts can be summarized as nanocrystalline zeolites, aluminium pillared clays, conventional acid solids, mesostructured catalysts, superacid solids, gallosilicates, metals supported on carbon, and basic oxides. [28] Among the mentioned catalysts, nanocrystalline zeolites have been extensively studied for polyolefin pyrolysis and this type of catalysts will be discussed in more details as follows.

Zeolite properties: pore size (structure) and Si/Al ratio (acidity)

A zeolite is a crystalline aluminosilicate with a three-dimensional framework structure that forms uniform pores of molecular dimensions. [70] Zeolites act as sieves on a molecular scale and exclude molecules that are too large to pass through the pores. The

three-dimensional frame structure significantly increases the area of the sieves and absorbs molecules that have similar sizes as the pores. According to the structure of zeolites, 176 zeolite framework types have been confirmed.[71] A three-letter code, such as MFI, is assigned to framework types by the Structure Commission of the International Zeolite Association.[53-54] The codes are normally derived from the name of the zeolite, for example, MFI from ZSM-5 (Zeolite Socony **M**obil-**fi**ve).[72] The MFI framework type of ZSM-5 is described as shown in Figure 2-7, with pentasil chains running parallel to z.

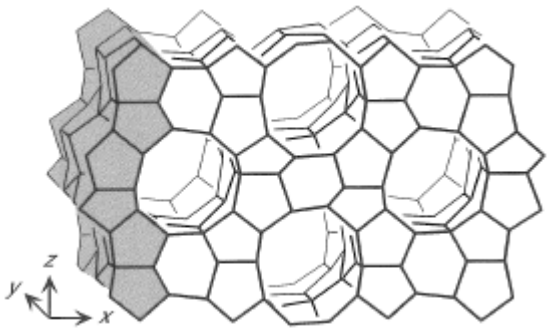


**Figure 2-7 The framework type ZSM-5 with pentasil chain parallel to z [71]**

The pore openings and sizes are key parameters for the catalytic effect in the plastic pyrolysis, which are determined by the size of single ring and the structure features (cages, cavity, chains, and channels). Rings are the basic units characterize the pore size. However, the channel wall in Figure 2-8 is composed of 6-rings and forms a 12-ring channel. Consequently, pore opening can be influenced by the other factor, structure feature.

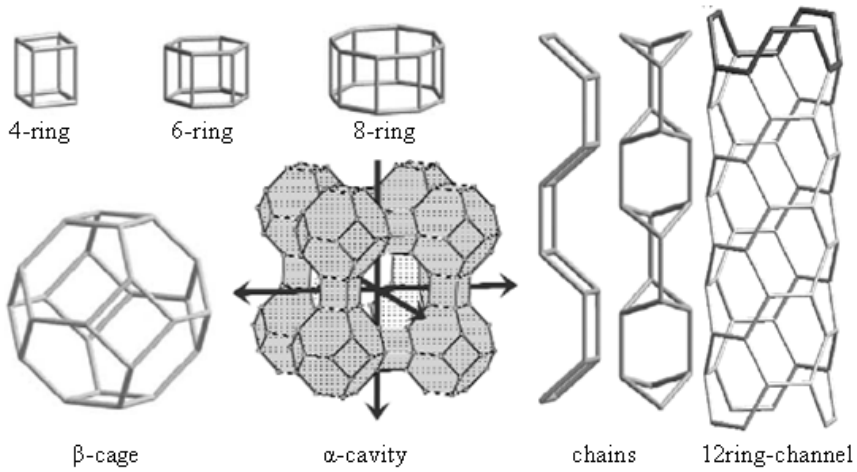


**Figure 2-8 Framework types of zeolite [52, 54]**

Zeolites are crystalline micro-porous aluminosilicates. Therefore, Si/Al ratio is also an most important parameter for zeolites which is applied to classify the zeolites.[73] The high-silica zeolites, with a Si/Al ratio greater than five such as ZSM-5, are widely used in petrochemical industries. [70] The high silica content in the catalyst makes the framework to stand high temperatures that this type catalyst is suitable for high temperature pyrolysis and regeneration cycle. A high dispersion of acidic protons assures that each proton performs maximum acidity. [74-75] Consequently, acidity is also an indicator to reflect the property of zeolites. Aguado *et al.* tested three types of nanocrystalline zeolite with different Si/Al ratios and specific surface area. [30] High Si/Al ratio implies a high total acidity of zeolites.[76] These zeolites are preferred for polyolefin cracking. Lower Si/Al ratio implies lower acidity and smaller crystal size of zeolite provide higher efficiency in terms of conversion. (Figure 2-9) The use of catalyst is dependent on the difficulty of changing catalyst, the cost of catalyst, and the efficiency of the catalyst. This varies in different situations.

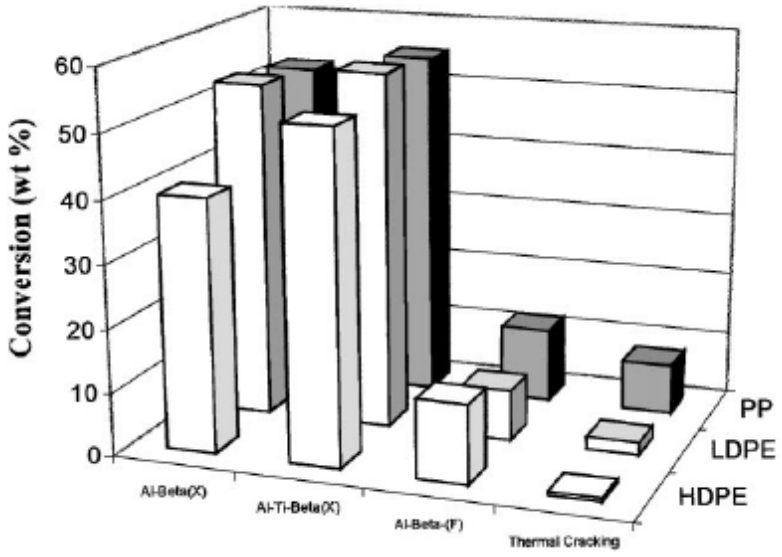


**Figure 2-9 Conversion obtained in the thermal and catalytic pyrolysis of HDPE, LDPE, and PP (400ºC, 0.5h, plastic/catalyst = 50% w/w) [30]**

### 2.1.6. Pressure

Operating pressure has significantly effect on both the pyrolysis process and the products. The boiling points of the pyrolysis products are increased under higher pressure, therefore, under pressurised environment heavy hydrocarbons are further pyrolyzed instead of vaporized at given operation temperature. [49, 77-78] Figure 2-10 shows the effect of pressure on hydrocarbon number and their fractions in the pyrolysis products of PE. In effect, under pressurized pyrolysis, more energy is required for further hydrocarbon cracking. It was also found that high pressure increases the yield of non-condensable gases and decreases the yield of liquid products. (Figure 2-11) The average molecular weight of gas product also decreases with the increase of pressure. [77] The influence of pressure on the concentration of double bond, C=C, of the liquid product was not significant as reported by Murata *et al.* [77] In summary, pressure has major effects on the pyrolysis reaction and the distribution of PE pyrolysis products, but has minor effect on the double bond components.

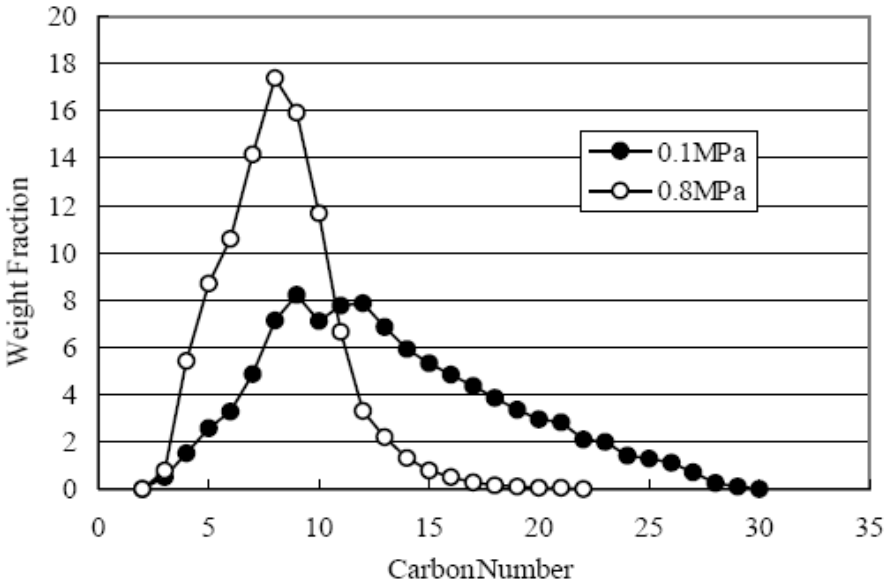


**Figure 2-10 Effect of pressure on the distribution of PE pyrolysis products [77]**

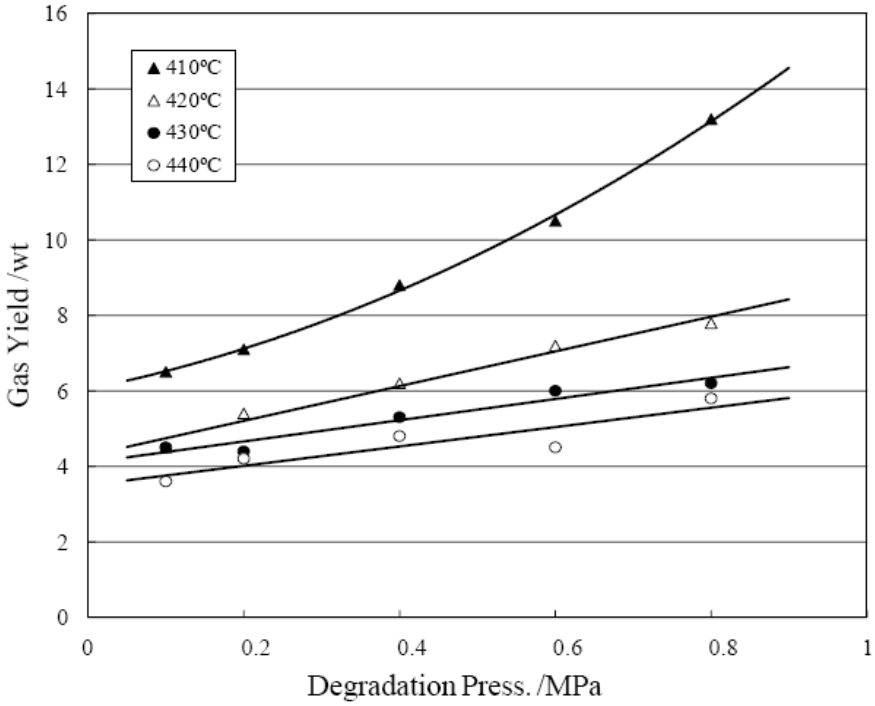


**Figure 2-11 Effect of pressure on the yield of gas at different temperature [77]**

## 2.1.7. Other Influencing factors

There are a number of other factors which also affect pyrolysis process to a certain extent. For example, reactive additives such as air, oxygen, or hydrogen are sometimes

present in the reaction for different purposes, which will interfere with the reactions and affect the quality of the products.

Further pyrolysis of the primary product occurs in most processes. Secondary cracking reactions were found in many reports which are enhanced by high pressure, long residence time, low heating rate and high refluxes.[39, 41, 46, 59] Although many researchers observed the impact of secondary cracking, few have investigated the influence of secondary cracking process on the yield and the quality of the products. Most secondary cracking occurred during the pyrolysis of PE and very limited cracking was found in PS pyrolysis. This is possibly due to the difference in their primary products. The primary products produced from PE pyrolysis contain large proportion of heavy hydrocarbons with carbon chain number up to 80. The average molecular weight of the primary products from PE is much higher than that of other plastics, PS, PP, PVC and PET.[34, 60] The secondary cracking is mainly effective for heavy hydrocarbons, hence, has less effect on the pyrolysis of PS, PVC, PET and other plastics. The importance of secondary cracking on PE pyrolysis has intensively been studied in this research.

### 2.1.8. Multi-factor effect on pyrolysis process

It is difficult to directly compare the product yields obtained for a specific plastic in different researches as the operating conditions and reactors can be very different. In general pyrolysis processes, thermal degradation occurs in the initial stages of the pyrolysis with absence of oxygen. The pyrolytic products immediately after the pyrolysis consist of solid residue, oil vapour and non-condensable gases among which the oil vapour will become liquid after cooling down. According to the residence time or the heating rate during the pyrolysis process, the pyrolysis can be classified into slow carbonization, slow pyrolysis, fast pyrolysis, and flash pyrolysis. The pyrolysis process and its target products are given in Table 2-1. [47]

With slow heating rate (less than 10K/min), the carbonization occurs and the process proceeds from the outer surface to the core of the plastic particles with the local carbonization temperature of above 300 ºC. The carbonization process is determined by the heat transfer rate to the material surface and the heat transfer rate within the material. At given temperature and heating rate, the residence time is also the most important variable to achieve the desired carbonization. [47] The residence time required is also related to the dimensions of the material. If the size of material is too large which needs much longer residence time, incomplete carbonization may occur at the centre of the plastic particles.

On the other extreme situation, if the operation temperature is very high, for example 800 to 1000 ºC, gasification process occurs and in this case, the plastics are directly converted to short chain gases and the yield of non-condensable gases in the product is maximized. High heating rate is required to minimize the proportion of solid char production and rapid quenching favours the liquid production before further cracking into gaseous products. [33]

The above mentioned processes are applied to all of the plastic types to be examined including HDPE, LDPE, PP, and PS all of which have similar cracking temperature from 320 to 500 ºC. However, in the pyrolysis of PVC the cracking temperature (250 ºC) is much lower than that of other common plastics mentioned above. [54, 78-79]

In most practical pyrolysis processes, particularly those applied in industries, preheating and melting the plastic feedstock between 200 and 300 ºC are applied in order to reduce the volume of the feedstock and to eliminate the oxygen from the feeding system. The melting temperature is also high enough for PVC to crack and form hazardous gases and acid. Therefore, a preheating chamber is commonly used in the commercial process to remove gases generated from the PVC degradation in the preheating.

## 2.2. Quality Comparison of Pyrolysis Products and Petroleum Fuels

### 2.2.1. Review of pyrolysis monitoring and product analysis

Pyrolysis process monitoring

In the plastic pyrolysis, plastic type and operation conditions applied in the researches and the industries varied largely. Consequently, the variation of the yield and the quality of the pyrolysis products are significant in the literature. However, when the same plastic is used and same operation conditions are applied, there are similarities in the product yield and production distribution. In most of the research work, the pyrolysis rate of feedstock plastics is measured by using thermogravimetric analysis (TGA) in fix-bed batch pyrolysis reactor. [9, 53] The percentage of gaseous products is measured simultaneously with the occurrence of the reactions. In fluidized bed reactor or continuous reactor, feeding rate is controlled and monitored to determine the reaction rate. Operation temperature is normally monitored by using thermocouples along the process line, which is used for estimating thermal reactions including heating-up, decomposition, cracking, and condensation. Some studies used high pressure pyrolysis in which pressure gauge is applied to control and monitor the operation pressure. With these monitoring devices, the processes can be controlled by adjusting the operating factors such as heating power, feeding rate, pressure and carrier gas flow rate when needed. .

Product analysis method

The pyrolysis products of plastics are mainly hydrocarbons presenting in gaseous, liquids and solid wax phases under standard conditions of temperature of 25 ºC and pressure of 100 kPa. Minor amounts of char and hydrogen gas may be found in the products. The char product can be analyzed by elemental analyzer or electron-microscope dispersive X-ray analyzer. In research, the hydrocarbon products can be firstly separated though gas chromatography (GC) and then identified by either comparing with hydrocarbon standards or passing through mass spectrometry (MS).

The structure and the proportion of individual components are investigated in laboratory analysis. [12, 27, 42, 56, 62, 65, 80-81]

Hydrocarbon products from industrial pyrolysis of waste plastics are used as a substitute for commercial fuels. Instead of investigation on individual components, the commercial fuel regulation requirements focus on the physical and chemical properties of fuels relate to engine performance. The New Zealand regulation requirements on the properties of petroleum fuels such as LPG, petrol and diesel adapted standard test methods from the American Society for Testing and Materials (ASTM) and institute of petroleum (IP) testing methods. [82] The properties of plastic pyrolysis fuels are analyzed in some studies. [10, 22, 29, 34, 44, 52, 58, 78, 83] It was found that the pyrolysis products from PE, PP, and PS are mainly hydrocarbons with molecular weights similar to the petrol and diesel range. A certain amount of non-condensable gases and insignificant amount of heavy wax were also found in the pyrolysis products. Heavy hydrocarbon wax can be processed into gases or light liquid by further high temperature treatments or catalytic cracking so that the yields of non-condensable gases and wax vary largely in different studies. [52] The plastic derived fuels were also found to have higher unsaturated hydrocarbon content and lower stability than those of commercial fuels. [17]

### 2.2.2. Comparison of diesel with plastic derived fuels

The New Zealand diesel regulations have 18 requirements those can be characterized into four groups: thermodynamic properties, flowing properties, component distribution, and performance properties.

In the regulation for commercial diesels, one of the most important thermodynamic properties is cetane number or cetane index that can be a substitute as cetane number, which indicates the auto-ignition conditions of the fuel. [82, 84] Cetane index is calculated from fuel density and distillation range which is also listed in the regulation

requirements. Therefore, cetane number, density, and distillation range are all important properties to diesel fuel.

The next important properties are the fuel flow properties which include viscosity, cloud point, pour point, cold filter plugging point and flash point. The importance of these properties will depend on the extent of known information of fundamental properties mentioned above, e.g., density and distillation range. If all of the fundamental properties are well known, the flow properties are less critical.

Miscellaneous properties reflects the effects of the minorities in diesel fuels, including carbon residues, sulphur content, water content, ash content and polycyclic aromatic hydrocarbon content. The carbon residue is fine solid particles in the fuel that may form combustion chamber deposits. The sulphur content in the fuel above a certain level causes high engine wear and poisons catalysts. The water content can contribute to corrosion in tanks and fuel injection equipment whereas the ash content is the solid residue when fuel is burnt off. The polycyclic aromatic hydrocarbon content is used to increase the cetane number due to their low boiling point and high density.

The properties of fuel performance consist of colour, particulate, filter blocking tendency, lubricity, oxidation stability and copper corrosion. [84] These properties result from one or more effects of the fundamental and the miscellaneous properties. For example, the copper corrosion is an indicator mainly due to sulphur content in the diesel.

Based on the diesel regulation, the fundamental properties of plastic derived fuels are examined in most studies because the diesel fuel is produced from synthetic hydrocarbon polymers that do not contain any other elements except for carbon and hydrogen. Therefore, some of the miscellaneous properties are not important for the diesel from plastic pyrolysis, such as sulphur content and water content. The quality of

the liquid fuels from pyrolysis of plastics will vary with pyrolysis operation conditions, pyrolysis reactor type and types of plastic feedstock. However, comparison of the plastic pyrolysis fuels and petroleum derived fuels has both been found in the literature review and thus this study will investigate this in details.

The quality of plastic derived fuels varies largely based on the process and the feedstock. The diesel range products in the LDPE derived fuels contain the same linear chain alkanes as those in the fresh diesel. The content of alkene in LDPE derived products is much higher than that in diesel, which decreases the storage stability of fuel. [17] Compared to naphtha, aromatic compounds, and branched hydrocarbons, linear alkanes have relative higher cloud point with the same carbon number or density. Therefore, many catalysts and processes were used to reduce linear hydrocarbons and increase the proportion of others.[17] It was found that plastic derived diesel contains high proportion of linear alkane that has low solubility in diesel. This can significantly increase the cloud point that is the temperature at which the first crystals appear in diesel. Dewaxing, hydrogenation, isomerization, and cyclization are normally used in the pyrolysis processes to change the chemical composition in the products. [25, 33, 70] Some other properties of plastic derived fuels are controlled in the producing processes such as distillation range and carbon residue in the fuel.

## 2.3. Existing Commercial Plastic Pyrolysis Technologies and Processes

The waste plastic pyrolysis plants were developed and built in many countries. The selection of the process and the plant is determined mainly on the feedstock composition and the target products.

### 2.3.1. Feedstock effects

According to a summary of existing processes and technologies reported by Arena and Mastellone, the most important property of plastic feedstock is whether it contains PVC. [61] PVC pyrolysis has different the thermal cracking process and different products from those of other common waste plastics including PE, PP and PS. In the PVC pyrolysis, the products containing HCl are particularly hazardous for fuels. [54] If the feedstock contains PVC, the plants must have re-treatment system to remove and a solvent scrubber to remove HCl from the pyrolysis products.

The other important property for some current processes is the size of feedstock. The requirement for the feedstock size is to avoid the feeding blockage and to enhance the heat transfer between the heating medium and the plastics particles.

It was found that in most cases, the feedstock is a mixture of various waste plastic in municipal slid wastes or industrial residues. In pyrolysis of the mixed plastics, interactive effects among the different plastic types may occur due to the difference in cracking temperatures and different products. . However, no report has been found where the pyrolysis technology is designed for a specific type of the waste plastic. [61]

### 2.3.2. Technology

The selection of pyrolysis technology is based on the characteristics of the feedstock and the target products. In general, each pyrolysis technology consists of three parts: feeding system, pyrolysis reactor and separation system.

Feeding system

In most commercial processes, the raw materials are firstly heated and melted in the feeding system before flowing into the reactor. The air, moisture and other solid materials can be separated from the raw plastic materials in the feeding system. In addition, the pre-treatment may be required for cracking the PVC at 250 ºC. [62-63] In some rotary kiln reactors, solid plastic particles with appropriate sizes can be extruded into the reactor directly. Most feeding systems move the highly viscous melted plastics into reactors by its gravity or by an extruder. However, a required temperature gradient should be maintained from the feeding system to the pyrolyzer although this may not be an issue for the rotary kiln reactors. The required temperature gradient is to prevent melted plastic cracking before entering the pyrolyzer. For example, the cracking temperature of PS is 420 ºC thus any over heating in the feeding system should be avoided. Free-fall feeding system is widely applied in fixed bed and fluidized bed reactors.

Pyrolysis

The description and classification of pyrolysis reactors are given in Section 2.1 of this thesis and the existing commercial pyrolysis plants use various types of the reactors as summarized by Scheirs and Kaminsky. [23]

Continuous pyrolysis process is applied on most commercial plants with capability to use catalysts in which the plastic retention time is relatively short. Very few of the commercial plants use high pressure operation condition and most of the plants operate

at or slightly above atmospheric pressure. The operating temperature in the reactors varies largely from 250 ºC (Mazda fixed-bed catalytic process in Japan) up to 800 ºC (Compact Power fixed-bed pyrolysis in United Kingdom) but most of the pyrolysis reactors operate between 400 ºC and 550 ºC. [23]

It must be noted that if the operation temperature is above 800 ºC, the process becomes gasification and the products are mainly short chain hydrocarbons which remains as gases under room temperature and atmospheric pressure. All of the commercial plants are fast or flash pyrolysis. Three types of reactors including fixed-bed, fluidized-bed, and rotary kiln can be found in the literature review. [20, 29, 45, 60-61, 65, 69, 85-88]

Product separation and collection

The products from the plastic pyrolysis are mainly combustible gases and liquids. The liquids can be either combusted for power generation or for further refining to produce high quality fuels. In some plants, the pyrolysis products are simply separated into liquid, gas and solid whereas others have a more complete separation system by feeding the mixture of liquid and gas into distillation columns. Diesel range products can then be distilled out as in an oil refinery process. The non-condensable gases are mainly made of hydrocarbons, and a minor amount of hydrogen and carbon monoxide. The gases can be liquefied as fuels, or used as fuels to heat the pyrolysis reactor, or if the amount is insignificant, the non-condensable gases are sent to an incinerator flaring off with the air.[89] Ash may present in the non-condensable gases so most commercial processes have a gas scrubber for cleaning the gases.

# 3. Analysis of Plastic Pyrolysis Reaction Kinetics and Reaction Energies

## *3.1. Theory of Pyrolysis Reactions*

Plastic pyrolysis is a complex process of breaking the long polymer chains into short ones. In many books and researches, this thermal degradation process is usually considered as depolymerisation of polymers.[33] In this chapter, the fundamental phenomena involved in the pyrolysis process are investigated from both physical and chemical point of view. Following further literature review on the reactions kinetics of the pyrolysis reactions, heat companied with the reactions and energy demand in the pyrolysis are analysed.

### 3.1.1. Effect of thermodynamic on physical property of polymer

The physical property of plastic can be changed significantly at different temperature before the plastic decomposition temperature is reached. Over the temperature, the carbon backbone of the plastic is cracked into shorter carbon chains. The chemical structure of the plastics changes as well. These phenomena have been fully understood since thermal plastics have been developed and studied for more than 100 years.[1, 90] Under the same temperature, different types of plastics have different physical properties and the decomposition processed may also be different.

With temperature increasing, the plastics undergo three major thermal transitions: namely glass transition, the melting, and decomposition as shown in Figure 3-1 for the state changes with temperature for PET. At room temperature, all polymers are hard solids, which is also called glassy state. As the temperature rises above the glass transition temperature, $T_g$, thermoplastic acquires sufficient energy to enable the chains to move freely and becomes rubberlike. [2] With the temperature further increasing, the rubberlike plastic is changed to liquid-like substance when thee temperature rises above

the melting temperature, $T_m$. Following this, the plastic starts to decompose when the temperature reaches the decomposition temperature, $T_p$. These phenomena can be described by changes in elastic modulus of the plastics with temperature increasing as shown in Figure 3-2. Other properties of the plastics are also changed with the increasing temperature such as heat capacity and linage. [2]

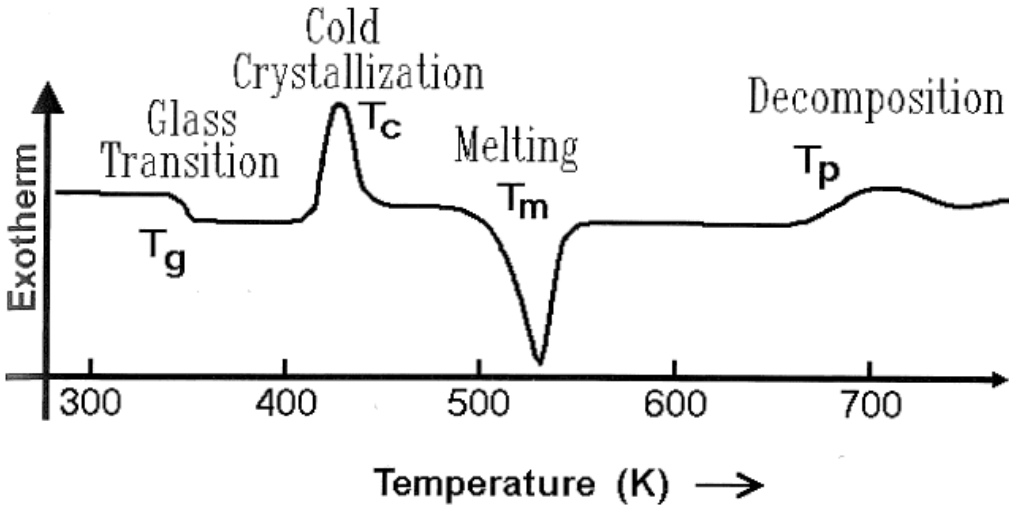


**Figure 3-1 The phase transitions of PET by differential thermal analysis [91]**

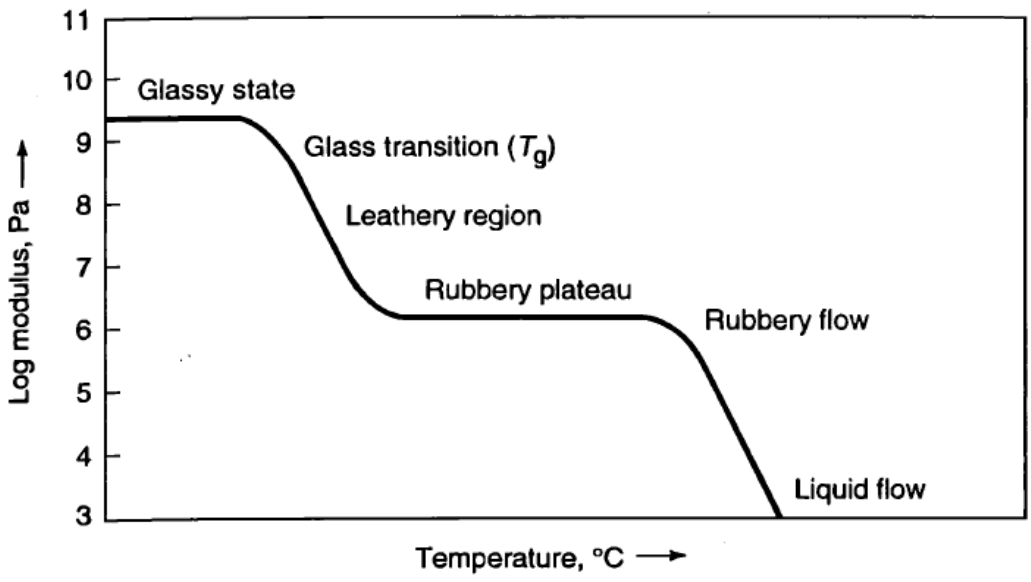


**Figure 3-2 Effect of temperature on elastic modulus of polymers [92]**

### 3.1.2. Chemistry of different chain cracking type

The chemical changes of plastics have been investigated in order to understand the cracking mechanism in the pyrolysis when the temperature rises above the decomposition temperature. With the temperature increasing, the vibration of molecules gets intensive and small molecule will escape the object surface when the vibration is intensive enough to overcome the van der Waals force, which is called evaporation. However, when the van der Waals force induced energy is greater than the bond enthalpy between atoms in the molecule structure, the molecule will crack rather than evaporate. The crackings occur at the most unstable bonds in the molecular structure. The stability of carbon bonds in then plastics varies with the carbon bond molecular structure and the order of stability of the hydrocarbons is shown in Figure 3-3 , in which R is a functional group in polymers. [93]

The energy required for bond breaking is called bond dissociation energy when the van der Waals force induced energy is equal to the bond enthalpy. The bond dissociation energies for C-C bond of primary, secondary, and tertiary carbons are 355, 351, and 339kJ/mol, respectively. [38] Therefore, the C-C bonds on the carbons with branches are likely to be broken first.

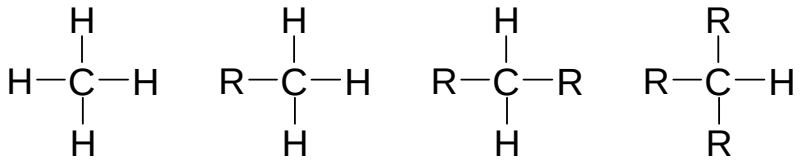


**Figure 3-3 Stability of carbon bonds [93]**

Based on the above theoretical analysis and other studies, three major types of cracking in the pyrolysis reaction are proposed as described in the following sections.[33]

### Random cracking

Most carbons in linear PE (HDPE) are on the long straight carbon chains (secondary carbon atoms) so that the cracking on these carbons has the same chance to occur, which is called random cracking. [51, 64, 94-97] There are a number of tertiary carbons at the branched knots of LDPE. The bonds on these tertiary carbons are less stable than secondary or primary carbons; hence, the C-C bonds at the branched knots start cracking first. This explains the reason why most hydrocarbons from cracking of branched LDPE carbons are straight chain hydrocarbons similar to those produced from linear HDPE. All C-C bonds in PP joint on tertiary carbons except for few of the C-C bonds at the ends of PP molecules. Subsequently, the bonds in PP are less stable than those in the PE. PP is more likely to produce smaller hydrocarbons than PE. Similar theories can be applied on the PS cracking. Random cracking is the major type of cracking in pyrolysis of PE, PP and PS.

### Chain strip cracking

Unlike the random cracking, the side carbon groups in the branched and cross-linked polymer units may come off the main carbon chains in the pyrolysis. This process is called chain strip cracking after which the unsaturated chains undergo further reactions including cracking, aromatization and coke formation.[72, 77] This is the major process in pyrolysis of polymers with reactive side groups. However, some side groups do not significantly react. For example, chain strip cracking is not significant in PP pyrolysis.

### End chain cracking

When plastic is heated to or above the decomposition temperature, the polymer may break up from the end groups. [33, 77, 95] Figure 3-4 shows the proposed mechanism

of the end chain cracking to produce volatile products at the gas-liquid interface in pyrolysis reactor. [77]

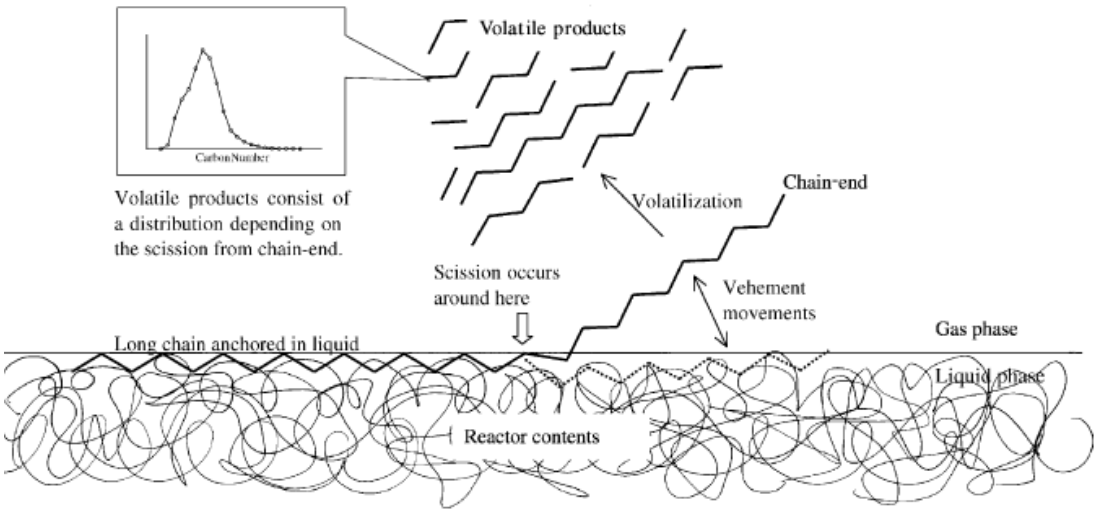


**Figure 3-4 Proposed macroscopic mechanism of the end chain cracking of polymers at gas–liquid interface [77]**

From Figure 3-4, it is observed that vehement molecule movements cause end chain cracking. When the stability of the C-C bonds in chains is uniform, the chains break up at the ends due to the vehemence of the molecule movements, which is promoted by the temperature increase. At higher temperatures, the movements of molecules are more vehement and thus shorter end chains will break off from the main C-C chains. This explains the reason why high reaction temperature promotes the yield of shorter hydrocarbon products such as in the fast pyrolysis and high temperature gasification. [78-83]

### 3.1.3. Pyrolysis reaction progresses

The polymer cracking is an important reaction in the plastic pyrolysis; however, the complete process involves other reactions as well. In this section, the full pyrolysis reaction process will be investigated. There are numerous reactions in the plastic

pyrolysis process, which can be considered to consist of four stages: initiation, propagation, hydrogen chain transfer and termination. [9, 68, 72, 77, 84-85] The possible product species in the pyrolyzing process can be classified into two groups: molecules including alkane, alkene, and dialkene, etc; and free radicals which also contain unpaired electrons either at the ends or in the middle of the free radicals.

Initiation reactions

Initiation reactions break the carbon chain of polymer and form smaller free radicals and molecules. There are three types of initial crackings according to the side group of the plastic, which was mentioned in section 3.1.2. Initiation reactions occur randomly or at the end chain positions in PE pyrolysis. These two types of scission reactions are illustrated, respectively, in Figure 3-5 for the random scission reaction and in Figure 3-6 for end chain scission reaction in the plastic pyrolysis. In the figures, G represents the side group in the polymer unit, which can be H, $CH_3$ or others. [95]


**Figure 3-5 Sketch of random scission reaction in plastic pyrolysis [95]**


**Figure 3-6 Sketch of end chain scission reaction in plastic pyrolysis [95]**

Massive free radicals are produced in initiation reactions; accordingly, propagation and termination reactions are considered to be reactions of the generated free radicals.

Propagation reactions

Propagation is scission of the free radicals generated from the initiation reactions, which are intermediate reactions during the pyrolysis process. From the literature review, β-scission was reported to be the main propagation reaction which also includes end chain scission reactions and mid-chain random scission reactions. [95] These two types of propagation reactions are shown in Figure 3-7 for the mid-chain random scission reaction and in Figure 3-8 for end chain scission reaction. The products from the propagation reactions are mainly 1-alkenes.

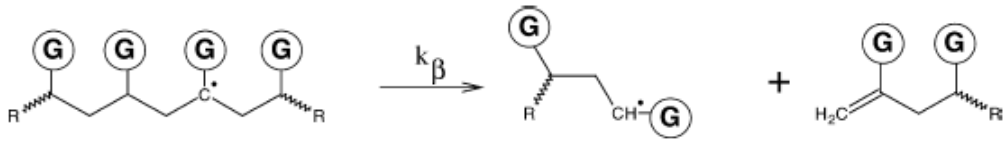


**Figure 3-7 Illustration of mid chain β-scission reaction [95]**

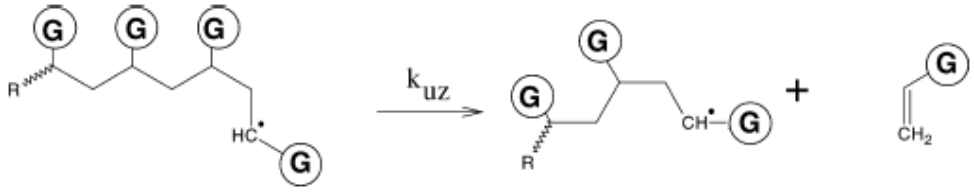


**Figure 3-8 Illustration of end chain β-scission reaction (unzipping reaction) [95]**

Propagation reactions crack the large free radicals generated from the initiation reactions and produce alkene molecules and smaller free radicals. In macroscopic scale, longer chain free radicals in the vapour phase are further cracked to smaller products through the propagation reactions. This theory can be applied to explain the relationship between residence time and the molecular weight of the pyrolysis products.

Hydrogen chain transfer reactions

Hydrogen chain transfer is proton transfer to other locations. This type of reactions decreases the polymer molecular weight, which can be found in many polymerization systems. [2] Hydrogen chain transfer reactions include intermolecular transfer reaction (Figure 3-9 and Figure 3-10) and intra-molecular transfer reaction (Figure 3-11). [33] Intermolecular transfer reaction occurs between free radicals and other components. Saturated hydrocarbon molecules are formed from the corresponding radicals.

Most free radicals from the initiation are end chain free radicals, which have a positive charge at the ends. (Figure 3-9) Some intermolecular transfer reactions on the mid-chain radicals are shown in Figure 3-10. In the contrast, the intra-molecular transfer reactions transfer the free hydrogen proton from the end to the middle of the free radicals. This reaction encourages isomer production in the pyrolysis process.

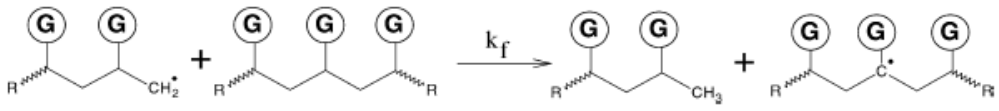


**Figure 3-9 Intermolecular transfer reaction on to the end chain radicals [95]**

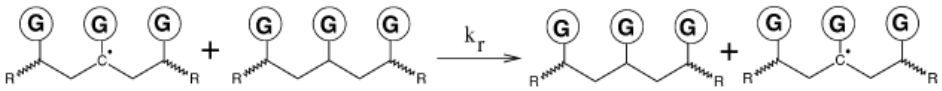


**Figure 3-10 Intermolecular transfer reaction on the mid-chain radicals [95]**

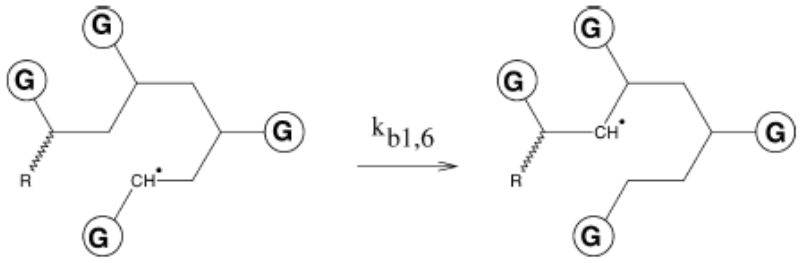


**Figure 3-11 Intra-molecular transfer isomerization via (1, 6) hydrogen transfer [95]**

Termination reactions

Termination reaction occurs by disproportionation of the free radicals or combining of two free radicals as shown in Figure 3-12. [2, 33] This reaction directly affects the product chain length.

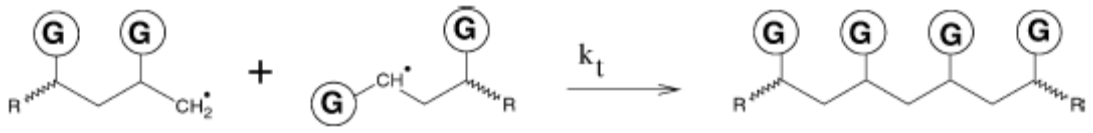


**Figure 3-12 Sketch of termination reaction or radical combination reaction [95]**

As a result of the combination reaction, the final products vary largely when free radicals from different plastics are present in the pyrolysis process.

According to the above reactions in the plastic pyrolysis, 1-alkenes are produced in β-scission reactions (propagation) while the initiation and the termination reactions produce unsaturated compounds. Plastics like PE, PP, and PS can be considered as saturated alkene molecules due to their large molecular weight. Therefore, the number of unsaturated bonds in the product indicates the magnitude of initiation and termination reactions, and the amount of 1-alkenes indicates the magnitude of propagation β-scission reactions.

The above reactions can also be described as the following reaction formula. [77, 86]

Initiation reaction:

$$Molecule \longrightarrow 2R^{\bullet} \qquad (1)$$

Propagation (β-scission) reaction:

$$R_n^{\bullet} \longrightarrow O_j + R_{n-j}^{\bullet} \quad (2)$$

Termination reaction:

$$2R^{\bullet} \longrightarrow products \quad (3)$$

Where $R_n^{\bullet}$ is a free radical with a chain length *n*. $O_j$ is an alkene (olefin) with a chain length j.

### 3.1.4. Reaction modelling

Due to the large number of reactions in the plastic pyrolysis processes, the reaction models are complex and numerous. The product compounds and intermediate-products compounds involved in the plastic pyrolysis process can be classified into **molecules** such as alkane (P), alkene (O), and dialkene (D), and **free radicals** such as end chain radicals and mid-chain radicals. However, free radicals exist only as intermediate products during the pyrolysis and do not exist in the final products. [77, 86-87] Theoretically, the reaction process models can be simplified into the following steps in terms of the reactants and the products.

$$P_n \longrightarrow O_j + P_{n-j} \quad (4)$$

$$O_n \longrightarrow c_1(P_j + D_{n-j}) + c_2(O_j + O_{n-j}) \quad (5)$$

$$D_n \longrightarrow D_j + O_{n-j} \quad (6)$$

Where *j* varies along the total carbon chain length *n*. $c_1$ and $c_2$ are constants and their values are dependent on the reactions and the processes. [95, 97] The straight chain polymers can be described as large molecular weight alkenes; $C_nH_{2n.}$ Other types of polymers may slightly be different. If the $C_nH_{2n}$ is assumed for all of the polymers, based on the hydrogen balance calculation in the above steps, the ratio of alkane to dialkene should be 1:1 if the products consist of alkanes, alkenes, and dialkenes only.

However, there are pure carbons and many other types of unsaturated hydrocarbons produced in the final products. The hydrogen extracted from the pure carbons may transfer to other products and form more saturated hydrocarbons. Large proportion of alkenes and alkanes were found both in other literature's data and this research, which indicates a significant effect of intra-molecular H-transfer reactions which are also called back-biting reactions. [95, 97]

To simulate the plastic pyrolysis reactions, some reaction models have been reported in many literatures. [62-63, 77, 86-88] Propagation reactions were extensively studied as they have major effects on the distribution of the pyrolysis product. [97] In this work, a more general kinetic reaction model will be developed based on the above analysis on the plastic pyrolysis reactions and products. The model is expected to be applied to a wider range of plastic types and pyrolysis conditions.

## 3.2. Kinetics of Plastic Pyrolysis Reaction

### 3.2.1. Reaction kinetics

Pyrolysis reactions of plastics are very complex. In addition, there are a number of factors affecting the process and the reactions such as catalysts, reactor type, the type of plastics and the secondary cracking process. A non-catalyst thermal degradation of plastics can be generally described using the Arrhenius equation. [62, 77, 88-89]

$$-\frac{dm}{dt} = km^n \tag{7}$$

The reaction kinetic constant in the above equation can be determined by

$$k = A_o e^{-\frac{Ea}{RT}} \tag{8}$$

In which $m$ is the mass ratio of unvolatilized sample residue to the initial models of the material before reaction and $n$ is the reaction order. $E_a$ is the activation energy (kJ/mol) and $A_o$ is the pre-exponential constant in the standard Arrhenius form. $R$ is the gas constant (J $K^{-1}$ $mol^{-1}$) and $T$ is the temperature in Kelvin (K).

Combining Equations (7) and (8) yields: [39, 77]

$$\frac{d\alpha}{dt} = A_o \exp\left(-\frac{E_a}{RT}\right)(1-\alpha)^n \tag{9}$$

Where α is the conversion ratio which is equal to (1-m) The kinetic parameters and the reaction order can be determined from experiments. [39, 63, 66, 77] Marongiu *et al.* applied the kinetic models for different plastics for non-catalyst pyrolysis and obtained values for Ea, n and $A_0$ as given in Table 3-1. [79, 95] Products from the primary cracking reactions can be further cracked in the subsequent reactions into lower molecular weight hydrocarbons. [94, 98-101] The latter is also called the secondary cracking which occurs both in non-catalyst and catalyst pyrolysis reactions.

**Table 3-1 Reaction kinetic parameters and values in pyrolysis of different plastics [79]**

| Kinetic model | Differential equations | $E_a$ (kJ/mol) | $n$ | $A$ (min$^{-1}$) | Yield coefficient |
|---|---|---|---|---|---|
| HDPE $\xrightarrow{k_1}$ V + R | $\frac{d[HDPE]}{dt} = -A_1 e^{\frac{-E_{a1}}{RT}}[HDPE]^{n_1}$ | 250 | 0.65 | $1.71\times10^{17}$ | |
| $\alpha_1$LDPE$_1$ $\xrightarrow{k_1}$ V$_1$ + R$_1$ | $\frac{d[LDPE_1]}{dt} = -A_1 e^{\frac{-E_{a1}}{RT}}[LDPE_1]^{n_1}$ | $E_{a_1} = 120$ | $n_1 = 1.40$ | $A_1 = 1.34\times10^{9}$ | $\alpha_1 = 0.10$ |
| $\alpha_2$LDPE$_2$ $\xrightarrow{k_2}$ V$_2$ + R$_2$ | $\frac{d[LDPE_2]}{dt} = -A_2 e^{\frac{-E_{a2}}{RT}}[LDPE_2]^{n_2}$ | $E_{a_2} = 220$ | $n_2 = 0.60$ | $A_2 = 1.47\times10^{15}$ | $\alpha_2 = 0.90$ |
| PP $\xrightarrow{k_1}$ V + R | $\frac{d[PP]}{dt} = -A_1 e^{\frac{-E_{a1}}{RT}}[PP]^{n_1}$ | 125 | 0.40 | $2.04\times10^{8}$ | |
| $\alpha_1$PS$_1$ $\xrightarrow{k_1}$ V$_1$ + R$_1$ | $\frac{d[PS_1]}{dt} = -A_1 e^{\frac{-E_{a1}}{RT}}[PS_1]^{n_1}$ | $E_{a_1} = 120$ | $n_1 = 1.60$ | $A_1 = 1.06\times10^{8}$ | $\alpha_1 = 0.10$ |
| $\alpha_2$PS$_2$ $\xrightarrow{k_2}$ V$_2$ + R$_2$ | $\frac{d[PS_2]}{dt} = -A_2 e^{\frac{-E_{a2}}{RT}}[PS_2]^{n_2}$ | $E_{a_2} = 185$ | $n_2 = 0.76$ | $A_2 = 2.32\times10^{13}$ | $\alpha_2 = 0.90$ |
| PVC $\xrightarrow{k_1}$ $a$HCl + $b$I | $\frac{d[PVC]}{dt} = -A_1 e^{\frac{-E_{a1}}{RT}}[PVC]^{n_1}$ | $E_{a_1} = 198$ | $n_1 = 1.04$ | $A_1 = 3.57\times10^{18}$ | $b = 0.52$ |
| $b$I $\xrightarrow{k_2}$ $c$V$_1$ + $e$R$_1$ | $\frac{d[I]}{dt} = b(A_1 e^{\frac{-E_{a1}}{RT}}[PVC]^{n_1} - A_2 e^{\frac{-E_{a2}}{RT}}[I]^{n_2})$ | $E_{a_2} = 143$ | $n_2 = 1.15$ | $A_2 = 9.95\times10^{10}$ | $e = 0.36$ |
| $e$R$_1$ $\xrightarrow{k_3}$ $f$V$_2$ + $g$R$_2$ | $\frac{d[R_1]}{dt} = e(A_2 e^{\frac{-E_{a2}}{RT}}[I]^{n_2} - A_3 e^{\frac{-E_{a3}}{RT}}[SR_1]^{n_3})$ | $E_{a_3} = 243$ | $n_3 = 1.58$ | $A_3 = 5.77\times10^{16}$ | $g = 0.06$ |
| | $\frac{d[R_2]}{dt} = g(A_3 e^{\frac{-E_{a3}}{RT}}[SR_1]^{n_3})$ | | | | |

[a] V, volatiles; I, intermediate; $SR_1$, residue generated in the first stage; $SR_2$, residue generated in the second stage.

From Table 3-1, it is noted that the Ea values vary from 120 to 250 kJ/mol, which may reflect the differences in experimental conditions and test materials in application of the kinetic reaction model. The influencing factors include molecular weight of the plastic tested, the method of kinetic parameter estimation, the detailed forms of the kinetic model used, the range of temperatures investigated, and other experimental conditions. The values of activation energy and coefficient of n and A in the kinetic reaction model (Equations 8 and 9) are summarized for different plastics types and operation conditions are summarized in Table 3-2 in which plastics types and cracking temperature are also given. [79, 95]

For pyrolysis reactions, Ea is the overall activation energy of all pyrolysis reactions. The pyrolysis process and each reaction will affect the value of Ea. All of the influences of those factors on the Ea value are not negligible, which make the evaluation of the Ea difficult. (Table 3-2) [79, 94, 99-101] Cracking process and temperature are two important factors affecting the value of Ea. The cracking process has very significant effects on the composition of the final product. Large molecular weight hydrocarbons from primary cracking can be cracked into small hydrocarbons through secondary cracking process. The energy required in this process increases the total Ea for the

overall reactions. It can be observed in Table 3-1 that the Ea value increases with the increase intensity of cracking of the products. The Ea value of LDPE cracking including secondary crackings consumes 220kJ/mol, which is above 150% of the Ea value of LDPE cracks into primary products only. Temperature also has effects on the Ea value because it has significant effect on the product distribution. The results of the Ea value at different temperature have been widely investigated and were collected by Miranda et. al. However, it is hard to identify the influence on the Ea value from temperature change because the experimental methods used in different literatures vary widely. (Table 3-2) Based on the differential equations (Table 3-1), it can be deduced that the factors influence on the Ea value by affecting the product composition. The product with higher proportion of small hydrocarbon requires more activation energy. [79]

**Table 3-2 Literature data on kinetic parameters for plastic pyrolysis [79]**

| Plastic (atmosphere) | Temperature range (°C) | $E_a$ (kJ/mol)[a] | $n$ | $A$ (min $^{-1}$) |
|---|---|---|---|---|
| *Polyethylene* | | | | |
| (vacuum, isothermal) | | 251–293 | | |
| (vacuum, isothermal) | | 276 | 0 | |
| (vacuum, isothermal) | 300–475 | 285 | 1 | |
| (vacuum, isothermal) | | 268 | | |
| (vacuum, isothermal) | 400 | 285–301 | 1 | |
| (vacuum, isothermal) | 246–480 | 280 | 1 | |
| (vacuum, isothermal) | 410–475 | 274 | | |
| ($N_2$, dynamic) | 20–600 | HDPE 233 | 0.74 | $5.58\times10^{15}$ |
| | | LDPE 206 | 0.63 | $7.20\times10^{13}$ |
| *Polypropylene* | | | | |
| (vacuum, isothermal) | 300–410 | 242.44 | | |
| (vacuum, isothermal) | 350–450 | 246.62 | | |
| (vacuum, isothermal) | 250–300 | 284 | | |
| (vacuum, isothermal) | 200–356 | 209 | | |
| (vacuum, isothermal) | 390–465 | (IPP) 257 | | |
| ($N_2$, dynamic) | 20–600 | 144 | | |
| ($N_2$, dynamic) | 20–600 | 183 | 0.90 | $3.72\times10^{12}$ |
| ($N_2$, dynamic) | 20–600 | 12.5 (1) | 1.0 | $4.8\times10^{-2}$ |
| | | 230 (2) | 0.5 | $1.2\times10^{16}$ |
| *Polystyrene* | | | | |
| (vacuum, isothermal) | below 340 | 187 | 0 | |
| (vacuum, isothermal) | | 209 | | |
| (vacuum, isothermal) | 360–420 | 243 | 0 to 1 | |
| (vacuum, isothermal) | 280–300 | 205 | | |
| (vacuum, isothermal) | 246–430 | 192, | 0.0 | |
| | | 251 | 1.0 | |
| (vacuum, isothermal) | 318–348 | 243 | | |
| ($N_2$, dynamic) | 20–600 | 172 | 0.5 | $3.0\times10^{12}$ |
| ($N_2$, dynamic) | 35–850 | 220 (1) | 0.51 | $3.0\times10^{12}$ |
| | | 276 (2) | 1.02 | $3.67\times10^{19}$ |
| | | 187(3) | 0.80 | $8.58\times10^{13}$ |
| ($N_2$, dynamic) | 35–850 | 2.1 (1) | 1.0 | $1.20\times10^{-2}$ |
| | | 272 (2) | 0.5 | $3.0\times10^{20}$ |

*: Numbers in brackets indicate the step of pyrolysis of single plastics in literatures.

### 3.2.2. Energy balance analysis

In the plastic pyrolysis, energy may be consumed or released from different stages of the process and reactions. This part of work aims to quantify the energy changes throughout the pyrolysis process thus the net energy input or output can be quantified. Three parts of energy changes are considered for the reactants and resultant substances: reaction energy change (ΔH), temperature change of the materials, and heat of evaporation of the products.

The energy change during a chemical reaction is called the Gibbs free-energy change, ΔG. [38, 93] ΔG consists of two terms, an enthalpy term, ΔH, and a temperature-dependent entropy term, TΔS.

$$\Delta G = \Delta H - T\Delta S \tag{10}$$

Where $\Delta H$ is the heat of reaction (kJ/mol) and is the change in total bonding energy during a reaction. $T$ is the temperature in Kelvin. Generally, the enthalpy component is dominant and much larger than the entropy component in a reaction. [38]

ΔG has a positive value when energy is absorbed from the environment, which is called endothermic reactions. Otherwise, it is called exothermic reaction. The relations among potential energy, heat of reaction ($\Delta H$) and activation energy ($Ea$) are illustrated in Figure 3-13 for both endothermic and exothermic reactions. [31]

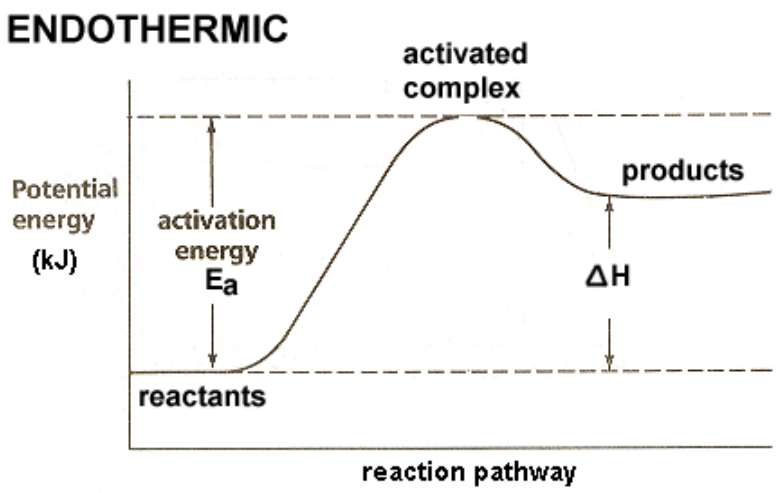


(a)

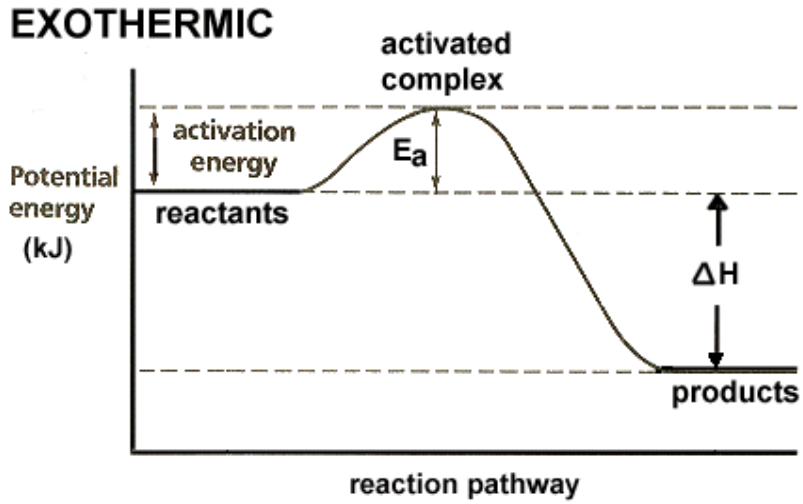


(b)

**Figure 3-13 Comparison of reaction energy diagrams for endothermic (a) and exothermic reactions (b) [38]**

As $\Delta H$ is the dominant part of $\Delta G$, the type of reaction can be distinguished by the value of $\Delta H$ because of $\Delta G = \Delta H - T\Delta S$. In a reaction, if enough bond dissociation energies (BDE) are known then $\Delta H$ can be calculated. For example, the bonds in polyethylene are almost secondary C-C bonds with bond dissociation energy of 355kJ/mol. Straight chain hydrocarbons are the dominant products generated from PE pyrolysis. Hence, a large number of C=C double bond and primary C-C bond at chain ends has been produced in the reactions. 1-alkene, n-alkane, and α, ω-dialkene are the major

hydrocarbons produced. 1-alkene is the major hydrocarbon product that has one C=C double bond at one end and one primary C-C bond at the other end. There are also minor n-alkane containing two primary C-C bonds and dialkene containing two double bonds produced at the same time. The bond dissociation energies of the primary C-C bond and the C=C double bond are 376 and 611kJ/mol, respectively. Both of the two types of product bonds formed require more energy than the energy released from the reactant secondary C-C bond breaking, 355kJ/mol. Therefore, pyrolysis of PE is an endothermic reaction which can be confirmed by findings of previous studies..[102-103] For a given plastic and given pyrolysis conditions, the value of $\Delta H$ is dependent on the composition of the final pyrolysis products.

In practical plastic pyrolysis processes, the theoretical energy required consists of heat for increasing plastic temperature, heat for pyrolysis reactions, and heat of evaporation of hydrocarbon products. In order to quantify the energy distribution in each part, mass flow analysis is needed and an example for non-catalyst pyrolysis of PE is shown in Figure 3-14 in which the pressure of the process is 101,325 Pa and the initial temperature, $T_1$, is the temperature of the feedstock at 20 ºC. The product temperature at the end of pyrolysis reactions, $T_2$, is 400 ºC at which LPG, petrol, and diesel are in gas phase, and wax is in liquid phase which is like fog carried out by other hot gases. In this example, LPG, petrol, diesel and wax range products are represented by hydrocarbons $C_1$~$C_4$, $C_5$~$C_{12}$, $C_{13}$~$C_{22}$, and $C_{23+}$, respectively. These ranges are used for the calculation in this study only, which do not represent actual carbon number range of the fuels.

$$PE(solid) \xrightarrow{pyrolysis} 10\%LPG(gas) + 30\%petrol(gas) + 40\%diesel(gas) + 20\%wax(liquid)$$

**Figure 3-14 Mass flow for reactant and products in PE pyrolysis**

For the plastic pyrolysis, the overall energy required for all of the matters involved can be calculated by the following equation: [102]

$$Q = \sum_{out} n_i H_i - \sum_{in} n_i H_i \tag{11}$$

Where:

Q is the overall energy required in the plastic pyrolysis process (kJ)

$n_i$ is the molar number of component i (mol)

$H_i$ is the enthalpy of component i (kJ/mol)

For pyrolysis of PE, the products are a continuous series of straight chain hydrocarbons which can be divided into four groups as LPG, petrol, diesel and wax represented by $C_3H_6$, 1-$C_8H_{16}$, 1-$C_{16}H_{32}$, and 1-$C_{28}H_{56}$, respectively. When a PE molecule is pyrolyzed into n 1-alkene molecules, there are n-1 C-C bonds broken in the long chain. Each secondary C-C bond is broken and turned into one C=C double bond. At the same time, the dissociation energy of C-H bonds on the carbons with the double bond and at the other end has also been changed. This process is described in Figure 3-15. Some bond dissociation energies are listed in Table 3-3. [31]

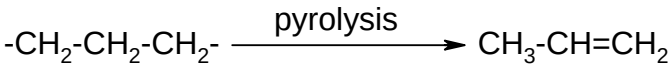


**Figure 3-15 Formation of a 1-alkene molecule from PE molecule pyrolysis**

Using bond dissociation energies given in Table 3-3, the reaction enthalpy, $\Delta H_r$, can then be calculated using Equation (11). The calculation of bond dissociation energy (BDE) required for forming 1-$C_3H_6$ in the PE pyrolysis is shown below and the results are given in Table 3-4. The BDE calculation for formation of 1-alkenes is similar to the above because the mid chain does not change during the reactions and the results are also included in Table 3-4.

**Table 3-3 Some bond dissociation energies [38]**

| Bond | Bond dissociation energy (kJ/mol) |
|---|---|
| $C_2H_5$ - H | 420 |
| $(CH_3)_2CH$ - H | 401 |
| $H_2C$=CH - H | 444 |
| $H_2C$=$CHCH_2$ - H | 361 |
| $H_2C$=$CHCH_2$ - $CH_3$ | 310 |
| CH3 - CH3 | 376 |
| $C_2H_5$ - $CH_3$ | 355 |
| $(CH_3)_2CH$ - $CH_3$ | 351 |
| $(CH_3)_3C$ - $CH_3$ | 339 |
| $H_2C$=CH - $CH_3$ | 406 |
| $H_2C$ = $CH_2$ | 611 |

**Table 3-4 Calculation of reaction energy change**

| Product bonds formed | BDE (kJ/mol) | Reactant bonds broken | BDE (kJ/mol) |
|---|---|---|---|
| $H_2C$ = $CH_2$ | 611 | 4 x $(CH_3)_2CH$ – $CH_3$ | 4x351=1404 |
| $H_2C$=CH – $CH_3$ | 406 | | |
| $C_2H_5$ – $CH_3$ | 355 | | |
| 3 x $H_2C$=CH – H | 3x444=1332 | 6 x $(CH_3)_2CH$ – H | 6x401=2406 |
| 3 x $H_2C$=$CHCH_2$ – H | 3x361=1083 | | |
| Total | 3787 | Total | 3810 |

From the results given in Table 3-4, the enthalpy change in the reactions at standard conditions, $\Delta Hr^o$, is the difference between the total BDE in the reactants and that in the

products, e.g., 3787 kJ/mol – 3810 kJ/mol = -23kJ/mol. This means that each mole of 1-alkene molecular formed from PE cracking will absorb 23kJ. The energy absorbed from the pyrolysis reactions then depends on the quantity of the molecules in the product broken off from the polymer molecules. This result shows that pyrolysis is an endothermic reaction.

The energy required for changing the temperature of plastic and the products can be calculated with the following equations: [102]

$$\Delta H(T_2) - \Delta H(T_1) = \int_{T_1}^{T_2} Cp(T)dT \tag{12}$$

Where $\Delta H(T_2)$ and $\Delta H(T_1)$ are the enthalpy of the formation of the hydrocarbons at temperatures $T_2$ and $T_1$, respectively. The phase of the hydrocarbons may change from liquid to gas when the temperature increases from $T_1$ to $T_2$.Cp is the heat capacity of the hydrocarbons at a given temperature $T$.

When there is a phase change of the hydrocarbon between $T_1$ and $T_2$ (for example $C_{16}H_{32}$ reaction in the following calculations), the phase changes of the products are illustrated in Figure 3-16. In this case, an evaporation energy term needs to be added and Equations (12) is then re-written as Equation (13). In Figure 3-16 and Equation (13), $l$ and $g$ represent, respectively, the liquid and gas phases of the hydrocarbons. $T_b$ is the temperature at the boiling point of the hydrocarbons. The properties of the hydrocarbons studied here are listed in Table 3-5, in which $\Delta H_v$ is the heat of evaporation of the hydrocarbon. [104]

$$C_{16}H_{32}(l,T_1) \xrightarrow{\Delta H_1} C_{16}H_{32}(l,T_b) \xrightarrow{\Delta H_v} C_{16}H_{32}(g,T_b) \xrightarrow{\Delta H_g} C_{16}H_{32}(g,T_2)$$

**Figure 3-16 Products and products phases changes from PE pyrolysis**

$$\Delta H(T_2) - \Delta H(T_1) = \int_{T_1}^{T_b} Cp(l,T)dT + \int_{T_b}^{T_2} Cp(g,T)dT \quad (13)$$

**Table 3-5 The properties of the three 1-alkenes in PE pyrolysis [104-105]**

| | Cp gas J/mol K | Cp liquid J/mol K | $T_b$, 1 atm | $\Delta H_v$ kJ/mol |
|---|---|---|---|---|
| $C_3H_6$ | 64.32 | 112 | -47.70 | 18.42 |
| 1-$C_8H_{16}$ | 176.10 | 241.40 | 121.280 | 33.76 |
| 1-$C_{16}H_{32}$ | 357.43* | 470.18* | 284.873 | 50.42 |
| 1-$C_{28}H_{56}$ | 628.98* | 810.98* | 429* | |

Numbers with " * " are the calculated value from this work.

The heat capacity of gas ($C_{p,g}$) and that of the liquid ($C_{p,l}$) are in linear relationship with the carbon numbers of n-alkane and 1-alkene as shown inFigure 3-17 and Figure 3-18 [105] It is interesting to note that with the same carbon number, the heat capacity values of n-alkane and 1-alkene are very similar. This is true both for gas phase and liquid phase although the values for 1-alkene are slightly lower than those of n-alkane. (Figure 3-17 and Figure 3-18) However, for heavy molecular weight hydrocarbons some properties can not be found in the literature review, therefore, these values have been estimated based on the existing data and linear relationship with the carbon number.

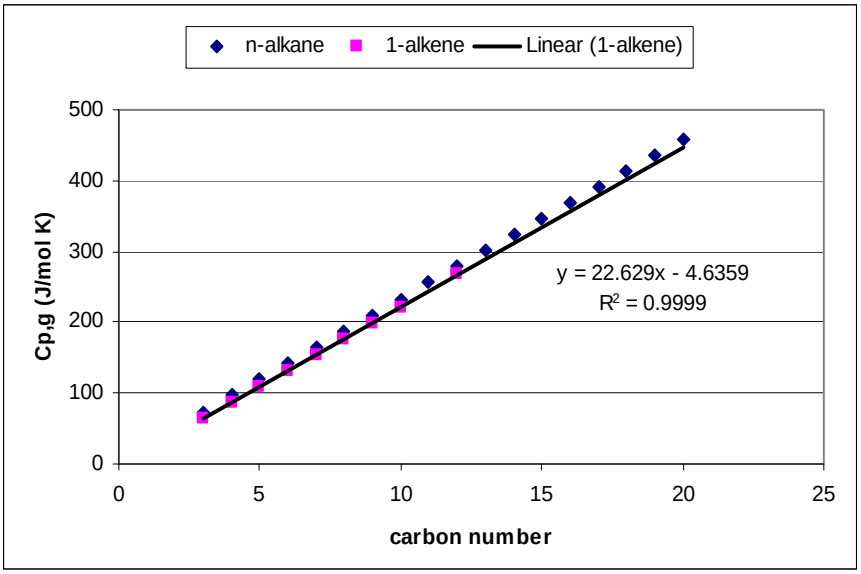


**Figure 3-17 Relation of $C_{p,g}$ of hydrocarbons with carbon numbers [104]**

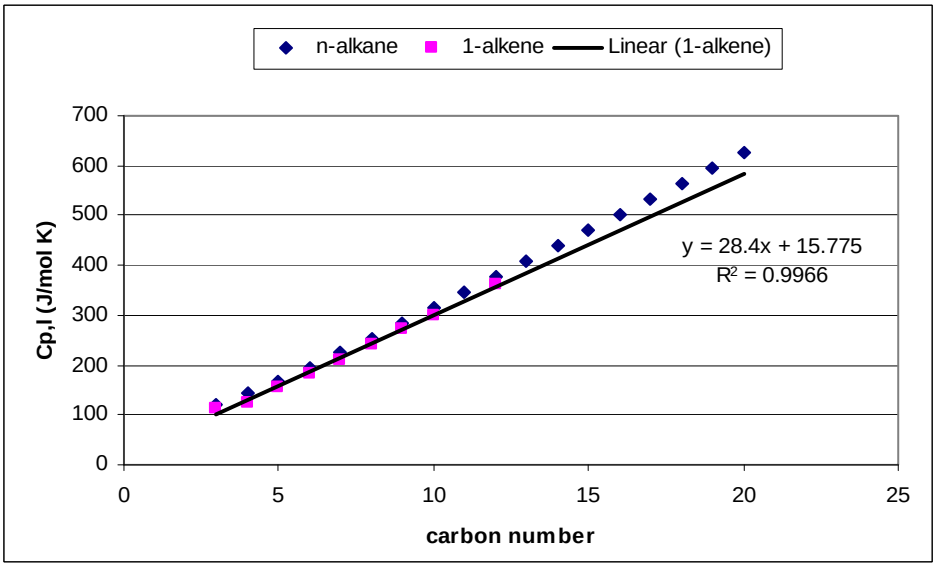


**Figure 3-18 Relationship of $C_{p,l}$ of hydrocarbons with carbon numbers [104]**

The boiling points of n-alkanes from $C_1$ to $C_{100}$ and those of 1-alkene from $C_2$ to $C_{20}$ were measured at 1 atm in Wilhoit and Zwolinski's study and the results are shown in Figure 3-19. [104] It was observed that the boiling point of 1-alkene is slightly lower than that of n-alkane with the same carbon number in a molecule. The difference between the boiling points of 1-alkene and the corresponding n-alkane with the carbon number greater than 20 is less than two Celsius degrees. Therefore, the boiling point of the corresponding n-alkane greater than $C_{20}$ can be accepted as that of 1-alkene in this case.

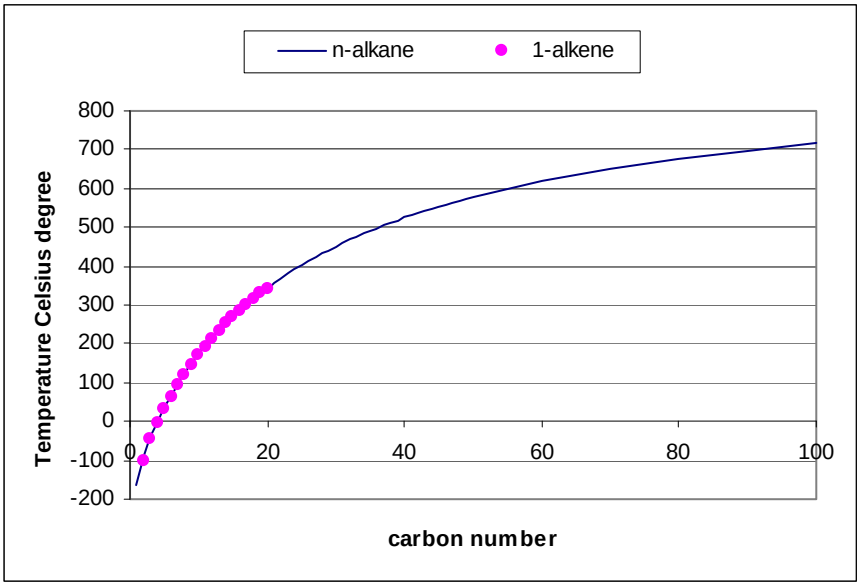


**Figure 3-19 Boiling point of n-alkane and 1-alkene [104]**

Based on Equations (13 and 14) and using data in Table 3-5, the energy required for heating and vaporizing the product, $\Delta H$, can be determined and an example is shown as Equations 15 to 18. In these equations, $T_1$ is the initial feedstock temperature at 25 ºC and $T_2$ is the temperature at the end of the pyrolysis reactions, 400 ºC.

$$\Delta H_{C_3H_6} = \Delta H(T_2) - \Delta H(T_1) = \int_{T_b}^{T_2} Cp(g,T)dT = 24.12 kJ/mol \quad (14)$$

$$\Delta H_{C_8H_{16}} = \Delta H(T_2) - \Delta H(T_1) + \Delta H_v = \int_{T_1}^{T_b} Cp(l,T)dT + \int_{T_b}^{T_2} Cp(g,T)dT + \Delta H_v = 106.08 kJ/mol \quad (15)$$

$$\Delta H_{C_{16}H_{32}} = \Delta H(T_2) - \Delta H(T_1) + \Delta H_v = \int_{T_1}^{T_b} Cp(l,T)dT + \int_{T_b}^{T_2} Cp(g,T)dT + \Delta H_v = 213.76 kJ/mol \quad (16)$$

$$\Delta H_{C_{28}H_{56}} = \Delta H(T_2) - \Delta H(T_1) = \int_{T_b}^{T_2} Cp(l,T)dT = 304.12 kJ/mol \quad (17)$$

Based on the pyrolysis product described in Figure 3-14 and Equation 15 to 18, the energy required for each individual process and the total energy required for the overall

process have been determined and the results are calculated in Table 3-6. The energy required for pyrolysis of 1kg PE is 169.18 kJ. The pyrolysis process requires 697.98kJ to heat the materials and 180.46kJ to vaporize the products. Hence, the pyrolysis reaction is endothermic reaction. The total energy for pyrolyzing 1kg PE into products with such distribution requires 1047.62 kJ. These figure is about 20% lower than that proposed (1316.1 kJ/kg) by Yuan. [102] The difference is possibly due to the difference in the reaction conditions and the distribution of products.

**Table 3-6 Energy balance of 1kg PE pyrolysis**

| 1kg PE | $C_3H_6$ | 1-$C_8H_{16}$ | 1-$C_{16}H_{32}$ | 1-$C_{28}H_{56}$ | Total |
|---|---|---|---|---|---|
| w/w | 10% | 30% | 40% | 20% | 100% |
| mol | 2.38 | 2.68 | 1.79 | 0.51 | 7.36 |
| ΔHr kJ/mol | 23.00 | 23.00 | 23.00 | 23.00 | 169.18 |
| ΔH kJ/mol | 24.12 | 72.32 | 163.34 | 304.12 | 697.98 |
| ΔHv kJ/mol | - | 33.76 | 50.42 | - | 180.46 |
| Total Energy kJ | 112.19 | 345.75 | 422.79 | 166.90 | 1047.62 |

Assuming the calorific value of these four groups of products from PE pyrolysis is close to that of LPG, petrol, diesel, and residual oil (wax), respectively, the net energy gain by pyrolysis of the PE plastics can be determined by $Q_{net} = \sum w_i Q_i - Q_r$ (18)

Where $Q_{net}$ is the net energy gain. $w_i$ is the percentage of product i, which can be LPG, petrol, diesel or wax. $Q_i$ is the calorific value of product i. $Q_r$ is the energy required in the process which does not include the heat loss from the system. Based on the calorific value of those commercial fuels [10, 91], the net energy gain is calculated and the

results are shown in Table 3-7. This net energy gain, 42.3MJ/kg, is similar to the value reported in Yuan (41.7MJ/kg). [102]

**Table 3-7 Calorific values of plastics pyrolysis products and net energy gain of the process MJ/kg [10, 91]**

| Products | LPG | Petrol | Diesel | Residual oil | Net energy profit |
|---|---|---|---|---|---|
| Composition (w./w., %) | 10% | 30% | 40% | 20% | |
| Calorific values (MJ/kg) | 46.1 | 44.0 | 43.0 | 41.8 | 42.3 |

## 3.3. Conclusion

Pyrolysis of hydrocarbon polymers is a very complex process, which consists of hundreds of reactions and products. Several factors have significant effects on the reactions and the products. Based on previous research, this chapter investigated the fundamental plastic processes and reactions. With temperature increasing, plastic will go though glassy state, rubbery state, liquid state, and decomposition. Decomposition of plastic in an inert environment into liquid is called pyrolysis. There are four stages of reactions during the plastic pyrolysis process: initiation, propagation, hydrogen transfer, and termination reactions. In the initiation reactions, the polymer molecules undergo three types of cracking processes: random, end chain, and chain strip cracking; which is determined by the side functional group on the plastic molecular carbon backbone. In the propagation reactions, especially β-scission, the cracking of large molecular weight free radicals is an important process which produces smaller compounds. Hydrogen transfer reactions increase the variety of the free radicals and that of the final product. Termination is the reaction that combines all free radicals into molecules.

Since the basic pyrolysis process and reactions are understood, a kinetic model was established for energy calculation of the reactions. According to the kinetic model and estimated product, the theoretical energy requirement for pyrolysis of PE was calculated, 1047.62 kJ/kg. The net energy gain of the process is 42.3 MJ/kg.

# 4. Experiments: influencing factors for plastics pyrolysis with the horizontal fixed-bed reactor

The objective of this study is to maximize the proportion liquid range product from pyrolysis of hydrocarbon plastics. In order to optimize the liquid range product, the effects of factors which influence the pyrolysis process need quantifying. Many of these factors affecting the distribution of the products were identified in previous studies and this has been discussed in Section 2.1. However, some of the factors can not be controlled in the process under the reaction conditions. Those adjustable factors will be controlled to optimize the process and to achieve the study objective. In this part of the study, a series of experiments were designed to identify and quantify the effect of the factors on the process and the distribution of the products. According to the results and the findings from each experiment, the apparatus and reaction conditions were modified to maximize the proportion of liquid product.

## *4.1. Temperature profile of plastic pyrolysis*

### *4.1.1.* Materials and methods

In this work, a horizontal fixed-bed batch reactor was designed and constructed as shown in Figure 4-1. The goal for this experiment was to understand the process of the plastic pyrolysis by monitoring and analyzing the temperature profile. In the system, a M303PY Gallenkamp electronic furnace was applied to heat the reactor as an external heating resource. There are two heating sources in the furnace. The front one was used for heating the reactor in this experiment, which has a maximum power output of 881 W. The output power was dialled at Load 100 to provide its maximum power. The reactor was made of stainless steel pipe with an inner diameter of 28 mm and thickness of 2 mm. The system also consists of nitrogen purging bottle and a water-cooling

condenser, both of which are connected to the reactor. Connected to the condenser are a liquid collector and a gas collector. The temperature on the outer wall of the reactor was measured by using thermocouples 1 (Thermal-well 1) and the centre space temperature in the reactor was measured using thermocouple 2 (Thermal-well 2). Thermal-well 2 is shown in Figure 4-2(left).

The experiments used materials supplied by a plastic recycling company which was a mixer of 50% PE, 25% PP, and 25% PS (weight) in the form of post-consumer plastic chips. During the experiment, 10.00 grams of the supplied materials sample chips were placed in the centre section of a combustion boat inside the reactor that was for maintaining consistency of the sample location in the reactor. The combustion boat was half of a pipe that was separated into three sections. (Figure 4-2 right) The centre section was at the heating zone of the furnace, which had the highest temperature in the process.

After the test plastic chips were placed in the reactor, the system was sealed and the nitrogen gas was used as an inert gas to purge the whole system before the furnace started heating. This lasted about one minute. ) When the pyrolysis started and the plastics was heated and then decomposed once the temperature is high enough, the gases produced went through the water-cooling condenser and the temperature was reduced to about 30 ºC. Liquid and non-condensable gases were separately then collected separately. The process ended when no more products came out and the space temperature raised above 500ºC.

Non-condensable gas product was collected by a water sealed gas cylinder with which the volume of collected gases can be read during the reaction process. It was found that brown wax accumulated at the two ends in the combustion boat. The liquid products are yellow-brown oils.

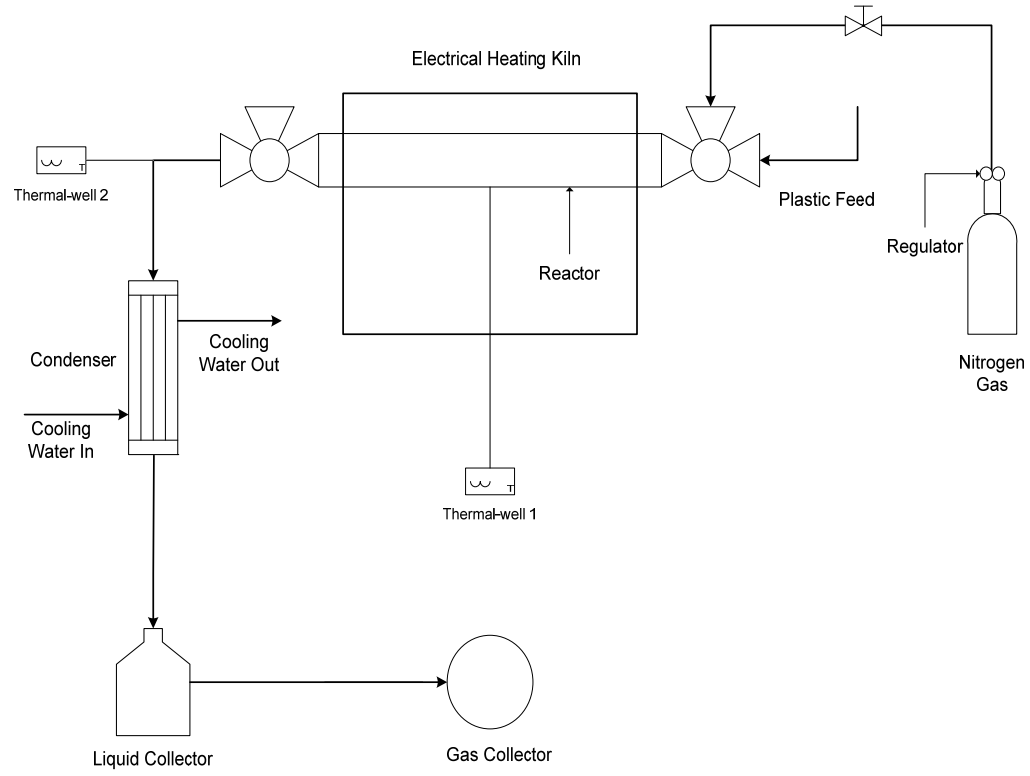


**Figure 4-1 Scheme and picture of horizontal pyrolysis apparatus**

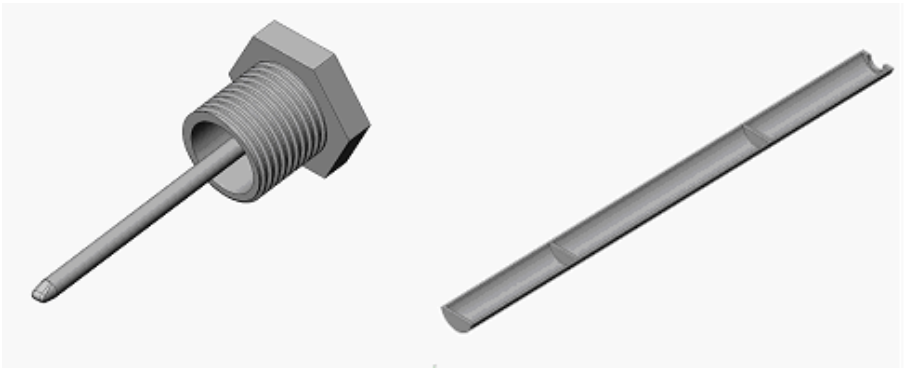

**Figure 4-2 Thermal-well 2 (left) and the combustion boat (right)**

In order to analyse the temperature changes during the plastics pyrolysis, a separate experiment was performed without any feedstock under the same conditions as the previous one. In the experiments, the temperature and the non-condensable gas volume was recoded every one minute.

### 4.1.2. Results and discussion

The 10g plastic mixture was completely pyrolyzed and after the experiment almost nothing was left in the central section of the combustion boat. The products collected included non-condensable gases in the gas collector, dark brown liquid in the liquid collector, yellow or brown wax and char in the reactor. Then the non-condensable gas was pumped into a balloon with an aluminium inner layer.

The wall temperature, $T_1$, and the space temperature, $T_2$, were simultaneously measured during the experiments and the results are shown in Figure 4-3 for the experiment with plastics in the reactor. From Figure 4-3, it was found that large temperature gradient existed between the reactor outer wall and the space inside the reactor. Towards the end of the experiment, both temperatures ($T_1$ and $T_2$) approached constant values of 1030 ºC

and 500ºC, respectively. This was also found in the temperature profile from other researches. [9, 34-35] There was an increase on the $T_2$ curve from the 16th minute to the 20th minute. However, this is not observed on the $T_1$ curve. This means the temperature of the gas in the reactor had a sudden change during this period. Due to the small quantity of the mass of gas, the effect of this temperature change on the wall of the reactor was too minor to be detected by $T_1$. (Figure 4-3)

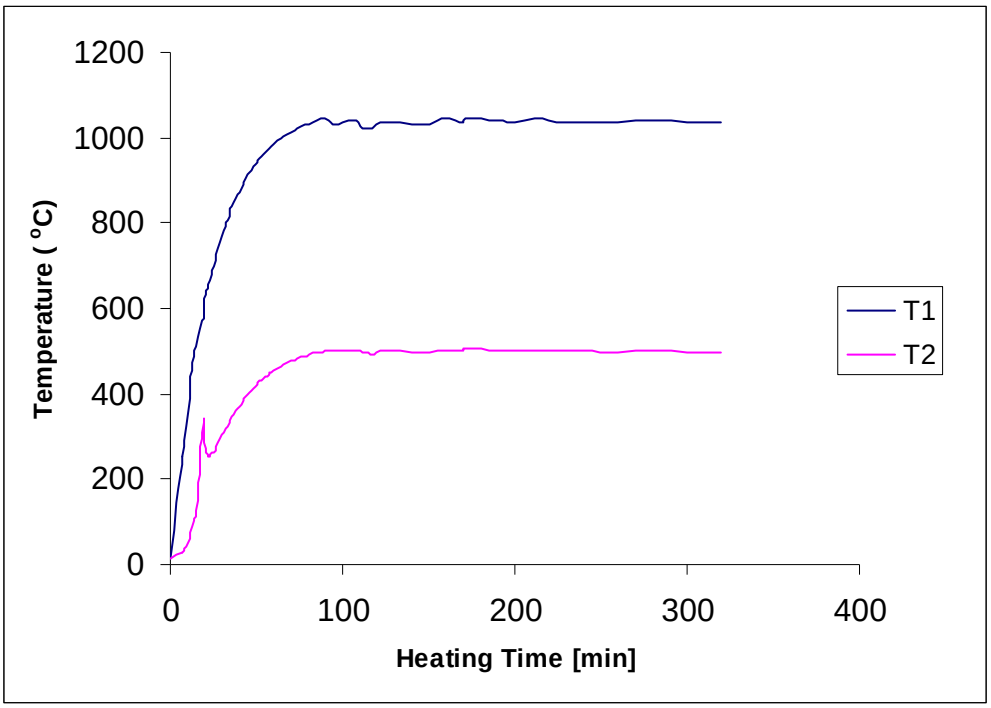


**Figure 4-3 Temperature profile of $T_1$ and $T_2$**

In order to examine and explain the sudden increase on the $T_2$ curve at the pyrolysis period of 16 to 20 minutes from the start, the temperature profiles from the separate experiment without plastics can be used as the baseline. In the latter experiment (without plastics), other conditions remained the same as those in the previous experiment so that the baseline curve can be plotted to compare with the temperature curve with 10g plastic mixture in the reactor. (Figure 4-4) The two temperature profiles are the same from the beginning to the 16th minute. The temperature curve with 10g plastic rapidly increased from the 16th and reached the peak at the 18th minute. The temperature then dropped to the baseline curve at the 20th minute. The 10g plastic

reaction temperature curve is slightly lower than the baseline curve after the 20th minute.

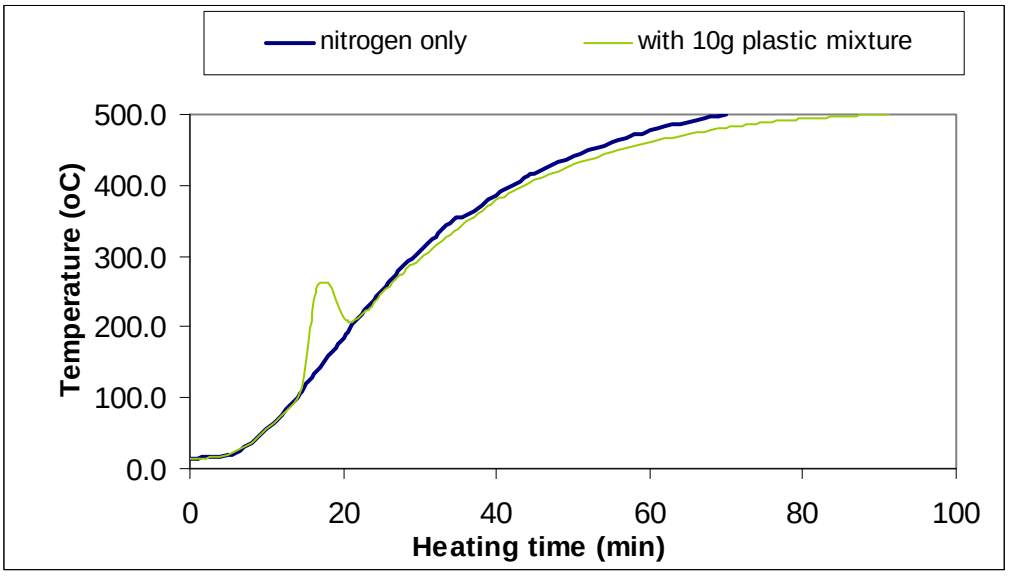


**Figure 4-4 Comparison of space temperatures between experiment of plastic pyrolysis and experiment without plastics**

At the 16minute of plastic pyrolysis experiment, the temperature of the reactor wall reached 480ºC. Considering the high heat conduction rate of the 2 mm thick stainless steel pipe, the temperature of the plastics in the reactor was very likely to be below but close to the reactor wall temperature of 480 ºC. The specific cracking temperature of the plastic tested cannot be identified because the feedstock plastic was a mixture of 50% PE, 25% PP, and 25% PS. In addition, the post-consumer plastics were possibly contaminated during the consumption process. In the further studies, virgin plastics were tested individually in order to determine the cracking temperature of each type of plastics and this will be described in Chapter 5.

From Figure 4-4, it is also observed that the space temperatures in the two experiments were almost the same from the starting to the 16th minute which means the energy required for increasing the plastic temperature was not significant enough to make

difference on the space temperature. That is due to the small quantity of mass and relatively low heat capacity of the plastics. At the 16$^{th}$ minute, plastics were cracked and vaporized into the reactor space. The temperature of the hydrocarbon vapour was close to 480 ºC which is higher than the baseline space temperature of 110 ºC. According to other literatures and previous discussion in section 3.1.3, plastics start with random cracking during which a series of hydrocarbon products such as non-condensable gases ($C_1$ to $C_4$) will be produced. [13, 33, 52, 106-107] As the volume of the pipe reactor is 250 ml, the volume expansion could be detected instantly with negligible time delay. Therefore, the gases could flow out of the reactor instantly once being generated.. This can be confirmed by the volume increase of the non-condensable gases and in this way the on-condensable gas volume measurement can be regarded as the most sensitive parameter for indicating the random cracking at the beginning of the plastic pyrolysis. The condensable vapour formed liquid products during the cooling process in the condenser.

By further examining the temperature profiles in the plastic pyrolysis (Figure 4-3) and comparison with the baseline temperature (Figure 4-4), it is believed that the sudden increase in the space temperature towards the outer wall temperature occurred when the gases were generated. Hence, during the plastic pyrolysis experiments, a rapid temperature rise in space temperature, $T_2$, caused by the hot vapour can be used as another sensitive indicator of vaporization and cracking of plastics. In the plastic pyrolysis experiment, the fast vaporization period lasted bout 2 minutes from 16 to 18$^{th}$ minutes from the start. It is interesting to see that the space temperature rise followed a single curve indicating the three types of plastics were vaporized during this period; therefore, they had similar cracking temperatures.

After the short period of fast cracking, it took another two minutes for the space temperature to drop back to the baseline, which means the energy required for the plastic cracking and vaporizing were not detectable and insignificant compared to the heat used for heating up of the system.

In the experiment, because a horizontal reactor was used, some of the heavy molecular hydrocarbons could be condensed bear the cooler ends of the reactor which were exposed to the ambient air. With increase in the reactor outer wall temperature, the condensed hydrocarbons may be re-vaporized and re-condensed at the ends of the reactor. This reflux process absorbed and caused loss of a significant amount of heat. In addition to the above heat consumed and lost, the outflow gases would carry away some heat from the reactor. As a result, the space temperature curve in the plastic pyrolysis was lower than the baseline curve in the experiment without plastics after 20 minute from the start (Figure 4-4), and the difference between them became greater while the process proceeded. The energy consumption of the process was estimated in chapter 5.

### 4.1.3. Conclusions

Post-consumed polyethylene, polypropylene, and polystyrene were tested in order to understand the first cracking process on these common waste plastic. It was found that these plastics have similar cracking temperature and the cracking process which lasted about two minutes. All of the three types of waste plastic were cracked when the reactor outer wall temperature was below 480ºC. It was found that condensation and vaporization of the pyrolysis vapour near the ends of the reactor required and caused loss of a significant amount of heat. However, the energy required for cracking the plastics was insignificant to be to be detected. Large temperature gradient between reactor wall and inside space was detected in the experiment. The temperature on the reactor wall is believed to be close to the cracking temperature of the plastic.

Based on the above findings, the production of non-condensable gases can be used as a sensitive indicator for random cracking reactions (primary cracking), thus the measurement of gas volume can determine the time when plastic starts cracking. The space temperature is another sensitive indicator for detecting when the product vapour generated by the cracking process.

## 4.2. Effect of Heating Rate

"Heating rate" can be defined in many terms on various pyrolysis plants and researches. In a fast or flash pyrolysis, plastic will be cracked and vaporized very quickly once entering the pyrolysis reactor. In these cases, the heating rate hereby means the rate of temperature increasing per unit time during the contacting time, which can range from 100 up to 10000 K/s. [10] On contrast, in a slow pyrolysis or a batch process, heating rate is normally from 10 to 100 K/s or less. [10] However, in practice, the most convenient way to control the heating rate is to control the heating load to the pyrolysis reactor at given feeding rate. The effect of the heating rate has been discussed in Section 2.1.2. It has been found that heating rate has both effect on the pyrolysis reaction rate [51] and the effect on the distribution of products. [10, 31, 42, 44, 106, 108]

The aims of this part of experimental studies were to experimentally examine the effect of heating rate on the pyrolysis process and the product distribution, and to identify how temperature triggered the cracking of the plastic mixture under the experimental conditions.

### 4.2.1. Experimental

The apparatus described in previous section was used in this part of the study as illustrated in Figure 4-1. The key part of the system is the M303PY Gallenkamp electronic furnace which provides heat with adjustable output power load controlled at scale from 0 to 100. The same post-consumed plastic mixture as that in the previous experiment was used in this experiment. The experiment consisted of three runs with different power load settings at 60, 80 and 100 with the full scale (100) being equivalent to the maximum power output of 881 W. 10g post-consumed plastic mixture was used in each run. Pyrolysis products of non-condensable gas, liquid and solid were collected separately. The volume of gas product, reactor outer wall temperature ($T_1$), reactor space temperature ($T_2$) were measured and recorded every minute simultaneously during each run of the experiment.

### 4.2.2. Results and discussion

The measured accumulated volume of non-condensable gas product was shown in Figure 4-5 for each run of the experiment. From the figure, it is found that the non-condensable gas started to be generated when the wall temperature reached a certain temperature, 450 ºC, in all three runs. This start of gas generation indicated the corresponding start of plastic cracking. To examine the pyrolysis process, the temperature variation within the reactor needs to be considered. As the heat is transferred from the heating element to the plastics through firstly the reactor wall and then the combustion boat, a temperature gradient must exist in the reactor radius direction. Therefore, a temperature gradient exists between the reactor wall and the surface of the combustion boat. In addition, there is also a temperature gradient alone the horizontal direction (length) of the combustion boat due to heat loss from the two ends of the reactor. Consequently, the central part of the reactor is hotter than the two ends and this was also observed in other study. [12]

In the experiment, the test sample of plastic mixture was placed horizontally in the combustion boat. The plastic at the central zone of the boat would start cracking earlier than those at the ends because of the temperature gradient along the reactor length. Although it was unable to determine exactly the hottest spot in the combustion boat, the outer wall temperature at the middle of the reactor was used as an indicating factor that determined the start point of the plastic cracking. It should be noted that the actual cracking temperature can be slightly different and likely to be lower than the outer wall temperature due to the temperature gradients both in the reactor radius and along the length of the combustion boat. This has also been discussed in other studies. [12, 31, 54-55, 79, 87, 109]

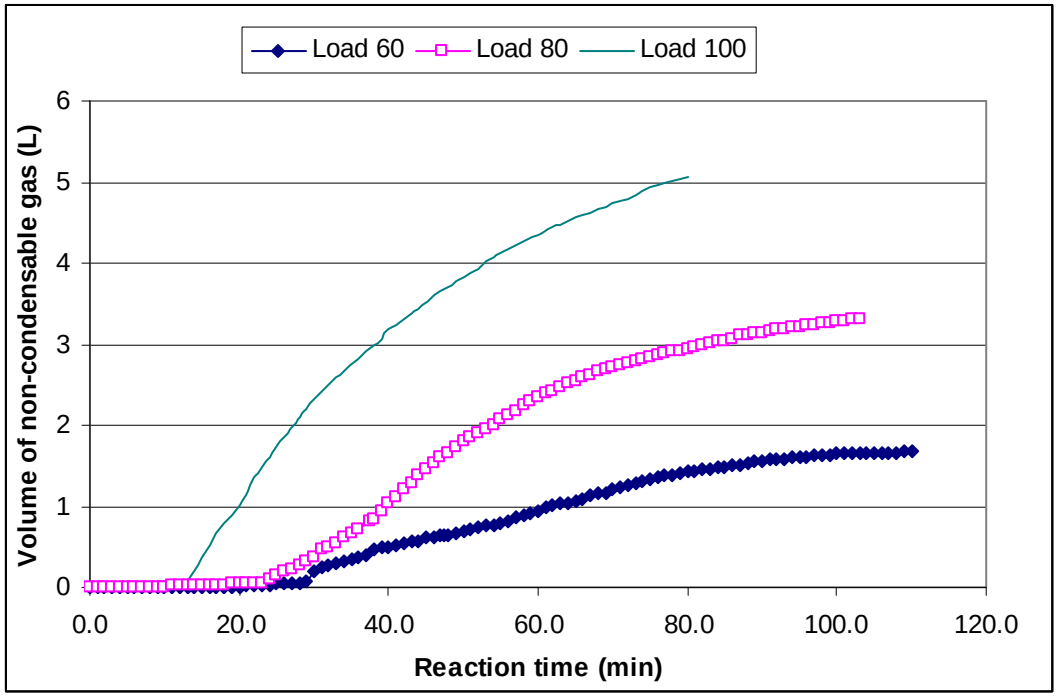


**Figure 4-5 Non-condensable gas production at different heating rates**

During the plastic pyrolysis, the changes in space temperature in the reactor were caused by the vapour generated from the plastic cracking reactions and the space temperate was lower than the plastic temperature in the combustion boat. Therefore, it is not suitable to use the space temperature as the plastic cracking temperature but this indicates the temperature of vapour leaving the reactor.

As the heating rates in the pyrolysis experiments increased with increasing of the power output from setting scale of 60 to the scale of 100, the corresponding heat-up times were 30, 22 and 13 for the reactor to be heated to the temperature when the plastic cracking occurred. The LDPE cracking point can be identified by the start of gas generation as well as the space temperature rapid increase. (Figure 4-5 and Figure 4-4) The LDPE cracking point remained at 450 ºC, which does not affected by the heating rate As Figure 4-5 shows the accumulated volume of the non-condensable gases, the slope of the curves are the generation rate of the non-condensable gases per unit time. The results of the slope calculations show that the gas generation rate was the lowest for the 60 scale power output and the highest for the 100 scale power output. In other words,

the gas production rate also indicates the intensity of the random cracking during the plastic pyrolysis. Therefore, the heating rate has a positive relationship with the intensity of random cracking reactions.

From the temperature profiles shown in Figure 4-3, it is found that the space temperature inside the reactor reached a constant value towards the end of the pyrolysis process. In a similar way, the reactor wall temperature also approached a constant value towards the end of the pyrolysis process and the value of the constant wall temperature was also positively related to the power output. At the same ambient conditions, the constant wall temperature was 617, 680, and 800 ºC with power load setting at 60, 80, and 100, respectively.

**Table 4-1 Product distribution at different power output**

| Product (g) | Power output scale | | |
|---|---|---|---|
| | 100 | 80 | 60 |
| Oil | 2.08 | 3.5 | 4 |
| Gas* | 5.86 | 3.49 | 1.87 |
| Gas volume (L) | 5.10 | 3.30 | 1.67 |
| Char | 1.22 | 1.28 | 1.3 |
| Wax | 0.84 | 1.73 | 2.83 |
| Total | 10 | 10 | 10 |

Note that: * the mass of gas product is a calculated from mass balances based on other collected products and the total mass of the feedstock.

The non-condensable gas and liquid products collected are given in Table 4-1. In addition to the gas and liquid, wax product was also found in the combustion boat (at the two end zones) after the plastic pyrolysis was completed. The quantity of the wax

collected was more for lower heating rate test and less for the high heating rate test. The explanation for this is that at high temperatures, wax initially condensed at the ends was further cracked and vaporized into gas and liquid products. Therefore, the run with maximum power output has the highest proportion of gas product and the lowest proportion of wax. (Table 4-1) The gas production and the wax production have a reverse proportional relationship.

In the plastic pyrolysis, char product was also found accumulating near the two dams in the combustion boat which was mainly from the labelling in the waste plastic. (Figure 4-6) According to other study, slow pyrolysis promotes char production. [47] The heat from the bottom of the combustion boat was conducted to the dams, which created slow pyrolysis zones. This can be confirmed by the observation that the char was found on both sides of the dam but was not found at the centre of the combustion boat. It is interesting to note that some small quantity of char was found in the end zones of the combustion boat near the dams which indicates that secondary cracking of the condensed wax would also produce some char in addition to gas and light liquid. The char could have effect on the heat transfer of the combustion boat.

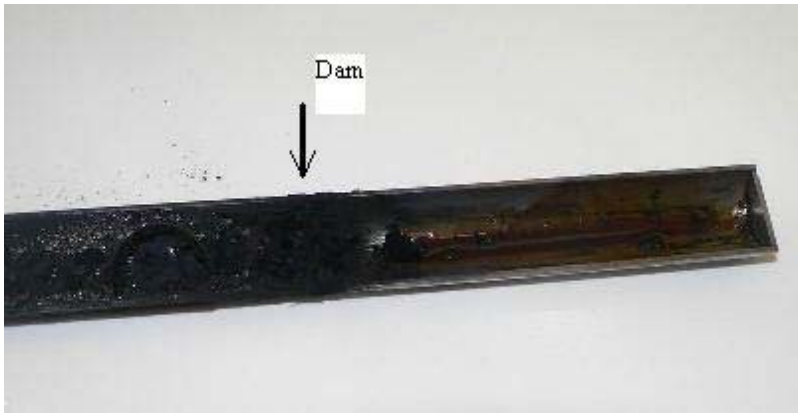


**Figure 4-6 Char accumulated on both sides of a dam in the combustion boat**

In order to avoid wax accumulation and char production inside the pyrolysis reactor, the reactor was later modified and reinstalled vertically, and this will be discussed in the following chapter of this thesis.

At the beginning of the pyrolysis reactions, the curves of non-condensable gas volume in the three runs increased with various slopes. This phenomenon may be due to the heterogeneity nature of the plastic mixture because PE, PP, and PS has different thermal properties and produces different pyrolysis products. In order to identify the process and the products precisely for each type of the plastics, further investigation was performed for pyrolysis of individual type of plastics and this will be described in next chapter.

### 4.2.3. Conclusions

Non-condensable gas, oil, wax, and char were the final products in the pyrolysis of waste plastic. From this part of study, it was concluded that the rapid production of non-condensable gases were generated from random cracking at the beginning of the pyrolysis. Heating rate has a positive relationship with the intensity of random cracking reactions thus more non-condensable gas, less liquid oil and less wax were produced with higher heating rate pyrolysis. The heating rate does not significant affect the char production although the char content tended to be less with high heating rate.

The temperatures measured at the reactor wall and in the inside space were both affected by the heating rate in the plastic pyrolysis. Both temperatures were higher for higher heating rate, which promotes further cracking of the wax and produces lighter hydrocarbons. Due to the variations in the reactor, the plastic cracking first occurred at the hottest spots which temperature would be close to but lower than the reactor wall temperature. Space temperature can be used as an indicator as the temperature of outflow vapour from the reactor.

The current batch pyrolysis system has shown the wax condensation near the ends of the reactor thus it was modified and installed vertically. This new reactor will be used to investigate the pyrolysis process of individual types of plastics and to examine the effects of other operation parameters. This will be discussed in the following chapter.

# 5. Pyrolysis of Polyethylene and effects of reflux and catalysts

## *5.1. Pyrolysis of Polyethylene*

### 5.1.1. Materials and apparatus

As different types of plastics behave differently in pyrolysis process, the major three types of plastic, polyethylene (PE), polypropylene (PP) and polystyrene (PS) were investigated on the batch pyrolysis apparatus. The plastics used in this series of experiments were virgin plastic particles for the fundamental investigations thus the material variability can be eliminated. All of these particles were granular particles with dimensions of approximately 3 mm long and 3 mm wide. (Figure 5-1) This chapter will discuss the pyrolysis of low density polyethylene (LDPE) with high density polyethylene (HDPE) is also pyrolyzed for comparison studies. In this chapter, effects of catalyst and reflux distillation are also presented.


**Figure 5-1 Virgin LDPE feedstock**

The low density polyethylene particles were produced by the state-of-the-art DSM Stamicarbon tubular process for blown film process. The chemical and physical properties of the LDPE were provided by PETLIN (Malaysia) Sdn Bhd. (Table 5-1)

**Table 5-1 Physical and chemical properties of LDPE (LD N103X)**

| Properties | Units | Typical values | Test methods |
|---|---|---|---|
| Relative density | $kg/m^3$ | 921 | ISO 1183 (A) |
| Bulk density | $kg/m^3$ | 590 | - |
| Melting point | ºC | 110 | DIN 53765 |
| Softening point | ºC | 91 | ISO 306 |
| Modulus of elasticity TD | $N/mm^2$ | 260 | ISO R527-3 |

In the experiments of this chapter and next chapter, the pyrolysis apparatus was modified to a vertical pyrolysis reactor in order to control the wax and to generate a distillation zone above the pyrolysis reactor. The modified apparatus is shown in Figure 5-2, which consists of three major components: a furnace, a reactor with a distillation pipe and a condenser. The pyrolysis reactor and the distillation pipe are connected together and became two functional zones: the bottom zone for the pyrolysis and the top zone above the furnace for the distillation. The reflux rate in the distillation zone can be adjusted by changing the length of the pipe which is naturally cooled by the ambient air around the top part. Three different pipes were used which had lengths of 380 mm, 280 mm and 200 mm, respectively, corresponding to high, medium and low reflux rates in the pyrolysis tests. With high reflux rate in the process, the residence time of the heavy products will be longer than that with low reflux rate process.

Three thermowells were mounted on the apparatus for installing thermal couples. (Figure 5-2) Thermal couple 1 ($T_1$) is for measuring the space temperature over the

pyrolysis reactor and below the distillation zone. The thermocouple locates 200mm below the top of the reactor pipe. Thermocouple 2 ($T_2$) is located at the entrance of the condenser that also is the outlet of the distillation zone, which measured the temperature of the product flowing out of the distillation zone and into the condenser. Thermocouple 3 ($T_3$) was inserted from the bottom of the furnace and fitted on the outer wall surface of the reactor, which measured the reactor outer wall surface temperature. As the temperature gradient from the outer wall to the inner wall (3 mm thick) is insignificant, the temperature measured by $T_3$ can be regarded as the temperature of the reactor inner surface which is also close to the temperature of the feedstock in contact with the reactor wall.

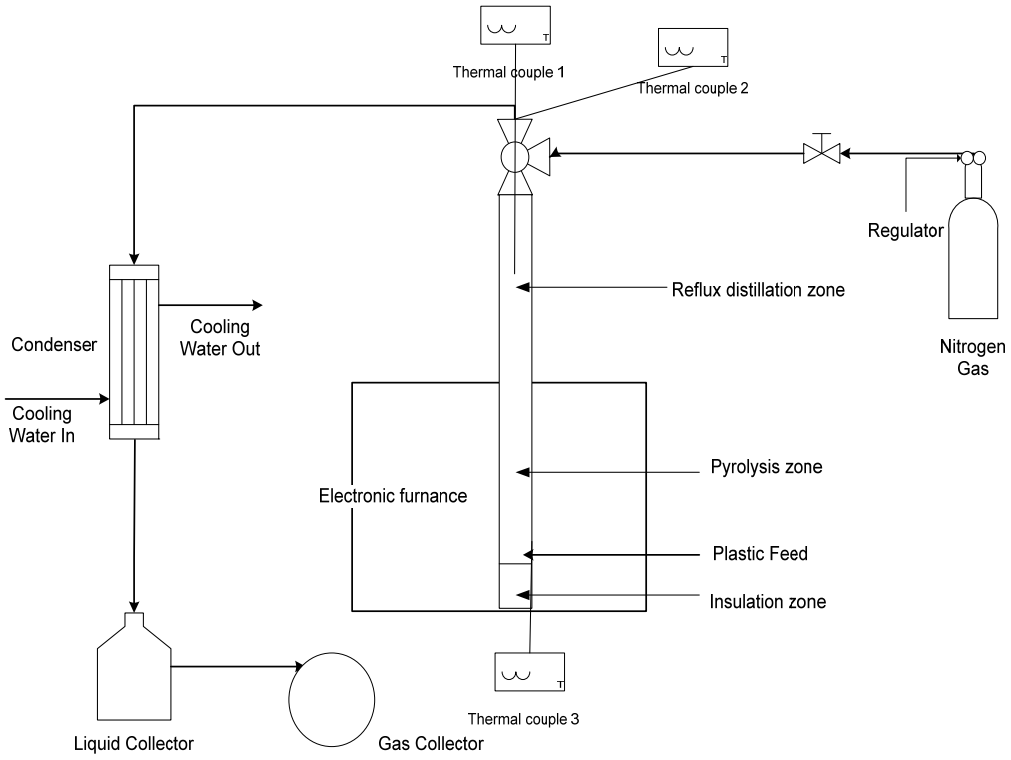


**Figure 5-2** Scheme of the vertical pyrolysis apparatus

In the experiment apparatus, a M303PY Gallenkamp electronic furnace was used to heat the reactor as an external heating resource. In the modified system, a 60 mm long stainless steel pipe was placed beneath the reactor pipe thus the reactor is located at the

hottest position within the furnace. [12] In this way, char production is minimized by avoiding the relatively slow pyrolysis in the low temperature zone. In addition, the bottom empty 60 mm long pipe also reduced heat loss from the reactor.

In the experimental system, nitrogen bottle supplied the pure nitrogen to purge the air out of the system before the experiment started. The condenser is a tube-shell heat exchanger where the pyrolysis gases flew inside the tube and cooling water flew between the tube and the shell. The cooling water was directly from tape at a temperature of 10 to 15 ºC. The condenser was effective enough to drop the temperature of the pyrolysis product to less than 30 ºC. The temperature in the laboratory room was 15 ºC. After the condenser, liquid and non-condensable gases were separated in a two-way beaker in which the liquid was collected and weighed after each run of the experiment. The non-condensable gases which were cooled down to less than 30 ºC in the condenser were then collected by a water sealed cylinder which measured the volume continuously during the experiment. After the experiment, the non-condensable gases were collected by a balloon with an inner aluminium layer for gas analysis.

The non-condensable gases from the experiment were analysed using Agilent 3000A Micro Gas Chromatography (Micro-GC) which has two columns (A and B), thus, two streams of gases can be analysed simultaneously. (Figure 5-3) Column A used argon as a carrier gas, which measured hydrogen and relatively heavy hydrocarbon gases. In column B, helium was used as the carrier gas to measure nitrogen, oxygen, carbon monoxide, carbon dioxide and methane.

Liquid products were analyzed using a Varian Gas Chromatography (GC) CP-3800. (Figure 5-4) The column applied was a Varian CP-SIL capillary column of 15 mm long and 0.32 mm in diameter with 1 μm wall thickness and wax coating on the inner wall surface. This column was able to identify hydrocarbons from C5 to C45. An alkane standard mixture supplied by Sigma-Aldrich was used for the assay of the GC's performance. The standard mixture contained all even n-alkanes from C10 to C40 with

50 mg/L in n-heptane. The liquid samples were also analyzed by using Gas Chromatography-Mass Spectrometry (GC-MS) at Hill Laboratories, Hamilton, New Zealand.

**Figure 5-3 Agilent 3000A Micro Gas Chromatography**

**Figure 5-4 Varian Gas Chromatography CP-3800**

Microstructure of the char produced from the plastic pyrolysis process was analyzed by using JEOL JSM 7000F high resolution scanning electron microscope (SEM) at the Department of Mechanical Engineering, University of Canterbury. (Figure 5-5) Element analysis in the scanning electron microscope and electron microprobe is performed by measuring the energy and the intensity distribution of the X-ray signal generated by a focused electron beam. When the electrons strike the sample, a variety of signals are

generated, and it is the detection of specific signals which produces an image or a sample's elemental composition. [110] Standardless ZAF method was applied for SEM-EDS (scanning electron microscope and energy-dispersive x-ray spectrometer).

**Figure 5-5 JEOL JSM 7000F high resolution scanning electron microscope**

### 5.1.2. Experiment method

At the beginning of the experiment, 20 grams of the LDPE particles were weighed using a four decimal place Mettler AE 200 balance and were filled into the pyrolysis reactor. Then, the system was sealed and purged using the nitrogen gas for one minute to create an oxygen free environment. After this, the furnace was turned on to full capacity with control scale at 100, equivalent to heating power of 881 W. During the experiment, three temperatures ($T_1$, $T_2$ and $T_3$) and the volume of the collected non-condensable gases were recorded every minute until temperature $T_3$ rose above 800 ºC when no product was left in the reactor. In order to investigate further cracking of the heavy pyrolysis product, three lengths of the distillation pipes (380 mm, 280 mm and 200 mm) were used separately in the experiments. The extra length above the furnace is cooled by the ambient air. Longer length of the reactor pipe leads to higher efficiency of condensation and higher reflux rate. In this section, only the results of high and low

reflux tests (using 380 mm and 200 mm distillation pipes) are reported while the effects of the reflux distillation will be discussed in the following section.

The collected liquid, non-condensable gases and char were collected and analysed. The non-condensable gases were analyzed by using Agilent 3000A Micro Gas Chromatography (Micro GC). In the gas analysis, both of the columns A and B were set at 90 ºC in the Micro GC. The injector temperature was set at 95 ºC. (Table 5-2) The run time of column A is four minutes and that of column B is 10 minutes. This time setting allows hydrocarbon gases with the retention time less than n-butane to come out, such as hydrocarbons from $C_1$ to $C_3$ and butene and butane isomers. Some of the gases were identified by running a gas standard with this method. (Table 5-3)

**Table 5-2 Micro GC set points and configuration**

| Micro GC Setpoints | A | B |
|---|---|---|
| Sample Inlet Temperature (°C) | 95 | 95 |
| Injector Temperature (°C) | 95 | 95 |
| Column Temperature (°C) | 90 | 90 |
| Sampling Time (s) | 15 | 15 |
| Inject Time (ms) | 10 | 15 |
| Run Time (s) | 240 | 600 |
| Post Run Time (s) | 120 | 60 |
| Pressure Equilibration Time (s) | 15 | 60 |
| Column Pressure (kPa) | 206.8 | 137.5 |
| Post Run Pressure (kPa) | 275.8 | 137.5 |
| Detector Filament | Enabled | Enabled |
| Detector Sensitivity | Standard | Standard |
| Detector Data Rate (Hz) | 20 | 20 |
| Baseline Offset (mV) | 0 | 0 |
| Backflush Time (s) | 15.0 | n/a |

| Table 5-2 Micro GC set points and configuration (Continued) | | |
|---|---|---|
| Injector Type | Backflush | Fixed Volume |
| Carrier Gas | Argon | Helium |
| Column Type | Molecular Sieve | Plot Q |
| Detector Type | TCD | TCD |
| Inlet Type | Heated | Heated |

**Table 5-3 Calibration table**

| Peak Name | Retention Time (min) |
|---|---|
| Hydrogen | 0.462 |
| Oxygen | 0.610 |
| Nitrogen | 0.777 |
| Methane | 0.876 |
| CO2 | 0.955 |
| Ethene | 1.099 |
| Methane | 1.139 |
| Ethane | 1.203 |
| CO | 1.340 |
| propane | 2.430 |
| butane | 7.561 |

The oils from low reflux rate process contained heavy molecular weight products and formed yellow cream; while the oils from high reflux rate process was clear liquid. (Figure 5-6) The cream product from low reflux rate process turned into clear liquid

when it was heated to 60ºC. The melted cream was able to be sucked by a one micro litre GC syringe for GC CP-3800 analysis injection.

**Figure 5-6 Oil product from low (left) and high (right) reflux processes.**

In the liquid oil analysis, the liquid was firstly flash-vaporized at 320ºC when it was injected into the GC. Then the vapour flew through the column which temperature was initially controlled at 80ºC for two minutes. After this, the column temperature was increased to 300ºC at a heating rate of 10ºC/min. The temperature remained at 300 ºC until no further peaks were observed. The total analysis time for the high reflux liquid product was 60 minutes and that for the low reflux product was 150 minutes. The GC allowed the hydrocarbons with carbon number between 7 and 40 to be separated and analyzed. In the analysis, the concentration of the liquid components was presented as molar percentage.

Char from the LDPE pyrolysis were found at the bottom of the reactor, which were black fine powder and particles. The char microstructure was analyzed by using the JEOL JSM 7000F electron microscope.

In the experiments, HDPE was also used for pyrolysis; however, it was found that the process and products from the HDPE pyrolysis were identical to those of LDPE pyrolysis. Therefore, this thesis only presents the results of the LDPE pyrolysis.

### 5.1.3. Results and discussion

Process analysis

During the pyrolysis experiments, the space temperature in the reactor ($T_1$), the reactor outer wall surface temperature ($T_3$) and the volume of the non-condensable gases were recorded every minute and the results are shown in Figure 5-7 for LDPE and in Figure 5-8 for HDPE. Both figures show the pyrolysis with high reflux rates. From the results of temperature profiles and non-condensable gas generation, the whole pyrolysis process can be divided into three stages: initial heating up stage (initial 18 minutes), fast pyrolysis stage (18 to 34 minutes) and decreasing pyrolysis stage (after 34 minutes). In the heating up stage, the space temperature ($T_3$) remained low until about 18 minutes when no non-condensable gases were generated. However, the reactor wall temperature continued increasing during the heating up stage.

After about 18 minutes, the generation of non-condensable gases increased dramatically and the space temperature kept increasing. However, the temperature on the reactor wall surface stopped rising one minute after the massive non-condensable gases produced and then remained almost constant for about 16 minutes. As discussed in previous chapters, the initial gas production rate indicates the random cracking in the early fast pyrolysis stage. However, from the previous analysis, the energy required for the cracking reaction is not large; therefore, significant amount of energy must have been consumed in somewhere else as the reactor outer wall surface temperature remained constant indicating constant heat transfer rate from the furnace to the reactor. In this stage, the vapour from the primary cracking went up into the distillation zone, then, were condensed and refluxed back to the pyrolysis zone. This process of condensation and re-cracking consumed a significant amount of heat which was carried up by the vapour from the pyrolysis zone to the distillation zone. Therefore, it has been observed that reactor space temperature ($T_1$) increased but reactor wall temperature ($T_3$) remained constant after 18 minutes from the start. Through this reflux process, low boiling point products flew gradually into the condenser.

In the final termination pyrolysis stage, less vapour was produced and less energy was required thus the reactor wall temperature ($T_3$) started increasing again. The high boiling point hydrocarbons were further pyrolyzed (secondary cracking) when the reaction surface temperature rose above 500 ºC. This secondary cracking was indicated through the second rapid increase on the gas production curve. (Figure 5-7) However, the less high boiling point vapour was produced in this stage; the total vapour product from the pyrolysis zone was reduced although the non-condensable gases kept increasing as less condensate must have been generated at this time. This resulted in a decrease in the reactor space temperature.

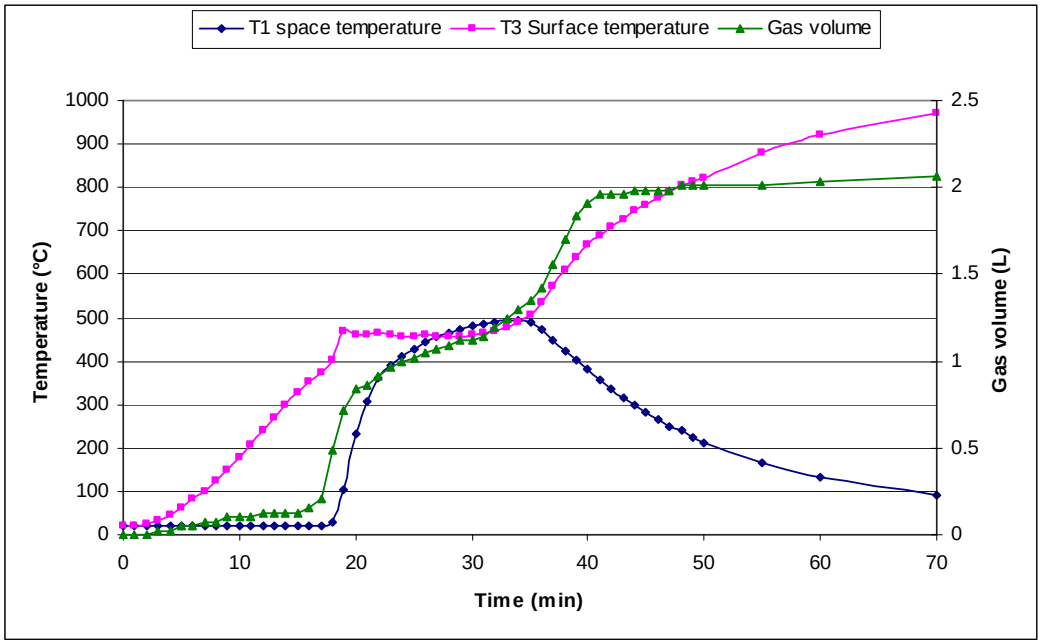


**Figure 5-7 High reflux rate LDPE pyrolysis process**

In the low reflux rate pyrolysis, the secondary cracking was less intensive than the high reflux rate pyrolysis, thus higher boiling point hydrocarbons were generated as liquid product. Higher boiling point hydrocarbons have higher viscosity than that of lower boiling point hydrocarbons; [104] therefore, the viscosity of the liquid product from low reflux rate process is higher. (Figure 5-6) the effect of reflux distillation on the product distribution was further investigated in the following experiments. (Section 5.2)

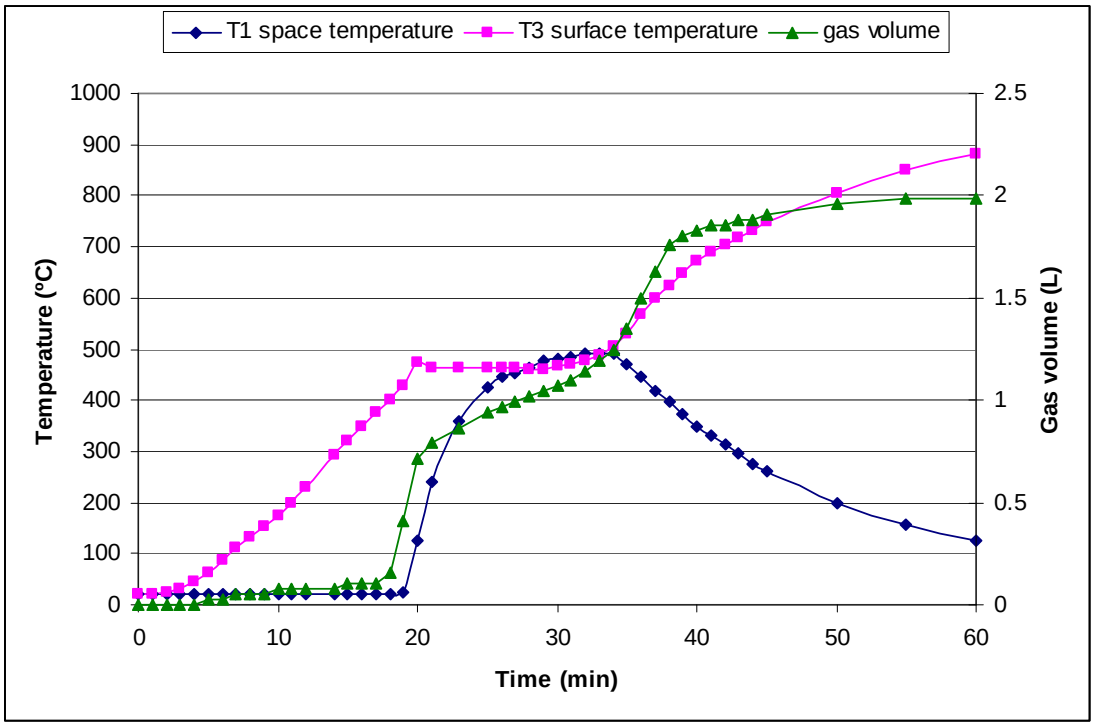


**Figure 5-8 High reflux rate process pyrolysis on HDPE**

The temperature profiles of high reflux rate HDPE process are listed in Figure 5-8. There was no significant difference in the pyrolyzing process between HDPE and LDPE. The temperature profile and non-condensable gas production are identical between pyrolysis of LDPE and pyrolysis of HDPE indicating similar cracking processes. Both of the LDPE and HDPE underwent secondary cracking when the low boiling point hydrocarbons were removed. Because of the above similarity and the higher value potential for recycled HDPE to be used in other products, LDPE is the most suitable for energy production using the waste plastic stream. [7-8] Therefore, LDPE was intensively studied in this study as a typical polyethylene material.

The results of product distribution of high reflux rate process LDPE pyrolysis are given in Table 5-4 from the results, it can be seen that the conversion of LDPE to hydrocarbons was over 99% and very little char was produced in the experiment as fine black powers and particles found at the bottom of the reactor. The high reflux rate

process experiments were repeated five times. The 95% confidence interval of the oil/wax mass was calculated, $16.7 \pm 0.1$ g.

**Table 5-4 Product distribution**

| | LDPE | | HDPE | |
|---|---|---|---|---|
| Product | Mass (g) | Percentage | Mass (g) | Percentage |
| Oil/wax | 16.6 | 83% | 16.7 | 83.5% |
| Char | 0.04 | < 1% | 0.03 | < 1% |
| Gas (estimated)* | 3.4* | 17% | 3.3* | 16 % |

*Note: The volume of collected LDPE gas was 2.03 L. The average molecular weight of the LDPE gases was calculated to be 38g/mol or 3.4g. The mass of HDPE gases was calculated from the difference between the mass of the feedstock and the oil and char products.

Non-condensable gas analysis

A typical Micro-GC analysis result for the non-condensable gases is shown in Figure 5-9 with the top chart from Column A and bottom chart from Column B. By integrating each peak through the GC program, the composition of the corresponding gas species was determined and the results from Figure 5-9 are given in Table 5-5. In Table 5-5, 'Norm%' is the normal percentage of a component in the gas sample. From the above results, it is known that the non-condensable gases consisted of oxygen ($O_2$), nitrogen ($N_2$), methane ($CH_4$), ethene ($C_2H_4$), ethane ($C_2H_6$), propane ($C_3H_8$), butane ($C_4H_{10}$) and other four unidentified species (peak6, peak 8, peak 13 and peak 23). The oxygen, carbon dioxide and some nitrogen gases were likely to be from contamination of air during the gas sampling and sample collection process. The remaining nitrogen is believed to be due to the purge gas left in the system. There were four peaks (peaks 6, 8, 13, and 23) in the GC analysis chart which needed to be identified from further analysis.

(Table 5-5, Figure 5-9) According to the result, methane, ethene, ethane, peak8, propane, peak13, and butane are the major components in the non-condensable gases from LDPE pyrolysis. The retention time of peak 8 was between propane and ethane; therefore, peak 8 was believed to be propene. Peak 13 could be one of butene and butane isomers, which would come out between propane and n-butane. [65] According to liquid product analysis and other identified gas species, it was most likely to be 1-butene because most of 1-alkene could be generated in the β-scission reactions. [52, 83, 97] The 1-butene was also identified by other researchers. [32, 51, 58, 79, 83, 88, 111-112] There was no $H_2$ detected in the gases. The hydrogen free radicals generated from initiation reactions may combine with alkenes and saturate the carbon double bonds. This has not been proven yet.

**Table 5-5 Non-condensable gas analysis results for high reflux LDPE pyrolysis**

| Signal | Retention Time [min] | Type | Area [μV*s] | Amt/Area | Norm % | Name |
|---|---|---|---|---|---|---|
| 1 | 0.596 | BP | 2198.09077 | 0.00117 | 2.610804 | Oxygen |
| 1 | 0.701 | VB | 23255.41966 | 0.00146 | 34.382758 | Nitrogen |
| 1 | 1.049 | BB | 11120.81796 | 0.00059 | 6.620348 | Methane |
| 2 | 0.948 | BB | 13830.48370 | 0.00006 | 0.840056 | CO2 |
| 2 | 1.083 | BP | 185789.32495 | 0.00006 | 11.284737 | Ethene |
| 2 | 1.190 | VP | 112918.37224 | 0.00006 | 6.858597 | Ethane |
| 2 | 1.494 | BP | 15869.99013 | 0.00006 | 0.963934 | Peak6 |
| 2 | 2.196 | VV | 217008.82366 | 0.00006 | 13.180991 | Peak8 |
| 2 | 2.397 | VB | 148122.34698 | 0.00006 | 8.996866 | propane |
| 2 | 6.521 | BV | 123013.64673 | 0.00006 | 7.471778 | Peak13 |
| 2 | 7.477 | PB | 102309.27801 | 0.00006 | 6.214207 | butane |
| 2 | 8.326 | BB | 9465.42118 | 0.00006 | 0.574924 | Peak23 |

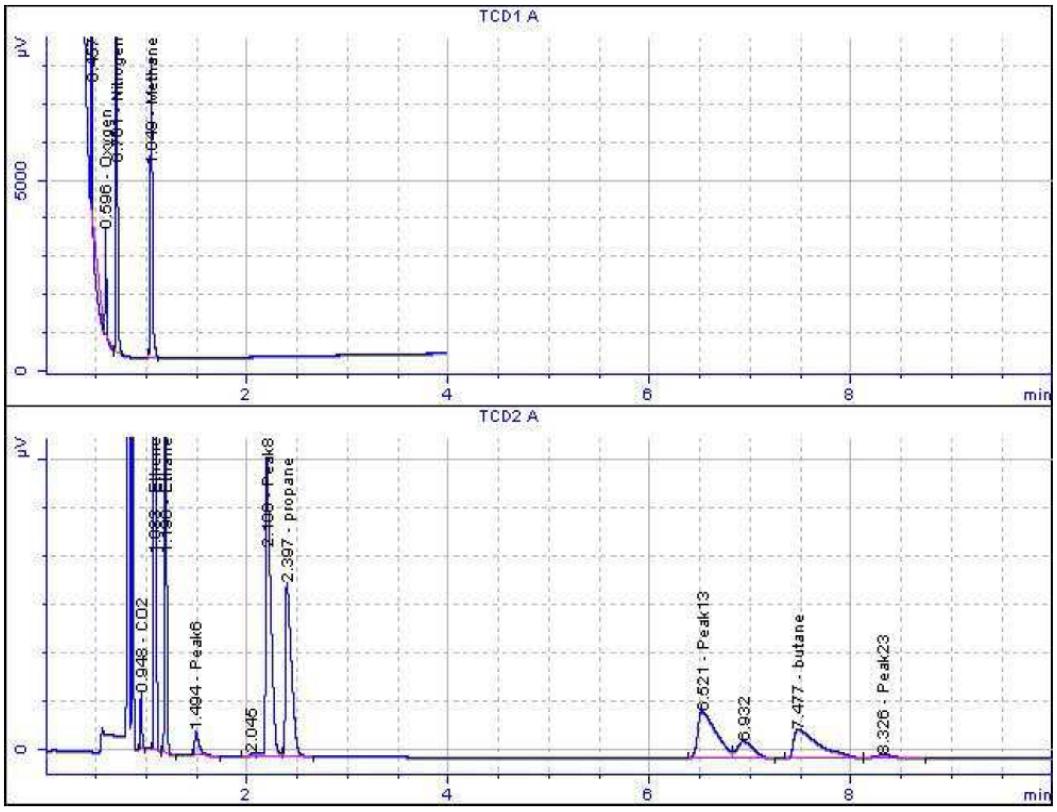


**Figure 5-9 Micro GC analysis chart for non-condensable gases from pyrolysis of LDPE with high reflux rate; column A (top), column B (bottom)**

The proportion of $C_1$, $C_2$, $C_3$, and $C_4$ are 12.2%, 32.0%, 34.7%, and 21.1%; respectively. 44% of the gas products are n-alkane. The rest should be alkenes and alkane isomers. The average molecular weight of the LDPE pyrolysis gases was calculated based on its distribution. (Table 5-6) Therefore, the average molecular weight of the gas product is 38g/mol. The distribution of the gas product also varies with the variation of reaction conditions. The difference of the gas products from the primary cracking and the secondary cracking reaction was also investigated.

**Table 5-6 Non-condensable gas distribution and its average molecular weight**

| Component | Norm% | Corrected | Carbon number | Percentage | Average MW |
|---|---|---|---|---|---|
| Methane | 6.53 | 12.2% | C1 | 12.2% | 16 |
| Ethene | 11.26 | 21.1% | | | |
| Ethane | 5.87 | 11.0% | C2 | 32.0% | 29 |
| peak6 | 0.70 | 1.3% | | | |
| peak7 | 0.12 | 0.2% | | | |
| peak8 | 11.32 | 21.2% | | | |
| Propane | 6.42 | 12.0% | C3 | 34.7% | 42* |
| peak13 | 6.14 | 11.5% | | | |
| Butane | 4.74 | 8.9% | | | |
| peak23 | 0.38 | 0.7% | C4 | 21.1% | 56* |
| Total | | 100.0% | | 100.0% | 38 |

*Note that: Peak8 and peak13 components are assumed to be propene and 1-butene, respectively. Contaminated gases and very minor gas species are ignored.

Char product analysis

Char was analyzed through the JEOL JSM 7000F SEM-EDS in the Department of Mechanical Engineering at University of Canterbury. The SEM image of the char is shown in Figure 5-10 and the chemical elements in the char are given in Table 5-6. It was found that the char contained 92.88% solid carbon, 6.18% oxygen, 0.86% calcium and very tiny proportion of silica (0.08%). (Table 5-7) However, these values are only used for indication due to the data scattering ($R^2$=0.4474). This result was also in consistent with the finding by Shah *et al.*. [42] From the SEM image, it can be observed that the char particles were attached to each other and adhesion was formed with rough surface. (Figure 5-10) The adhesion behaviour of the char particles at high temperature

could a potential problem for a continuous fix-bed reactor which would form fouling on the reactor surface.

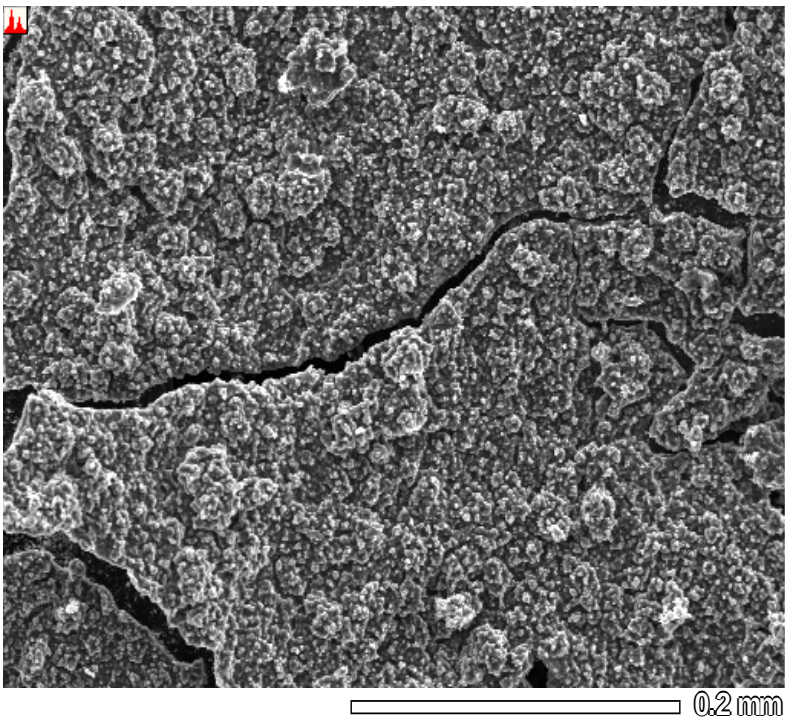


**Figure 5-10 Electron microscope photo of LDPE char surface**

**Table 5-7 ZAF Method Standardless Quantitative Analysis**

| Element | (keV) | mass% | Error% |
|---|---|---|---|
| C | 0.277 | 92.88 | 0.19 |
| O | 0.525 | 6.18 | 2.70 |
| Si | 1.739 | 0.08 | 0.82 |
| Ca | 3.690 | 0.86 | 1.89 |
| Total | | 100.00 | |

Note that: Fitting Coefficient 0.4474. The experimental error was significant; therefore, these numbers are not accurate.

### 5.1.4. Identification of the components in liquid product

The viscosity and colour of the LDPE pyrolysis oil varied with the pyrolysis condition as discussed in Section 5.1.2. It was clear yellow-brownish liquid from high reflux rate process but became creamy solid wax with low reflux rate process. (Figure 5-6) In analysis of the liquid product, a specially designed 1 µl GC syringe was used to transfer liquid product into the GC CP-3800. However, the syringe could only be used for liquid but not for wax. Therefore, in order for the wax to be sampled by this syringe, the wax was preheated to 60 ºC which turned into clear liquid for the GC analysis.

The GC analysis results for the LDPE pyrolysis liquid are shown in Figure 5-11 for high reflux rate (top) and low reflux rate (bottom). In total, 115 hydrocarbons were found in the high reflux process oil product and 121 peaks were detected in the low reflux rate pyrolysis. (Figure 5-11) The components from both the high and the low reflux rate processes had similar peak distribution in the first 60 minutes from the GC analysis. In the liquid from low reflux rate pyrolysis, the final 6 liquid peaks are high boiling point components ($C_{37}$ to $C_{42}$) which were not found in the high reflux process pyrolysis liquid product.

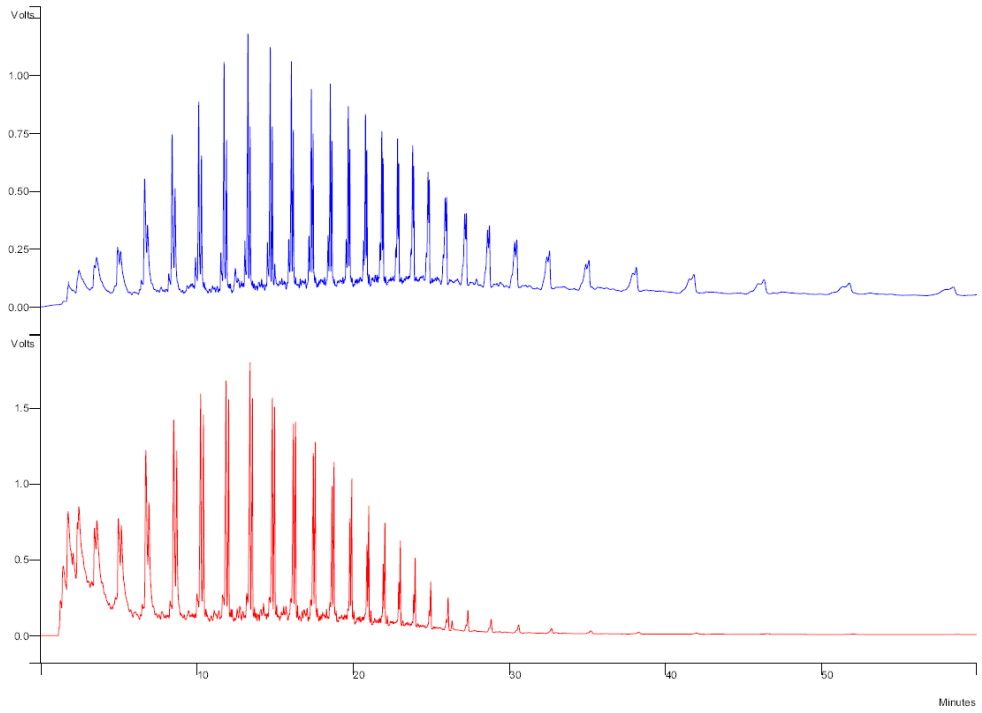


**Figure 5-11 Distribution of low (top) and high (bottom) reflux rate LDPE liquid pyrolysis products**

In the liquid product from the high reflux pyrolysis, the hydrocarbons chains ranged from $C_5$ to $C_{36}$ but those from the low reflux rate pyrolysis ranged from $C_5$ to $C_{42+}$. These results are in agreement with other studies. [18, 20, 27, 37, 49, 58, 60, 63, 86, 89, 98, 101, 103-106] Lee and Shin [50] found that the distribution of the oil product molecular weight ranges up to 500 which corresponds to $C_{40}$. The molecular weight of the major components is between 200 and 400, which is from $C_{14}$ up to $C_{30}$. Aguado *et al.* [29] found that the carbon chain length in the products is up to $C_{55}$.

From Figure 5-12, the components appeared on the GC analysis chart as peaks in sub-groups. Each sub-group consisted of a small peak in the front and two major peaks behind. (Figure 5-11) According to the literature review [28, 31, 87], the small peak in the front of each group is α, ω-dialkene. The following two peaks are 1-alkene and n-alkane, respectively, according to other studies. [58] This chromatogram obtained in this study is very similar to those obtained by other researchers. [27, 59, 88, 111-115] The oil products from both processes (high reflux and low reflux rate pyrolysis) had a normal distribution with the maximum peak value at the 13.4 minute ($C_{14}$ group). However, liquid from the high reflux rate pyrolysis contained lower proportion of the hydrocarbons with carbon chain length greater than 14 than that from the low reflux rate pyrolysis. On the other hand, the liquid from the high reflux rate pyrolysis contained lighter molecular weight hydrocarbons with carbon chain number less than 14 compared to that from the low reflux pyrolysis. (Figure 5-11) The heavy hydrocarbons with carbon number greater than 36 do not appear in the high reflux process product. This was due to the effect of secondary cracking of the liquid products, which was caused by the difference of reflux rates in the pyrolysis.

In order to identify the two major components in each sub-group, the liquid oil generated from the LDPE pyrolysis was firstly diluted in n-hexane with a ratio of 1:1000. Then, 1% v/v 1-Cetene (1-$C_{16}$) and 1% v/v n-Cetane (n-$C_{16}$) were added into the diluted oil, respectively. The GC results for these new samples are shown in Figure 5-12 with comparison with the only diluted oil. In theory, by adding known components in the liquid, the GC chromatogram will show a clear increase for the peaks of added

components. On the word, the increased peaks are the known components. From the results shown in Figure 5-12, 1-$C_{16}$ and n-$C_{16}$ were identified on the sample GC analysis graph, which appeared at the 16$^{th}$ minute on the graph. The $C_{16}$ group is the group with a clearly increased peak in the graph. (Figure 5-12 middle and bottom graphs) Therefore, it is determined that the front major peak in the group is 1-alkene and the second major peak is n-alkane. This technique was applied on all groups in the LDPE liquid product and thus the corresponding hydrocarbons were identified.

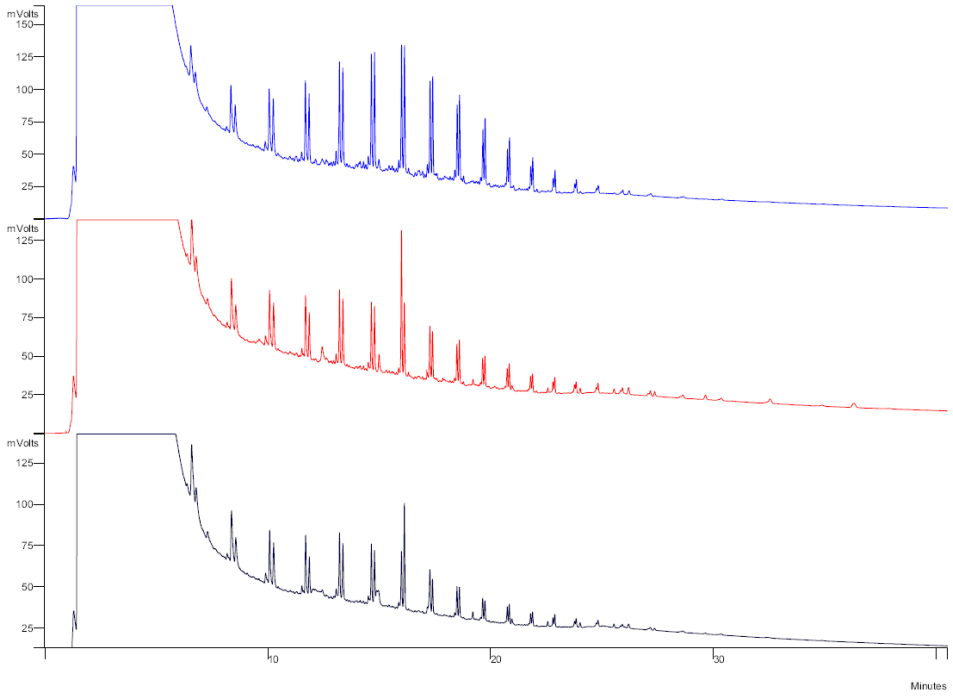


**Figure 5-12 Comparison of LDPE liquid sample (top) and the liquid with additive 1-$C_{16}$ (middle) and n-$C_{16}$ (bottom)**

Once a specific carbon number is known ($C_{16}$), other hydrocarbons with different carbon numbers can be determined by comparing the LDPE sample with a standard hydrocarbon mixture that consisted of even carbon number n-alkane from $C_{10}$ to $C_{40}$. (Figure 5-13 middle graph) Each component in the hydrocarbon standard was 50mg and diluted in n-heptane to 10ml. The correspondent even carbon number n-alkane peaks were increased when the LDPE product was mixed with the standard. (Figure 5-13 bottom graph) Therefore, the increased peaks were the even carbon number n-alkanes. As the increased peak at the 16$^{th}$ minute was initially identified to be n-$C_{16.}$, other peaks were thus determined based on these two experimental results.

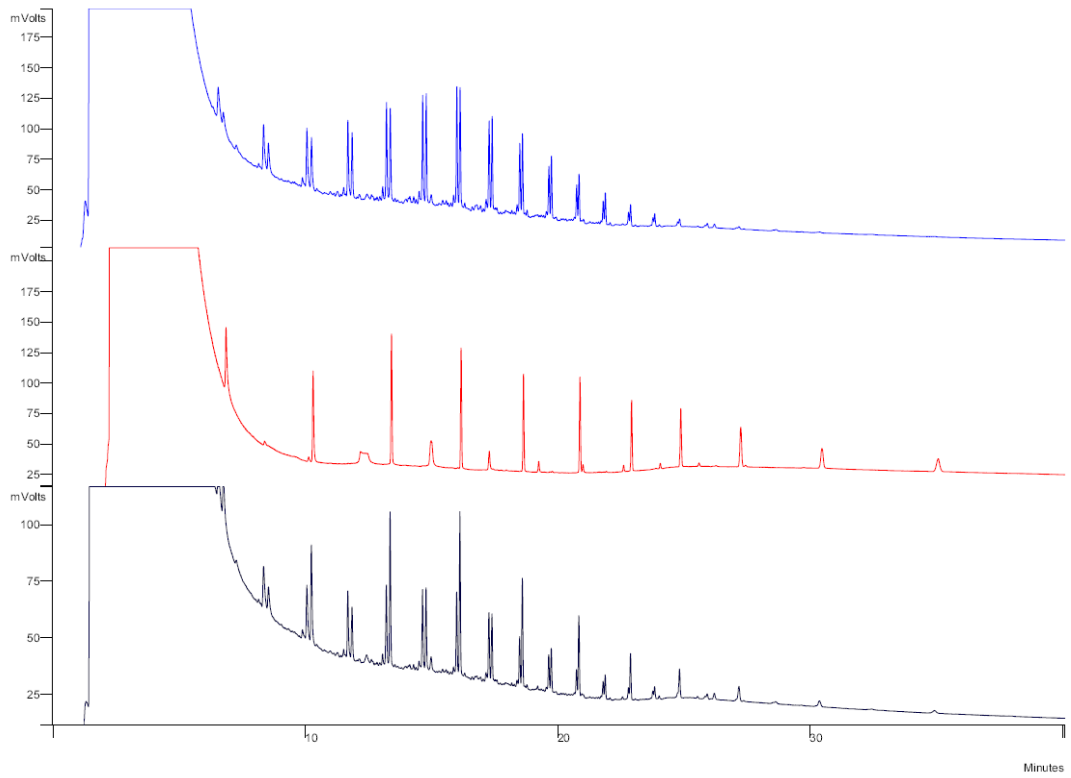


**Figure 5-13 Comparison of LDPE liquid sample (top) and hydrocarbon standards (middle and bottom)**

The liquid sample was also analyzed by GC-MS. The results from the GC-MS analysis clearly illustrated the carbon number in each hydrocarbon group. (Figure 5-14) However, it did not separate the 1-alkene and the n-alkane peaks adequately. The hydrocarbons with significant concentration were detected up to $C_{30}$ in the solution. The carbon number of each group is shown in Figure 5-14. The result on the individual component was not applied because the 1-alkene and the n-alkane peaks were overlapping each other.

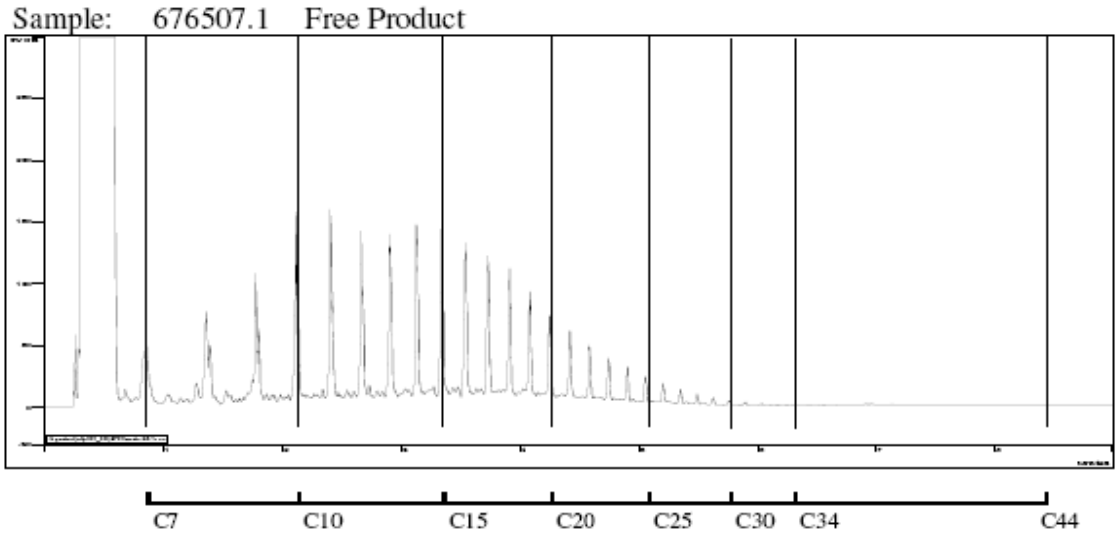


**Figure 5-14 GC-MS analysis on LDPE sample diluted in n-pentane**

### 5.1.5. Conclusions

PE is one of the most commonly used plastic materials. According to the pyrolysis processes and the product distribution, there is no significant difference between LDPE and HDPE, therefore, LDPE was extensively investigated and reported in this chapter of the thesis. The LDPE products consist of non-condensable gases, liquid or wax hydrocarbons, and char. The proportion of each product can be changed by changing the reaction conditions.

From this study, it is found that the product distribution was significantly influenced by reflux rate in the pyrolysis process. The products consisted of 83% oil/wax, 16% of non-condensable gases, and less than 1% char with high reflux rate pyrolysis. In the high reflux rate pyrolysis, heavy molecular weight hydrocarbons were refluxed into the pyrolysis zone and were further pyrolyzed into lighter hydrocarbons such as non-condensable gases and light liquid oil. Intensive secondary pyrolysis reaction was observed in the high reflux rate process. The char product was largely solid carbon with a small proportion of silica and calcium oxides.

The non-condensable gases ($C_1$ to $C_4$), oil and wax ($C_{5+}$) were analysed to be hydrocarbons with carbon chain number ranged from $C_1$ to $C_{42+}$. The hydrocarbons with the same carbon chain number were grouped together on the chromatogram and the highest concentration for the liquid product had a peak value of at the $C_{14}$ group. (Figure 5-11) In order to determine the sub-group peaks, an innovative method was developed by diluting the sample and adding standard liquid with known carbon numbers. It was identified that the front major peak is 1-alkene and the other major peak is n-alkane in each group, respectively.

The influence of reflux rate on the products is very significant. In the high reflux rate pyrolysis, hydrocarbons above $C_{36}$ were further pyrolyzed thus was not found in the liquid product. However, a significant amount of heavy hydrocarbons above $C_{36}$ were found the in the low reflux rate pyrolysis. The components in the liquid were also analyzed though GC-MS but the GC-MS method could not distinguish individual peaks in each sub-group. The effects of reflux rate and secondary cracking reactions on the products were further investigated in the following section.

## 5.2. Effects of reflux distillation

Based on the previous experiments, it was found that the reflux distillation has significant effect on the pyrolysis process and the products. Secondary cracking reactions on the heavy molecular weight hydrocarbons occurred when light hydrocarbons were removed from the pyrolysis reactor. These reactions converted the proportion of heavy molecular weight hydrocarbons into light molecular weight hydrocarbons. The effect of different reflux rates on the product and the process was further investigated in this series of experiments.

### 5.2.1. Experiments

The material used in this experiment was also virgin LDPE particles which were the same as the material specified in the previous section. (Section 5.1.1) The pyrolysis apparatus was also the same as used in Section 5.1. (Figure 5-2) Three different lengths of pyrolysis pipes, 200 mm 280 mm, and 380 mm, were applied in these experiments, representing low, medium and high reflux rates, respectively. In each experiment run, 20 grams LDPE was placed in the pipes at the beginning and the same experimental procedures as described in the previous section were followed. In the experiment, the temperatures in the reactor space ($T_1$), at outlet of the distillation pipe of the entrance of the condenser ($T_2$) and at the reactor wall outer surface ($T_3$). The non-condensable gas volume was measured during the experiment and collected after the experiment. Liquid product and char were also collected after each run of the experiment. The products of gas and liquid were analysed using the same methods as described in Section 5.1.1. .

### 5.2.2. Result and discussion

Effects of reflux rate on the pyrolysis process

For understanding of the pyrolysis process, temperatures at outer surface of the reactor wall ($T_3$) were firstly examined for high reflux rate, low reflux rate and for empty reactor run when the pyrolysis apparatus was tested without plastic in it. As discussed previously, the outer surface temperature ($T_3$) is close to the inner surface temperature thus it indicates the temperature profile of the internal reaction surface of the pyrolysis

reactor. The $T_3$ profile measured with the empty reactor can be used as a baseline of the temperature change to examine the effect of the filled plastics and reflux rate on the pyrolysis process as shown in Figure 5-15. From the profiles of $T_3$ of baseline, and pyrolysis with low and high reflux rates, it is found that these profiles were almost the same in the first 16 minutes from the start when the wall temperatures reached approximately 450°C. This result confirms that the heat consumed in this initial period was only for heating up of the reactor and the furnace and that the pyrolysis reaction had not occurred. However, after the 16$^{th}$ minutes, the $T_3$ profiles with LDPE in the reactor increased slower than the baseline, indicating the pyrolysis started occurring. This was apparent for the high reflux rate pyrolysis in which the wall temperature almost remained constant at 470 °C. When the wall temperatures rose to 500°C, they increased further at similar rate at the baseline.

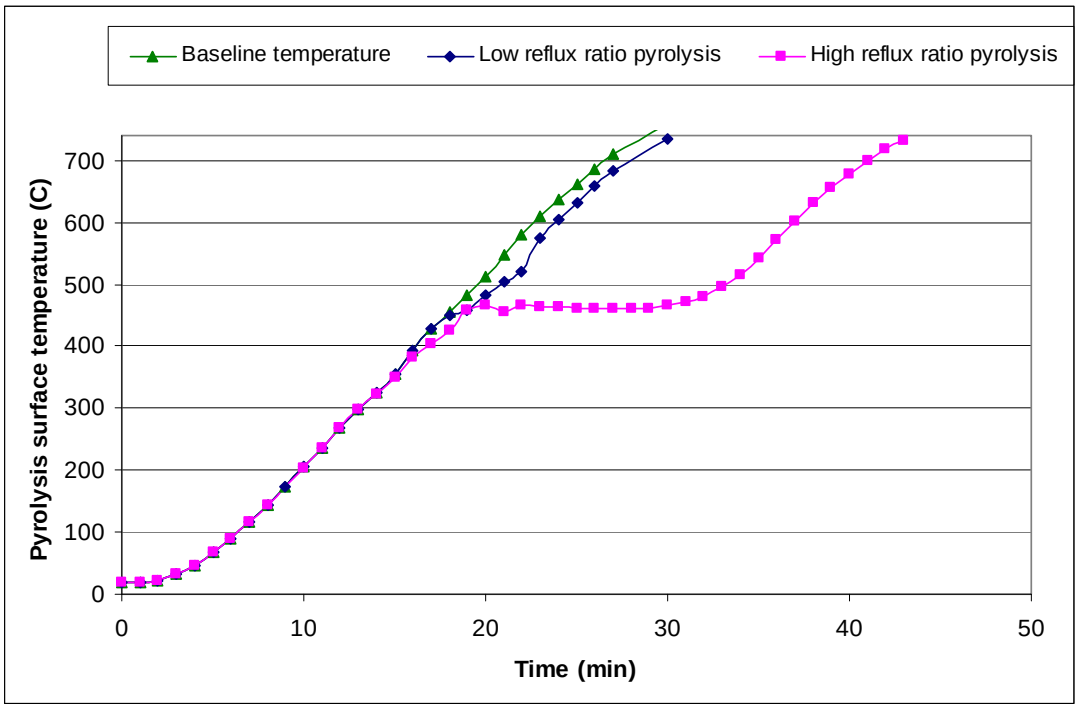


**Figure 5-15 Profiles of outer wall surface temperatures with empty reactor and during LDPE pyrolysis with low and high reflux rates**

For the low reflux rate pyrolysis, the wall temperature was only one minute apart from the baseline after the pyrolysis started; indicating that only the heat transferred in the

one minute was needed for the plastic pyrolysis reactions. From this finding, the energy consumed during the one minute can be calculated as the energy required for LDPE pyrolysis reactions including plastic cracking, vaporization and energy loss in reflux distillation. However, the pyrolysis with high reflux rate took much longer time and required more energy due to secondary cracking and heat loss in the distillation. According to the energy balance calculation in section 3.2.2 (Table 3-6 and equation 18), the energy required for LDPE pyrolysis and vaporization process is calculated in Table 5-8.

**Table 5-8 Energy balance of the 20g LDPE pyrolysis and vaporization**

| 20g LDPE | $C_3H_6$ | 1-$C_8H_{16}$ | 1-$C_{16}H_{32}$ | 1-$C_{28}H_{56}$ | Total |
|---|---|---|---|---|---|
| ΔHr, kJ/mol | 23.00 | 23.00 | 23.00 | 23.00 | |
| ΔH, kJ/mol | 24.12 | 72.32 | 163.34 | 304.12 | |
| $\Delta H_v$, kJ/mol | - | 33.76 | 50.42 | - | 181 |
| | | | | | |
| Low reflux products | 7% | 22% | 50% | 21% | 100% |
| mol of component | 0.033 | 0.039 | 0.044 | 0.011 | 0.128 |
| Energy required kJ | 1.57 | 5.09 | 10.51 | 3.54 | 20.71 |
| | | | | | |
| High reflux products | 15% | 31% | 44% | 11% | 100% |
| mol of component | 0.072 | 0.055 | 0.039 | 0.005 | 0.171 |
| Energy required, kJ | 3.39 | 7.08 | 9.22 | 1.77 | 21.45 |

Note: $\Delta H_r$ is the reaction enthalpy, which is calculated in Section 3.2.2; ΔH is the energy that increased the temperature of material from the initial status, $T_1$, to the final product status, $T_2$; $\Delta H_v$ is the vaporization heat of each component.

According to the results given in Table 5-8, the theoretical energy consumption for pyrolysis of the 20g LDPE varied from 20.71kJ for low reflux rate to 21.45kJ for high reflux rate based on product distribution.

The above theoretical energy consumption can be compared to the actual energy consumption based on the reactor outer wall temperatures. In the experiments, the total energy consumed consisted of both the energy for LDPE pyrolysis, vaporization, and the energy loss from reflux distillation. The output power of the furnace was 881 W. The difference between baseline curve and those of LDPE pyrolysis was used for determination of the energy consumption in the LDPE pyrolysis which is equal to the product of the furnace output power and the time difference to reach the same temperature by the end of the pyrolysis. As an example, the energy calculations for the low and the high reflux rate pyrolysis are listed below in which $E_{low}$ is the energy requirement for low reflux rate and $E_{high}$ is the energy requirement for the high reflux distillation. P is the power of the furnace.

$$E_{low} = P \times (t_{low} - t_{baseline}) = 881W \times 1\min = 881J/\sec \times 60\sec = 52.86kJ$$

$$E_{high} = P \times (t_{high} - t_{baseline}) = 881W \times 14\min = 881J/\sec \times 14 \times 60\sec = 740.04kJ$$

From the theoretical energy demand for the pyrolysis and the actual energy consumed in the experiment, the heat loss can be calculated. For example, in the low reflux rate pyrolysis, the energy lost was $52.86kJ - 20.71kJ = 32.15kJ$ . Hence, 60.8 percent of the total energy was consumed in the low reflux rate distillation process. In the high reflux rate process, the total energy consumed was the energy provided in 14 minutes or740kJ in total, in which only 21.45 kJ was consumed by the pyrolysis. Therefore, 97% of the total energy consumed was lost in the high reflux rate pyrolysis. The energy

consumption for the pyrolysis including vaporization and secondary cracking was only 3% of the total energy consumed in this case.

Secondary cracking of the primary hydrocarbon products was the major reactions during the high and medium reflux rate pyrolysis processes. The secondary cracking reduces the heavy molecular weight hydrocarbons to light molecular weight hydrocarbons thus producing more non-condensable gases. From the analysis of pyrolysis process, it is also known that the initiation reactions consist of random and end chain cracking on the polymer carbon chains, which also produce light hydrocarbon products, such as non-condensable gases. [33, 52, 77, 94-95, 100, 116-118] As mentioned in Section 3.1, the production rate of non-condensable gases is a sensitive indicator for the initiation reactions. This analysis can be confirmed by the experimental results of the non-condensable gas production rates as shown in Figure 5-16 for high flux rate pyrolysis, in Figure 5-18 for medium reflux rate pyrolysis and Figure 5-20 for low reflux rate pyrolysis. In the low reflux rate pyrolysis, only one peak was found for the non-condensable gas production at the early stage of the pyrolysis but there were two peaks for the medium and high reflux rate pyrolysis. In the latter two cases, the first peak was similar to that in the low reflux rate pyrolysis but the second peak appeared later in the process.

The above process can also be understood from the measured temperature in the reactor space ($T_1$). After about16 minutes from the start, the LDPE particles were pyrolyzed quickly and the product vapour rose into the distillation zone. Therefore the space temperature ($T_1$) increased rapidly. After four minutes rapid increase, the gas production slowed down, which was a sign of the primary initiation reaction completing. In high and medium reflux rate pyrolysis, most of the heavy molecular weight hydrocarbons were refluxed back to the pyrolysis zone for further cracking at the same time when the product vapour rose to the distillation zone. (Figure 5-2) The light molecular weight product vapour generated from the secondary cracking then flew out of the distillation zone, and condensed and collected.

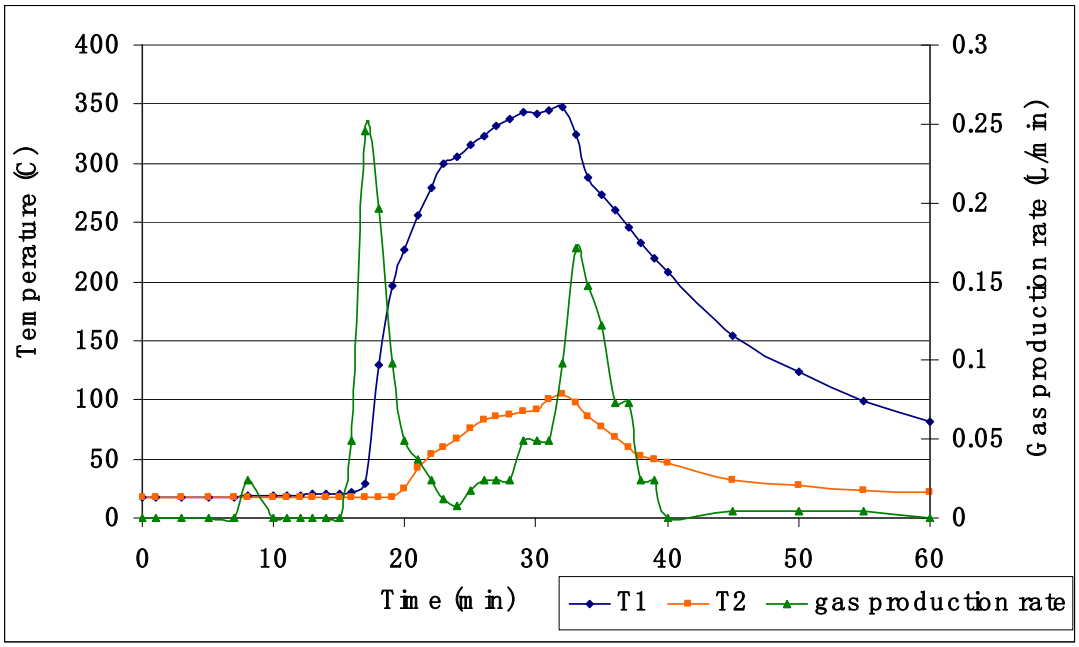


**Figure 5-16 Profiles of reactor space temperature ($T_1$), outlet temperature from distillation zone ($T_2$) and non-condensable gas production for high reflux rate LDPE pyrolysis process**

$T_2$ is the measured temperature at the exit of distillation pipe, which did not change unless the hot product vapour passed through the exit. Due to the fast heat loss from the distillation pipe, $T_2$ was also affected by the temperature of the product vapour. During the primary pyrolysis process, $T_2$ did not change instantly with the production of non-condensable gases and the increase of distillation space temperature $T_1$ because most of the hydrocarbons were refluxed back to the pyrolysis zone before reaching the exit point. In this case, the non-condensable gas was not sufficiently hot and the flow was not sufficiently high for $T_2$ to be increased. This can be confirmed by the observation that the liquid product was only formed when $T_2$ started increasing.

For the high reflux rate pyrolysis, the reactor space temperature ($T_1$) started to increase sharply from 16$^{th}$ minute and remained relatively stable at 300-350°C until 33 minutes from the start of the experiment. The relatively stable temperature was caused by the significant reflux of the primary products. According to the gas production rate, the effect of secondary cracking was not significant. The change of the vapour temperature was negligible in the reflux distillation zone. (Figure 5-17) However, the outlet

temperature ($T_2$) increased during this period, which indicates the increase of the high temperature products passing through the exit pipe. Some of the vapour passing through was condensed to form liquid product and the rest remained as non-condensable gases collected. Those products were the light hydrocarbons from the primary cracking.

After about 33 minutes, the pyrolysis was almost completed and no more heavy hydrocarbons were produced and refluxed back to the reactor, therefore, no more product vapour past the exit pipe. Hence, both $T_1$ and $T_2$ dropped towards the baseline temperature. (Figure 5-16 and Figure 5-17)

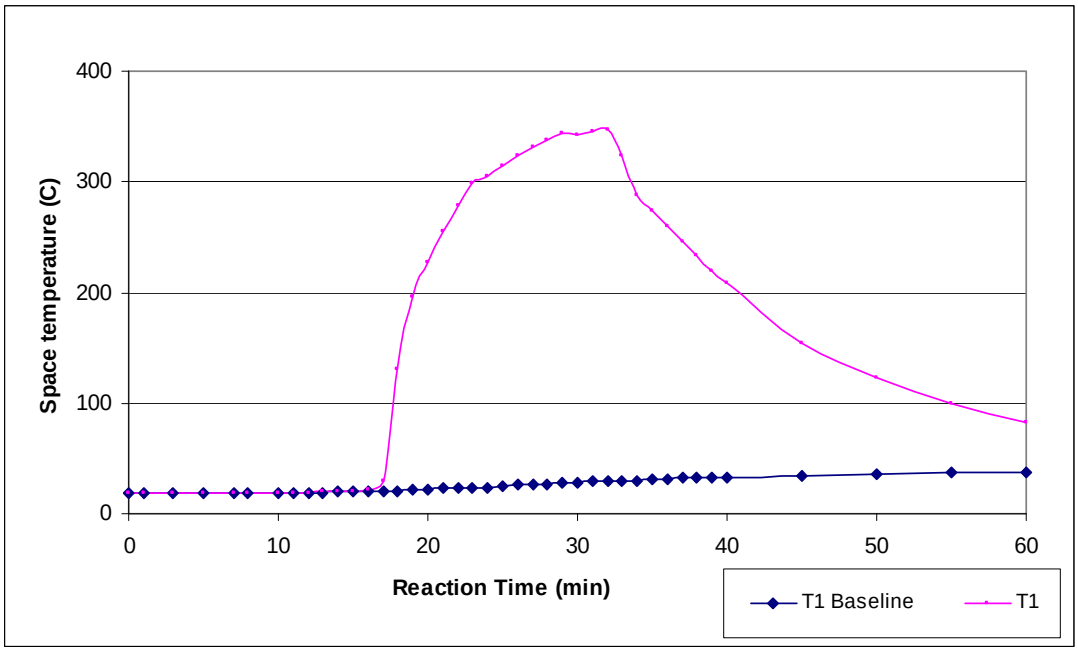


**Figure 5-17 Profiles of space temperature, $T_1$, from the distillation pipe during the high flux rate pyrolysis of LDPE with comparison with baseline**

The profiles of temperatures $T_1$ and $T_2$ in the medium reflux rate pyrolysis are to those of the high reflux rate pyrolysis as discussed before. (Figure 5-18) However, the interval (7 minutes) of the two peaks for the non-condensable gas production, representing the primary and the secondary pyrolysis was much less than that in the high reflux rate pyrolysis (14 minutes). With shorter length for the distillation pipe in the medium reflux

rate pyrolysis, light products were easier to be removed compared to the high reflux rate pyrolysis. Small amount of char was found at the top of the pyrolysis zone after the high reflux rate process. This indicates that the secondary crackings occurred there when the reflux product flew back to the pyrolysis zone.

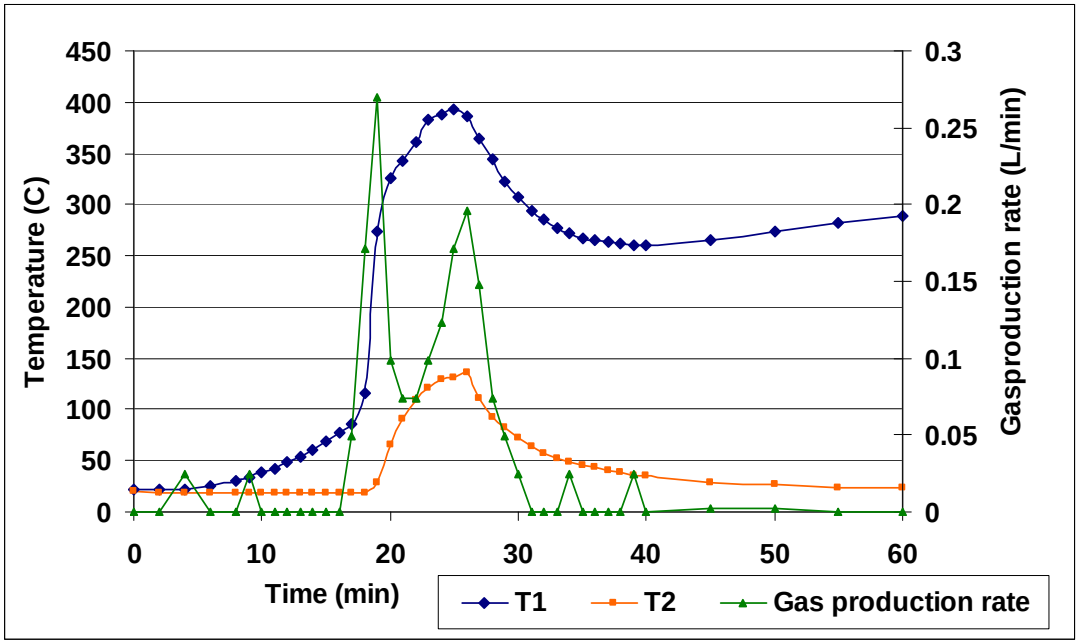


**Figure 5-18 Profiles of reactor space temperature ($T_1$), outlet temperature from distillation zone ($T_2$) and gas production for medium reflux rate LDPE pyrolysis**

In the low reflux rate pyrolysis, the reflux effect was very minor during the process as almost all the distillation pipe was covered by the furnace. Therefore, secondary cracking peak was not observed on the non-condensable gas production rate curve. (Figure 5-19) The primary pyrolysis product vapour, once produced, was removed quickly from the reactor. The heavy molecular weight hydrocarbons were condensed in the condenser. Some wax solidified in the water cooled condenser. Some products were left in the system. This is considered as the reason of the pyrolysis product loss in the material mass balance calculations.

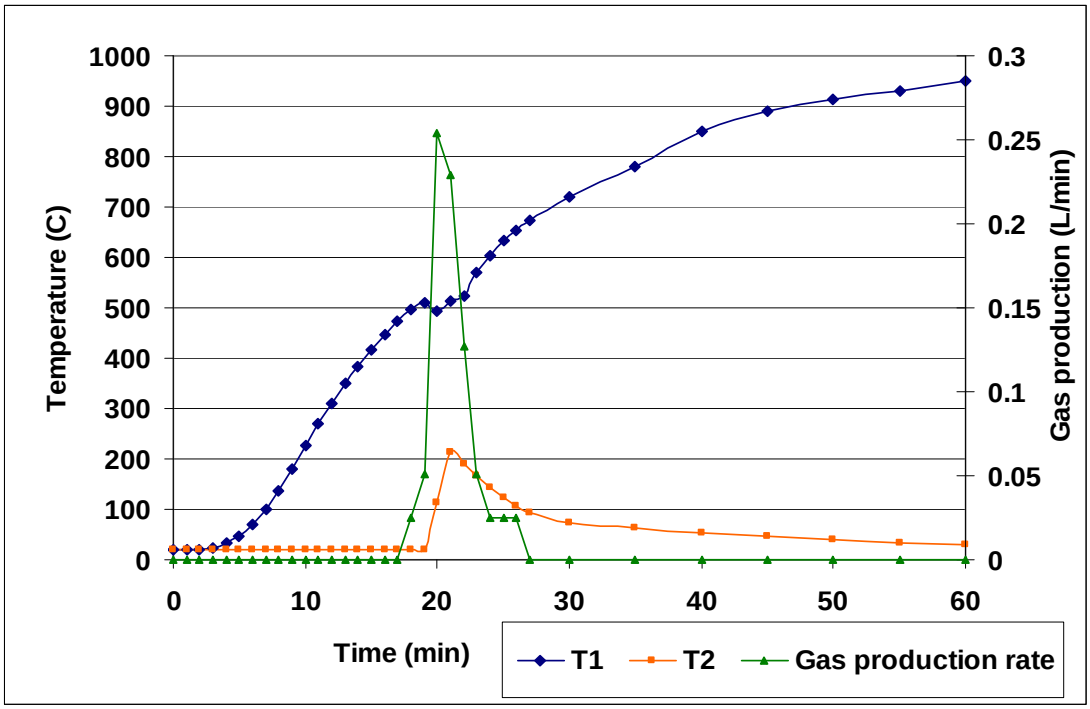


**Figure 5-19 Profiles of reactor space temperature ($T_1$), outlet temperature from distillation zone ($T_2$) and gas production for low reflux rate LDPE pyrolysis**

Effects of reflux rate on the product distribution

From the above discussion, reflux rate has a significant effect on the LDPE pyrolysis process and also on the product distribution. This has been noticed in previous plastics pyrolysis kinetic studies. [31, 46, 49, 58, 68, 79, 99, 112-113, 115, 117] However, due to the complexity of the products, no report has been found on the identification of individual carbon numbers of the hydrocarbon products. The quantification of the effect of secondary cracking on the product distribution has not been found in the literature review.

The product distribution for the LDPE pyrolysis with low, medium and high reflux rates are given in Table 5-9. In the table, the values were corrected with consideration of material loss such as wax sticking in the condenser. The proportion of the char was found to be less than 0.5% in any cases studied; therefore, the ahs was ignored in the material balance calculations. From the table, it is known that the liquid/wax products

were 93.1% for the low reflux rate pyrolysis but this was reduced to 83.3% for the medium reflux rate pyrolysis and to 81.8% for the high reflux rate pyrolysis. Correspondingly, the non-condensable gas proportion was increased from 6.9% in the low reflux rate pyrolysis to 16.7% and 18.3% in the medium and high reflux rate pyrolysis, respectively.

This clearly demonstrates that in the medium and high reflux rate pyrolysis, some of the heavy hydrocarbons in the primary cracking liquid product were converted into non-condensable gases through the reflux distillation. Although char content was not presented, it was found in the final products in the form of mainly fine black carbons attached on the reaction surface at the bottom of the reactor. Some char was also found in the pyrolysis zone in both high and medium reflux rate processes. The location of char formation may be regarded as an indicator for locations where cracking reactions had occurred in the pyrolysis. From this hypothesis, the primary cracking reactions occurred at the bottom of the reactor, and the secondary cracking reactions occurred on the wall of the pyrolysis zone where the condensed hydrocarbons were refluxed back to the reactor.

**Table 5-9 Product distribution from LDPE pyrolysis with different reflux rates**

| 20g LDPE | Reflux rate in pyrolysis process | | |
|---|---|---|---|
| Product | Low | Med | High |
| Gas (C1~C4) | 6.9% | 16.7% | 18.3% |
| Liquid (C5+) | 93.1% | 83.3% | 81.7% |
| Char* | - | - | - |

Non-condensable gas product

In this study, the non-condensable gases generated from the initial primary cracking and from the secondary cracking were collected and analysed separately. (Table 5-9) The conversion of PE into non-condensable gases has a positive relationship with reflux rate. Thus, the proportion of the gases reveals the level of secondary crackings because there is large amount of the gases produced in the random crackings of the refluxed heavy hydrocarbons. The results are given in Table 5-10. As far as the author is aware, this approach is the first in this area of studies.

**Table 5-10 Product distribution in non-condensable gas components from primary and secondary cracking processes**

| | | Primary gas product | | | Secondary gas product | | |
|---|---|---|---|---|---|---|---|
| Component | Product group | Norm% | Percentage | Average MW | Norm% | Percentage | Average MW |
| Methane | C1 | 12.2% | 12.2% | 16 | 11.0% | 11.0% | 16 |
| Ethene | C2 | 21.1% | 32.0% | 29 | 12.0% | 27.7% | 29 |
| Ethane | | 11.0% | | | 15.7% | | |
| peak6 | C3 | 1.3% | 34.7% | 42 | 0.6% | 41.9% | 42 |
| peak7 | | 0.2% | | | 0.3% | | |
| Propene | | 21.2% | | | 22.5% | | |
| Propane | | 12.0% | | | 18.5% | | |
| peak13 | C4 | 11.5% | 21.1% | 56 | 9.4% | 19.2% | 56 |
| Butane | | 8.9% | | | 9.1% | | |
| peak23 | | 0.7% | | | 0.7% | | |
| Total | | 100.0% | 100.0% | 37.6 | 100% | 100.0% | 38.2 |

From the results, it is found that the non-condensable gases were all hydrocarbons from $C_1$ to $C_4$. The interference of purging gas, nitrogen, has been eliminated in the normalized proportion of the gas components and most of the major components have been identified in the analysis as given in Table 5-10. Peak 13 was not identified but is supposed to be one of butene or butane isomers according to its retention time. Based on the analysis results, the average molecular weight of the non-condensable gases was calculated to be 37.6 and 38.2 g/mol for the primary and the secondary cracking processes, respectively.

Although the major non-condensable gas components from the two cracking processes were the same, the proportions of each individual gas components were different. The proportion of ethene from the secondary cracking (12%) was only about half of that from the primary cracking process (21.2%). However, the proportion of ethane and propane from the secondary cracking were, respectively, 43% and 54% higher than those from the primary cracking. Other gas components (methane, propene) had similar proportions between these two cracking processes. Overall, the proportion of the alkene decreased from 60% in the primary cracking gases to 45% in the secondary cracking gases.

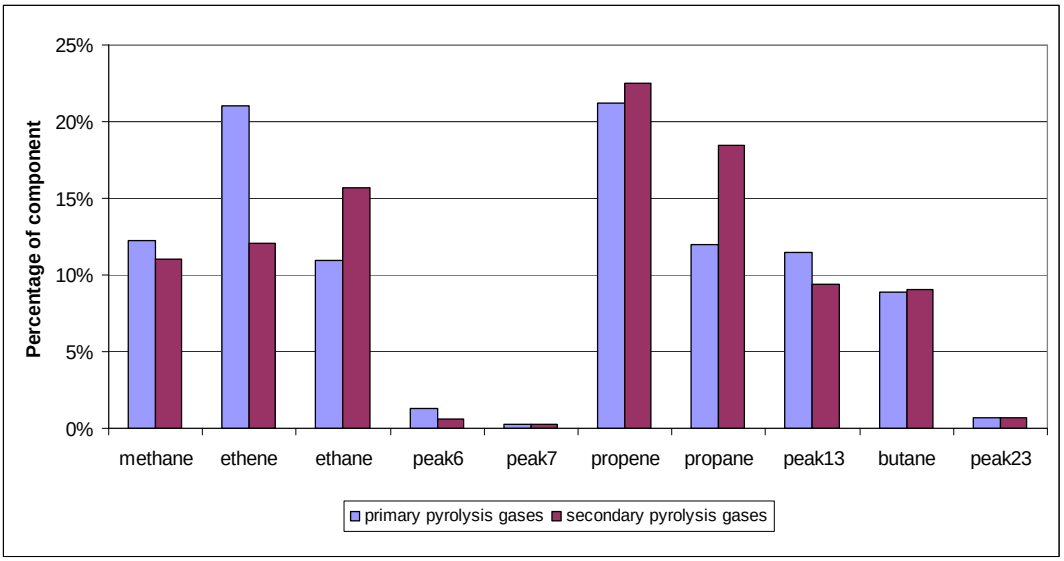


**Figure 5-20 Distribution of the non-condensable gas components from the primary and the secondary cracking in the LDPE pyrolysis**

Liquid and wax products

From the results presented in previous section, it is known that with high and medium reflux rates, the proportion of non-condensable gases were significantly increased and correspondingly, the heavier hydrocarbons ($C_{12+}$) were decreased. The results of the liquids and non-condensable gases from the high and low reflux rate pyrolysis of LDPE are given in Figure 5-20. From the table, the proportion of the heaviest hydrocarbon group ($C_{29+}$) was most reduced from 9.8% at low reflux rate to 1% at high reflux rate. Therefore, the primary hydrocarbon product with higher molecular weight was likely to be cracked in the secondary cracking process. (Table 5-11) The distribution of the final product can be significantly changed by adjusting the reflux rate in the distillation process.

**Table 5-11 Distribution of liquid and non-condensable gas products from different reflux rate pyrolysis processes**

| Hydrocarbon group | low reflux process product proportion w/w | high reflux process product proportion w/w |
|---|---|---|
| $C_1$~$C_4$ | 7% | 18.3% |
| $C_5$~$C_{11}$ | 17.0% | 29.5% |
| $C_{12}$~$C_{16}$ | 36.0% | 32.8% |
| $C_{17}$~$C_{20}$ | 18.8% | 10.8% |
| $C_{21}$~$C_{28}$ | 11.4% | 7.5% |
| $C_{29+}$ | 9.8% | 1.0% |

Further analysis revealed that the secondary cracking has different effects on alkanes and alkenes in each group with the same carbon chain number. Previous GC analyses results show that in each sub-group, n-alkane, 1-alkene, and α, ω-dialkene were the major components. By comparing the GC results between the liquid products from low reflux rate pyrolysis and those from the high reflux rate pyrolysis (Figure 5-21), the

proportion of α, ω-dialkene, that appeared as small peaks in the front of each sub-group for the low reflux rate pyrolysis, was greatly decreased to a very low level in the high reflux rate pyrolysis products. (Figure 5-21) Correspondingly, the 1-alkene and n-alkane peaks from 5 minutes to 15 minutes were significantly increased in the high reflux rate pyrolysis products. Obviously, the difference of the height of 1-alkenes and that of n-alkane peaks was reduced in the high reflux rate pyrolysis products. As a result, the ratio of 1-alkene to n-alkane decreased after the secondary cracking. Particularly, the reduction on the 1-alkene/n-alkane ratio was more significant in the heavy molecular weight hydrocarbons than the light hydrocarbons. For example, the ratio of 1-$C_{15}$/n-$C_{15}$ dropped from 1.2 to 1, while the ratio of 1-$C_{24}$/n-$C_{24}$ dropped from 1 to 0.4. (Figure 5-21) Therefore, the secondary cracking cracked more 1-alkenes than n-alkanes, particularly, heavy molecular weight 1-alkenes. The hydrogen free radicals may react with 1-alkenes and produced n-alkanes. These are not found in any other relevant research reports.

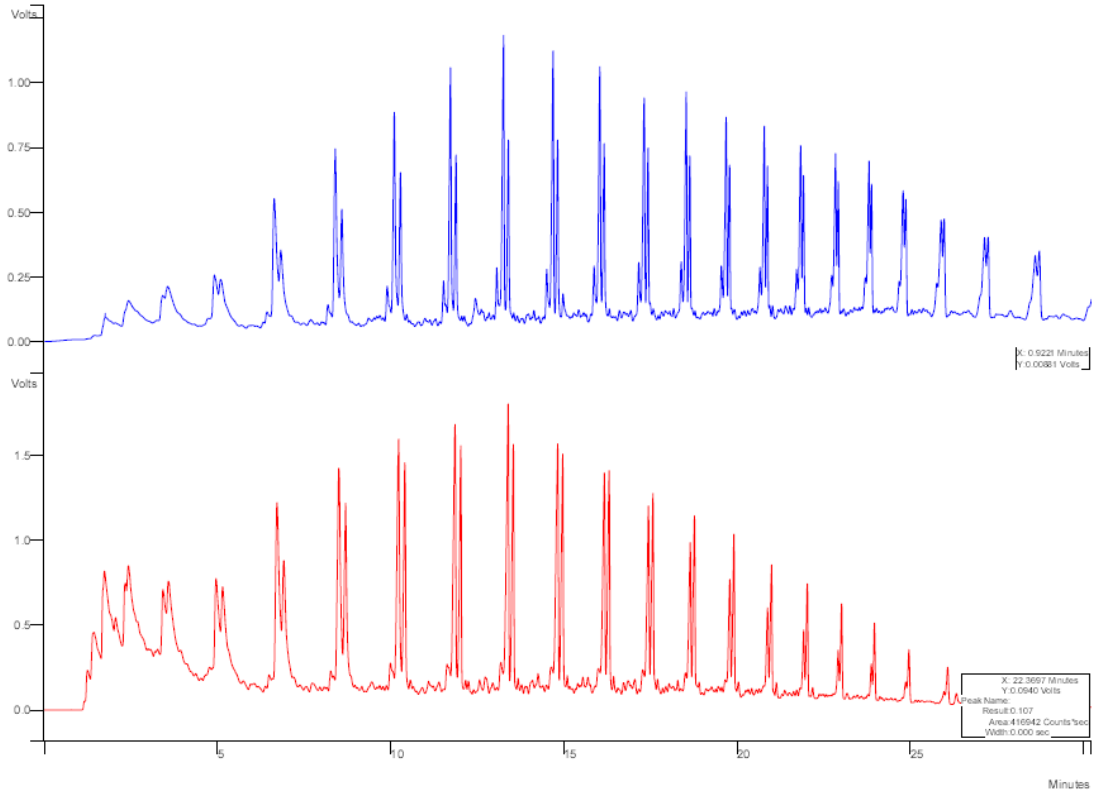


**Figure 5-21 Comparison of pyrolysis liquid components between low reflux rate (top) and high reflux rate (bottom)**

Note that: The scale of Y axis for the two charts is not the same.

Char product

Neither high nor low reflux process pyrolysis produced significant amount of char. The mass/mass proportion of char content in both processes was less than 0.5 percent. The amount of char was neglected in the analysis.

### 5.2.3. Conclusions

Secondary cracking in high and medium reflux rate pyrolysis has significant effects on the pyrolysis process and distribution of the pyrolysis products. However, the secondary cracking was not obvious in the low reflux rate pyrolysis. In the pyrolysis with reflux, majority of the energy consumed was lost in the reflux distillation process, accounting for 73% and 99%in the low and the high reflux rate pyrolysis, respectively.

With high and medium rate pyrolysis, a large amount of heavy molecular weight hydrocarbons were further cracked into non-condensable gases and lighter hydrocarbons through the secondary cracking. As a result, the conversion of non-condensable gases indicates the reflux rate or the level of the secondary crackings. The proportion of the non-condensable gases increased from 6.9% from the low reflux rate pyrolysis to 18.3% from the high reflux rate pyrolysis. The wax content ($C_{29+}$) decreased from 9.8% to 1% correspondingly. It is also found that in each carbon number sub-group, the 1-alkenes were more likely to be cracked than were the n-alkanes, particularly in the heavy molecular weight products. The percentage of α, ω-dialkenes was significantly decrease after the secondary cracking. The char content in every process remained below 0.5% w/w, which did not change much with the reflux rate and was negligible in the analysis.

## *5.3. Catalytic Pyrolysis on Low Density Polyethylene*

### *5.3.1.* Materials and equipment

Catalytic pyrolysis was studied previously and the published results show that catalyst can change the reaction process and the distribution of pyrolysis products, particularly, for PE that produced high molecular weight products in pyrolysis. [29, 56, 64, 119] As the proportion of wax (heavy molecular weight hydrocarbons) is high in the PE pyrolysis products, catalytic pyrolysis was investigated to convert the wax into diesel range fuels rather than use high reflux rate distillation that consumes a large amount of energy. According to previous studies (Section 2.1.5), pore size and the ratio of Si/Al are the two key factors determining the effect of zeolite catalyst because zeolites are crystalline micro-porous aluminosilicates. [70-71, 75]

In this study, the catalysts used in the experiment were provided by Nankai University Catalyst Co. Ltd., China. In order to maximize the diesel range and other liquid product and to reduce the proportion of wax, three types of catalysts, NKC-5 (ZSM-5), NKC-7 (NaY), and NKC-3A zeolite were investigated. The physical appearance of these catalysts is shown in Figure 5-22. The pyrolysis apparatus used for LDPE pyrolysis was also used in the catalytic pyrolysis experiments. (Figure 5-2)

(a) (b) (c)

**Figure 5-22 Catalyst appearance: (a) NKC-3A, (b) NKC-5, and (c) NKC-7**

The catalyst of NKC-3A zeolite mainly consists of alkali metals and silica aluminate, which adsorbs molecules with certain range diameters no larger than 3A (0.3 nm). The NKC-3A zeolite catalyst is widely used in petroleum processing for gas cracking, which can adsorb water molecules while excluding hydrocarbon molecules. [120] In the experiment, the effects of the zeolite with different pore sizes on the pyrolysis product were examined.

The catalyst NKC-5 is ZSM-5 zeolite based catalysts with the ratio of Si/Al at 25 and pore size of 0.5 nm. NKC-5 is used for converting hydrocarbons such as $C_5$ (alkene or alkane) into aromatics like benzene, toluene, xylene, etc. [121] The NKC-5 performance was tested by the manufacturer in a continuous fixed bed reactor with catalyst to feedstock ratio of 1:10. The results showed a conversion efficiency of 99% with gas yield of 31.3% and aromatic compound of 62%. [121] In this study, the NKC-5 was used to maximize the petrol range product or aromatics in the LDPE pyrolysis.

NKC-7 is an alkali metal silica aluminate based catalyst with NaY zeolite structure. The NaY zeolite can adsorb the molecules of certain range of diameter no larger than 1nm.[122] NKC-7 is a catalyst for cracking the heavy molecular weight hydrocarbons into lighter hydrocarbons during diesel production.

### 5.3.2. Experimental

In order to investigate the effects of catalyst on the pyrolysis products, lower reflux rate pyrolysis of LDPE was conducted. The results from experiments using the three catalysts were compared with the results of matching pyrolysis experiments without catalysts. (Section 5.2) In this way, the effect of catalyst on heavy molecular weight hydrocarbons was identified.

Four runs of pyrolysis experiment were conducted at low reflux rate: Run 1 (control) was pyrolysis of LDPE without any catalyst, Runs 2 to 4 were pyrolysis, respectively, with catalysts of NKC-5, NKC-7 and NKC-3A. In each run, 20 g LDPE was used and in Runs 2 to 4 2g catalysts was added.

In Runs 2 to 4, the LDPE was first placed in the pyrolysis reactor then, the catalyst was added into the reactor before the experiment started. The following procedures, measurements and product analysis methods were the same as those of the low reflux rate pyrolysis experiments described in Section 5.1.2.

### 5.3.3. Results and discussion

The pyrolysis products measured in the experiments are given in Table 5-12 for the contents of non-condensable gases and liquids. The char content was also lower than 0.5% thus it was not included in the product analysis. In the table, the results are mass proportion in the product. The mass proportion of the non-condensable gases was calculated from values measured gas and the estimated average molecular weight of the gases.

**Table 5-12 Pyrolysis product distribution w/w with catalytic and comparison with that without catalysts pyrolysis**

| | Gas | Liquid |
|---|---|---|
| No catalyst | 17% | 83% |
| NKC-7 | 25% | 75% |
| NKC-5 | 58% | 42% |
| NKC-3A | 24% | 76% |

From the product analysis results, it is found that the effect of the catalysts on the distribution of the pyrolysis product was significant. All of the three types of catalysts tested promoted the production of non-condensable gases and reduced the proportion liquid product. (Table 5-12)

The catalysis of NKC-5 had the most significant effect on the gas production with the proportion of the non-condensable gases increased from 17% to 58%. In addition, it was also observed that the liquid product from NKC-5 catalytic pyrolysis had relatively low viscosity while the liquid products from other runs (Run1, Run 3 and Run4) were creamy solid wax at ambient temperature (20°C). The other two types of catalysts (NKC-7 and NKC-3A) also increased the production of non-condensable gases but with mush less extent from 17% to 25% and 24%, respectively. Obviously, NKC-5 is the most effective catalyst examined for dewaxing and increasing the production of non-condensable gases.

The profiles of non-condensable gas production during four runs of LDPE pyrolysis are presented in Figure 5-23. The starting point of the pyrolysis can also be observed from the gas production curves in which the pyrolysis reactions started at the same time (17 min) in Run 1 (control), Run2 (NKC-7) and Run 3 started at the same elapsed time. Therefore, the profiles of reactor outer wall temperature ($T_3$), reactor space temperature ($T_1$) and outlet temperature from the distillation pipe were the same for these three runs.

However; in Run 4 where NKC- 3A was used, the non-condensable gas was generated at 15 minute from the start, 2 minutes earlier than other runs. Form the temperature profiles presented earlier, the heating up rate for the system was 30 ºC/minute with no difference for baseline run or for runs with catalysts. From this observation, it is concluded that the primary cracking temperature for the pyrolysis with NKC-3 catalysts was reduced by 60 ºC to 390 ºC due to the effect of the added catalyst (NKC-3A).

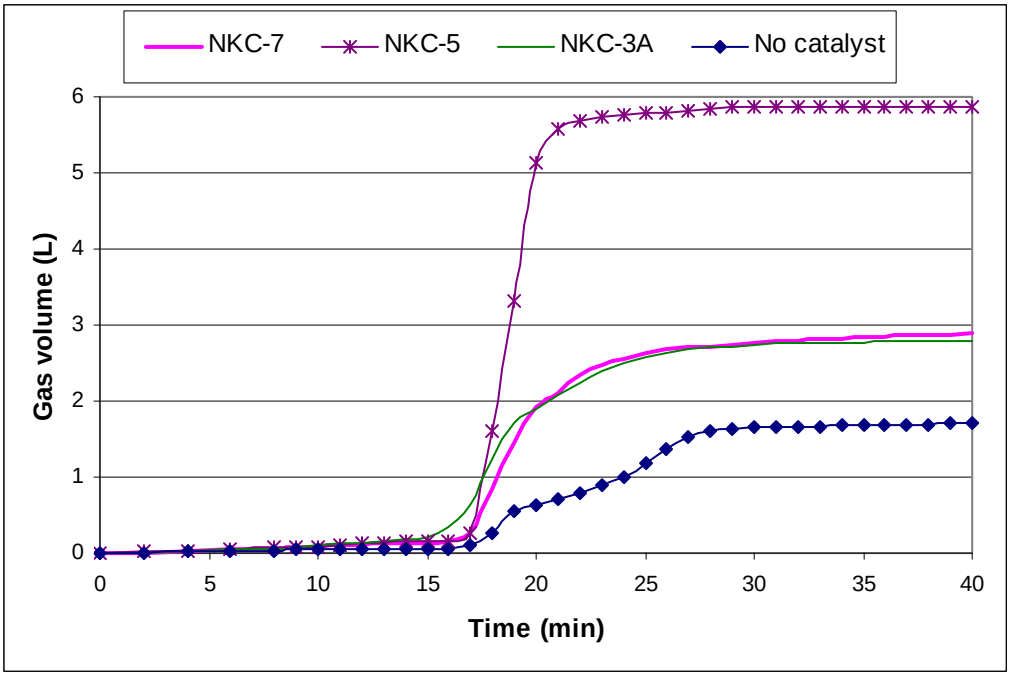


**Figure 5-23 Gas production of LDPE catalytic pyrolysis**

In the experiments with catalysts, it was found that the catalysts remained at the bottom of the reactor after the experiment but these catalyst particles turned into black after the reactions. It is believed that this colour change was mainly caused by the fine carbon residues left on the catalysts.

The liquid products were analyzed using GC as described before and the results are shown in Figure 5-24 in which the order of chromatographs from the top to bottom are for Run 1 (control), Run2 (with catalyst NKC-3A), Run 3 (NKC-5) and Run 4 (NKC-7), respectively. From these results, it is seen that the three types of catalysts had different influence on the composition of the liquid product. The quantitative results for the liquid products in each run are given in Table 5-13.

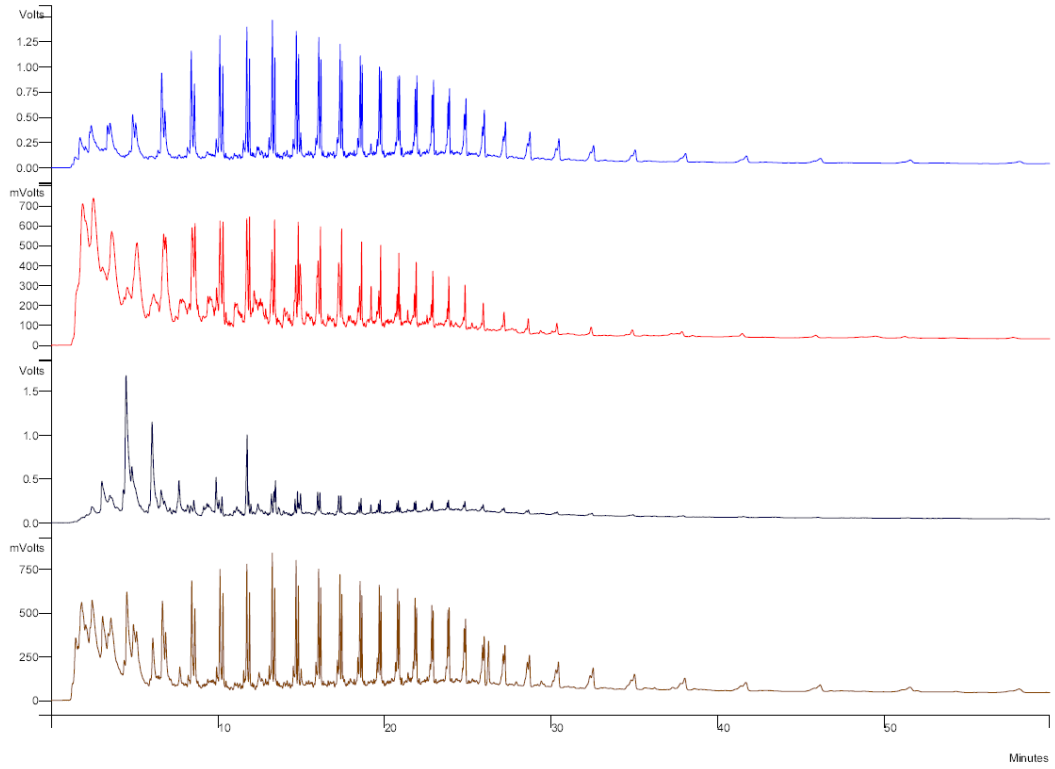


**Figure 5-24 GC analysis results for the liquid products from pyrolysis of LDPE Chromatographs from top to bottom are respectively: Run 1 (control), Run 2 (NKC-3A), Run 3 (NKC-5) and Run 4 (NKC-7)**

Note: The scales are different for the graphs.

From the results in Table 5-13, it is found that in the LDPE pyrolysis using catalyst of NKC-3A (Run 2), the heavy molecular weight hydrocarbons ($C_{28+}$) has decreased from 6% in the control to 1% while the diesel range product ($C_{11}$-$C_{27}$, New Zealand winter diesel from Mobil measured by Feng Gao) also had a significant decrease from 66% in the control to 37%. Additionally, from the GC chromatographs, the height of first peak in each hydrocarbon sub-group, 1-alkenes, was also significantly reduced compared to the n-alkanes, the second peak in the same sub-groups. On the other hand, the percentage of the LPG ($C_1$-$C_4$) and the petrol ($C_5$-$C_{10}$) range hydrocarbons has increased from 17% to 24%, and from 11% to 37%, respectively.

In Run 3 with catalysts NKC-5, the diesel and the wax range products were greatly reduced compared to the control. The LPG gas product increased from 17% to 58% and the petrol range product increased from 11% to 18%. (Table 5-13) The dewaxing effect of NKC-5 on the pyrolysis of LDPE is very significant. However, the structures of the components have also been changed with the NKC-5 catalyst which is reflected by the flat and irregular peaks GC chromatograph. (Figure 5-24) The concentration of the 1-alkenes and the n-alkanes was greatly reduced. A few aromatic compounds, benzene, toluene, and xylene, were significant in the liquid product. Further analysis shows that the concentrations of benzene, toluene, and xylene were 3.8%, 9.4%, and 5.6%; respectively. Therefore, the catalyst of NKC-5 has remarkable effect on converting straight chain hydrocarbons into aromatics and promoting LDPE pyrolysis gases. The results from this study are consistent with previous report of Uemichi, *et al.,* who tested the catalysts of zeolite ZSM-5. [62]

In Run 4 where catalyst NKC-7 was used, the diesel range product was significantly reduced from 66% in the control to 37%. (Table 5-13) However, the proportions of other hydrocarbons were all increased to a certain extent, including wax being increased from 6% to 14%, petrol range being increased from 11% to 24% and LPG gas from 17% to 25%. The overall composition of the NKC-7 liquid pyrolysis product was similar to that of the control except for higher proportion of petrol and wax range products. The GC chromatograph for the NKC-7 liquid pyrolysis products was similar to that of the control (Figure 5-24) where 1-alkenes and n-alkanes were the dominant components in the liquid.

**Table 5-13 Product distribution of catalytic pyrolysis of LDPE and comparison with control**

| Product distribution | C1-C4 | C5-C10 | C11-C27 | C28+ |
|---|---|---|---|---|
| No catalyst | 17 | 11 | 66 | 6 |
| NKC-3A | 24 | 37 | 37 | 1 |
| NKC-5 | 58 | 18 | 22 | 2 |
| NKC-7 | 25 | 24 | 37 | 14 |
| Commercial fuel range | LPG | Petrol | Diesel | Wax |

### 5.3.4. Conclusions

The effects of three types of zeolite based catalysts (NKC-3A, NKC-5, NKC-7) were investigated in this experiment on LDPE pyrolysis. The catalysts NKC-5 and NKC-7 did not affect the start of pyrolysis reactions compared to the control, but the pyrolysis reactions using catalyst NKC-3A started 2 minutes earlier controlled to the control, thus it is concluded that the cracking temperature was decreased by 60°C from 450 ºC to 390 ºC with catalyst NKC-3A.

All of the catalysts tested have promoted the proportion of non-condensable gases significantly. The catalyst NKC-5 has the most significant impact with the gas production being increased from 17% in the control to 58%. The other two catalysts, NKC-3A and NKC-7, promoted the proportion of non-condensable gases to 24% and 25%, respectively.

The diesel and the wax range products were reduced in the LDPE pyrolysis using both NKC-3A and NKC-5. However, the wax range product using NKC-7 was increased from 6% in the control to 14%. By using the catalyst NKC-5, the 1-alkenes hydrocarbons were significantly reduced in the carbon chain sub-group. NKC-5 assisted to convert most 1-alkenes and n-alkanes into aromatics (toluene, benzene, and xylene) in the liquid product of LDPE pyrolysis. Catalysts have significant effects on the product distribution and the pyrolysis process. However, the use of catalyst may include other issues like changing catalyst, loss of catalyst activity, etc.. This is depended on the reactor and the type of catalyst.

# 6. Pyrolysis of PP, PS and Plastic Mixtures

## *6.1. Pyrolysis of Polypropylene*

### *6.1.1.* Materials and apparatus

This part of study investigated the pyrolysis process and products using virgin polypropylene (PP) with trade brand of AR564 in order to maintain the consistency of the material. The virgin PP is in the form of oval particles with dimensions of 3 mm by 4 mm as shown in Figure 6-1. Other properties of the virgin PP are listed in Table 6-1.


**Figure 6-1 Appearance of virgin PP (AR564) used in this study**

**Table 6-1 Thermal and physical properties of virgin PP using in this study**

| Properties | Unit | Value | ASTM method |
|---|---|---|---|
| Melt flow rate | g/10 min | 24 | D1238 |
| Melting point | ºC | 160-165 | - |
| Density | g/cm3 | 0.90 | D792 |

This study also used the vertical batch pyrolysis apparatus which was used in Section 5. (Figure 5-2) In order to investigate the effect of reflux rate, three lengths of the reactor pipe were used (200 mm, 280 mm and 380 mm), which corresponded to low, medium and high reflux rates for the distillation. In a similar way to Chapter 5, water sealed cylinder was used to measure the volume of non-condensable gases generated. A balloon with an aluminium inner layer was used to collect the gas samples for analysis using the same 3000A Micro GC as that in the previous experiments described in Section 5.2. The liquid product was collected and analyzed with the same Varian Gas Chromatography CP-3800 as that used in Section 5.2.

### 6.1.2. Experimental

Before the experiment, 20g virgin PP was placed in the reactor. Then, nitrogen gas was used to purge the air out of the apparatus for one minute. After that, the M303PY Gallenkamp electronic furnace was turned on with the power load setting at 100 which corresponds to 881 W. The experiment stopped when no products were further collected. The objectives of part of study were to examine the process and products of PP pyrolysis and to compare with those of LDPE pyrolysis thus the main part of the experiments were conduced using the reactor length of 280 mm or the medium reflux rate pyrolysis. High and low reflux rate processes were also tested to investigate the effect of reflux rate on the products. For the detailed operation procedure and product analysis (gas and liquid), please refer to Section 5.2. The char content in this study was also very low thus no analysis was undertaken.

### 6.1.3. Results and discussion

Process Analysis

In a similar way as the pyrolysis of LDPE, the PP pyrolysis produced liquid and non-condensable gases. The reflux rate in the distillation process also had significant effects on the PP pyrolysis process and products. The liquid product collected after the

condenser was yellow creamy wax with low reflux rate PP pyrolysis, while it was clear yellow-brown oil from medium or high reflux rate PP pyrolysis.

Figures 6-2 and 6-3 show the profiles of reactor space temperature ($T_1$), temperature at the reactor outer wall surface ($T_3$) and the production rate of the non-condensable gases. Figure 6-2 is for the medium reflux rate pyrolysis and Figure 6-3 is for the high reflux rate. From the result of medium reflux rate pyrolysis (Figure 6-2), only a single stage of fast production of non-condensable gas which started 17 minutes from the beginning of the pyrolysis process. This is different from the pyrolysis of LDPE at the medium reflux rate. (Figure 5-18) The starting point for the non-condensable gas production indicates the starting time of the pyrolysis reactions. In the medium reflux rate process, the refluxing distillation time was only three minutes. Therefore, the two rapid increase period of non-condensable gases production were merged together. (Figure 6-3)

However, the PP pyrolysis with high reflux rate showed a second fast rate of non-condensable gas production after about 30 minutes which is similar to the LDPE pyrolysis (Figure 5-16) although the second fast production rate for the PP pyrolysis was less than that of the LDPE pyrolysis at the high reflux rates. These above observations may indicate that PP pyrolysis had less reflux using the same length of the reactor pipe as less condensable gas was generated from the secondary cracking process. This can be further confirmed by comparing the product distribution at the same reflux rate between pyrolysis of LDPE (Table 5-9) and pyrolysis of PP. (Table 6-2)

The pyrolysis process can be better understood by analysing the measured temperatures at the reactor outer wall surface and in the rector space. (Figures 6-2 and 6-3) From the temperature profiles at high reflux rate pyrolysis, it is found that the reactor outer wall surface temperature ($T_3$) increased continuously from the start and remained at about 450 ºC when the massive non-condensable gases were generated. This lasted about 13 minutes during which the gas production was gradually decreased. (Figure 6-3) During

this period, intensive reflux distillation occurred and the refluxed products consumed significant amount of heat thus maintaining the reactor temperature relatively constant. When the products were gradually removed, the temperature of $T_3$ increased again at about 30 minutes from the start and in the meantime more non-condensable gases were generated again, mainly from the secondary cracking. It is observed that the temperature reached 510°C when the secondary cracking started. The reactor wall surface temperature eventually reached about 700°C at the end of the pyrolysis.

The PP pyrolysis with medium and low reflux rates had similar temperature profiles but the second increase in the non-condensable gas production rate was not observed due to the lack of secondary cracking.

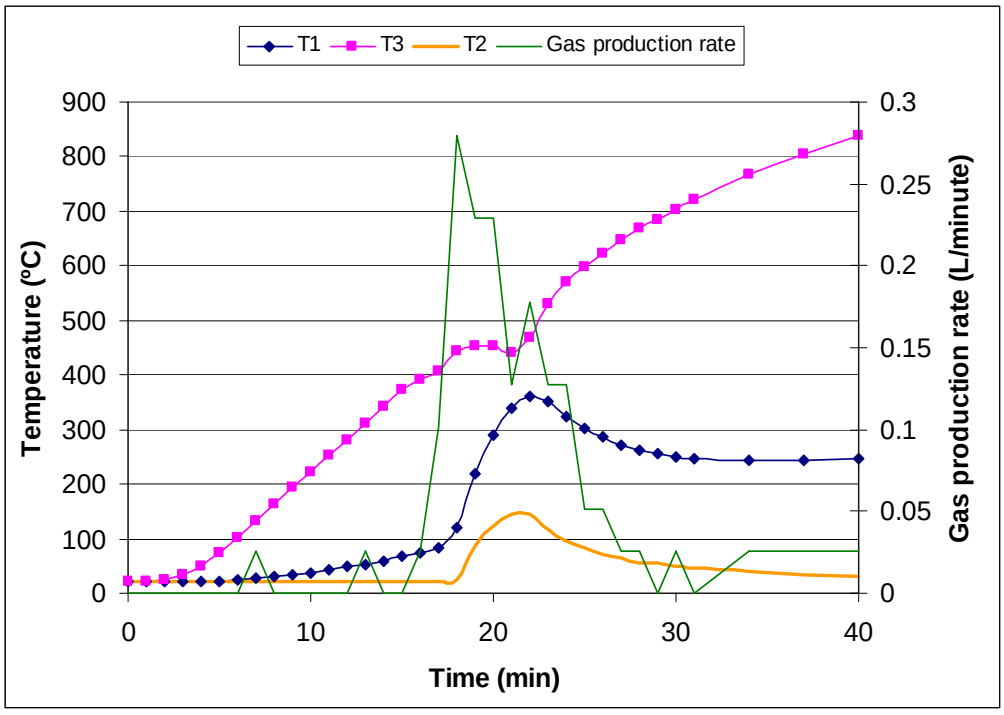


**Figure 6-2 Profiles of medium reflux rate PP pyrolysis**

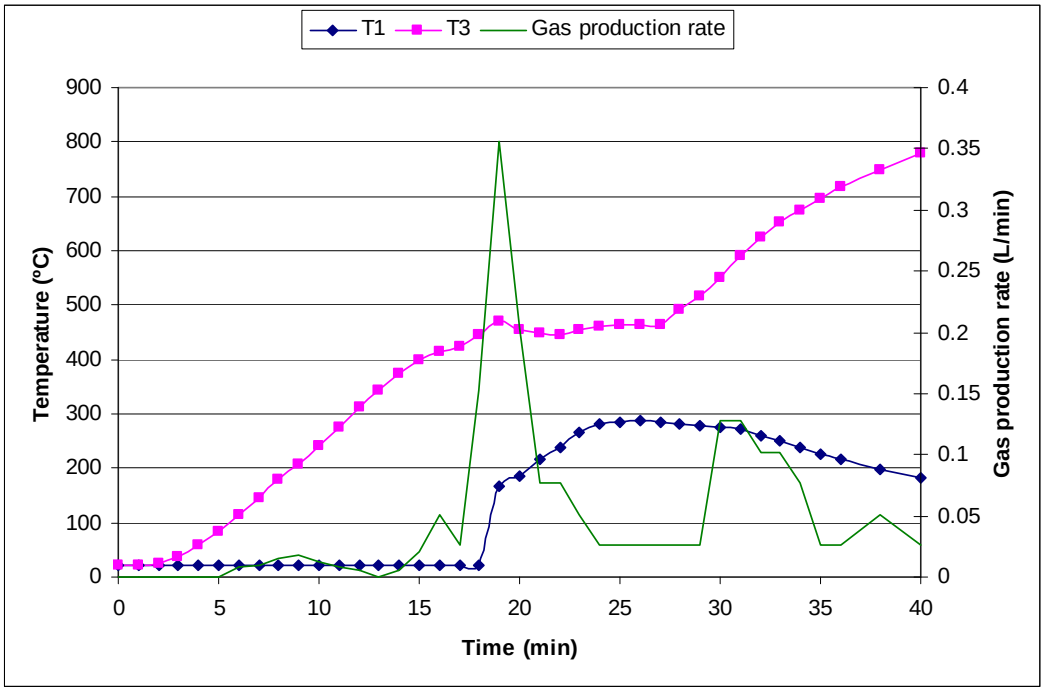


**Figure 6-3 Profiles of high reflux rate PP pyrolysis**

In the PP pyrolysis, non-condensable gases, liquid and char were collected and the results for the high reflux rate pyrolysis are given in Table 6-2. The char content was insignificant, less than 0.05g. The char was fine black power attaching on the inner surface of the pyrolysis zone. Hence, the mass of the char was hardly to be precisely quantified.

**Table 6-2 Products from PP high reflux rate pyrolysis**

| Product | Gas ($C_1 \sim C_4$) | Liquid ($C_{5+}$) | char |
|---|---|---|---|
| Collected values | 1.91 L | 16.63 g | - |
| Calculated and corrected values | 3.13g* | 16.83g** | Less than 0.05 |
| Proportion | 15.7% | 84.2% | Less than 0.25% |

Note: * The mass of non-condensable gases was calculated from the measured gas volume and the calculated average molecular weight of the gases. (Table 6-3)

** The 1% mass loss in the products from 20g PP, 0.2g, was assumed to be the residue liquid attached on the wall in the apparatus.

Non-condensable gas product

From the gas analysis, the composition of the non-condensable gases was determined and the results are illustrated in Figure 6-4 for medium reflux rate PP pyrolysis. From the results, it was found that there were seven main components in the gases which had concentration greater than 1%. The highest concentration component is propene which accounted for 44% in the total non-condensable gas product. Other significant gas components include methane (11%), ethene (10%), ethane (12%) and another unidentified one at peak 28. There was 4% hydrogen detected in the gases, which did not appear in the LDPE pyrolysis products. The identified peak 28 was located between propane and n-butane; therefore, it can be one of the butane isomers or butenes according to other studies. [34, 101]

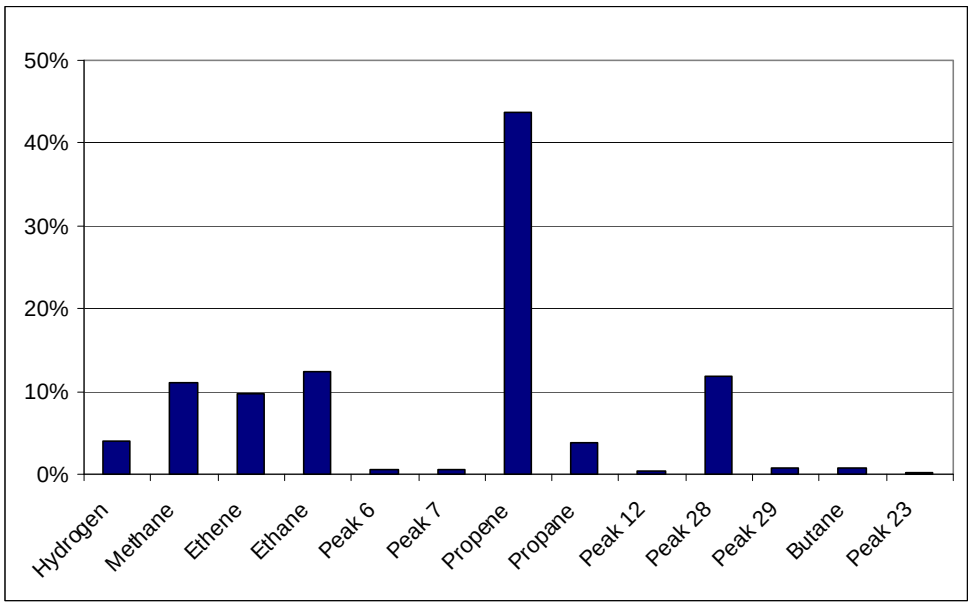


**Figure 6-4 Components in non-condensable gas from PP pyrolysis**

The proportion of each component is affected by the reflux rate and operation conditions (temperature and pressure). From previous studies, it is known that at a relatively low temperature, $C_1$ to $C_4$ are the main components. [47] Hydrogen gas is also

produced from PP pyrolysis while it was not found in the non-condensable gases from PE pyrolysis. Methane and ethylene are the main components in a high temperature PP pyrolysis. The pyrolysis experiment conducted in this study was a relatively low temperature process and the gas product composition results are similar to the reported gas results of PP pyrolysis at 400ºC. [21, 23, 61, 112]

**Table 6-3 Distribution of non-condensable gases from PP pyrolysis**

| Compound | Percentage | Expected MW |
|---|---|---|
| Hydrogen | 4.09% | 2 |
| Methane | 11.11% | 16 |
| Ethene | 9.69% | 28 |
| Ethane | 12.49% | 30 |
| Peak 6 | 0.53% | 42 |
| Peak 7 | 0.64% | 42 |
| Propene | 43.79% | 42 |
| Propane | 3.81% | 44 |
| Peak 12 | 0.32% | 56 |
| Peak 28 | 11.76% | 56 |
| Peak 29 | 0.79% | 56 |
| Butane | 0.82% | 58 |
| Peak 23 | 0.16% | 70 |
| MW avg | 100.00% | 36.7 |

Note: MW means molecular weight;

MW avg means average molecular weight of the gases

Assuming that peak 28 was one of the isomers of butane, the average molecular weight of PP pyrolysis non-condensable gases was calculated to be 36.7 g/mol. This is slightly lower than the average molecular weight of the gases from LDPE pyrolysis, 38 g/mol, (Table 5-6) because the proportion of $C_3$ and $C_4$ in PP non-condensable gases is less than that in LDPE gases. It is possibly due to the difference between the molecule structure of PP and PE. Different from the long chain hydrocarbons from random cracking of PE, initial cracking on the PP carbon chain likely occurs on the C-C bond attached to the tertiary carbons. The free radicals with methyl- side group that did not combine with other free radical groups formed propene. Thus, 44% of propene was found in the gases, which is much higher than that in PE and PS. The volume of the collected gases was 1.91 L. Therefore, the mass of the non-condensable gases is 3.13 grams. (Table 6-2)

Liquid product

The liquid from high and medium reflux rate PP pyrolysis processes was yellow-brown oils at medium reflux rate which was similar to PE pyrolysis oils. (Figure 6-5) The condensed product from low reflux rate process was yellow creamy wax that was also similar to that from LDPE low reflux rate pyrolysis. The liquid product was analyzed through GC and GC-MS and the results from the medium reflux rate pyrolysis of PP are shown in Figure 6-6. The GC chromatograph of PP pyrolysis oil has methyl-side groups on the carbon backbone which is different from that of the LDPE pyrolysis oil. As mentioned in the previously, in the tertiary carbons, the joints with methyl groups have the weakest C-C bonds which will break first in the initiation reactions. (Section 3.1.2) During pyrolysis, the free radicals with methyl groups combined together with each other at the ends formed many oligomers of propene. In the pyrolysis of PP, the intramolecular radical transfer is preferred to the intermolecular one in the PP pyrolysis process. Thus, the low oligomers predominate in the PP pyrolysis oil is more volatile than that of PE. [68] The difference between the PE pyrolysis oil and the PP pyrolysis oil can be observed on the GC analysis graphs. (Figure 5-11 and Figure 6-6)

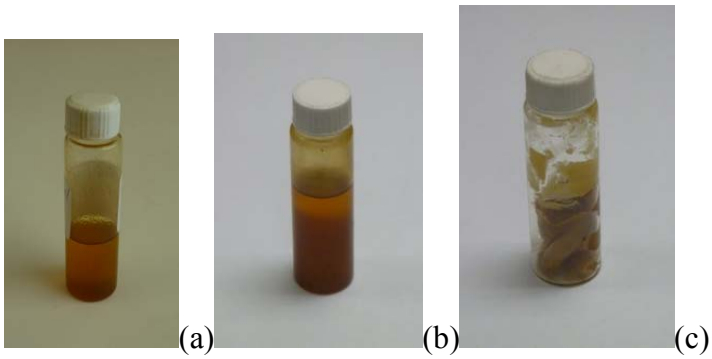


**Figure 6-5 Comparison of liquid oil from PP pyrolysis at high (a), medium (b), and low (c) reflux rates processes**

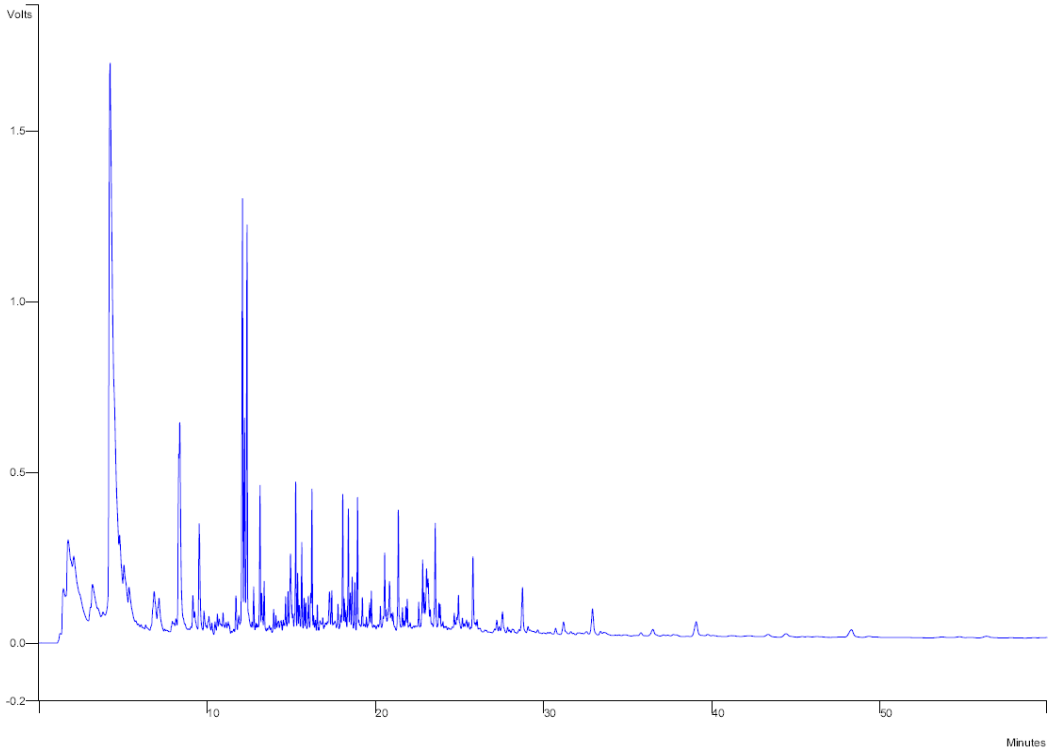


**Figure 6-6 GC analysis result of PP pyrolysis oil with medium reflux rate**

A similar pyrolysis product distribution to that of this study was also observed by other researchers (Figure 6-7) who found that the product distribution of PP pyrolysis is developed by a free radical mechanism. [123-124] When PP is pyrolyzed at about 400 ºC, propene gas were eluted and collected in the process. There were 99 peaks detected from the GC analysis in which the main oligomers of propene are dimers, trimers,

tetramers, and pentamers of propene in the first 13 minutes, which accounts for 68% of the concentration of liquid products. Both GC chromatographs (Figure 6-6 and Figure 6-7) show an outstanding high peak at 4.2 minutes and other significant peaks in the first 20 minutes, which accounts for 81% v/v of the total liquid product. The outstanding peak at the 4.2 minute was identified as 1, 3, 5 - trimethyl - cyclohexane ($C_9H_{18}$). This cyclohexane accounts for 21% in the liquid products. The peaks came out after the 13$^{th}$ minute were heavy boiling range oligomers, a series of which are α, ω-isodialkenes. Others can be isoalkanes and 1-isoalkenes. [68]

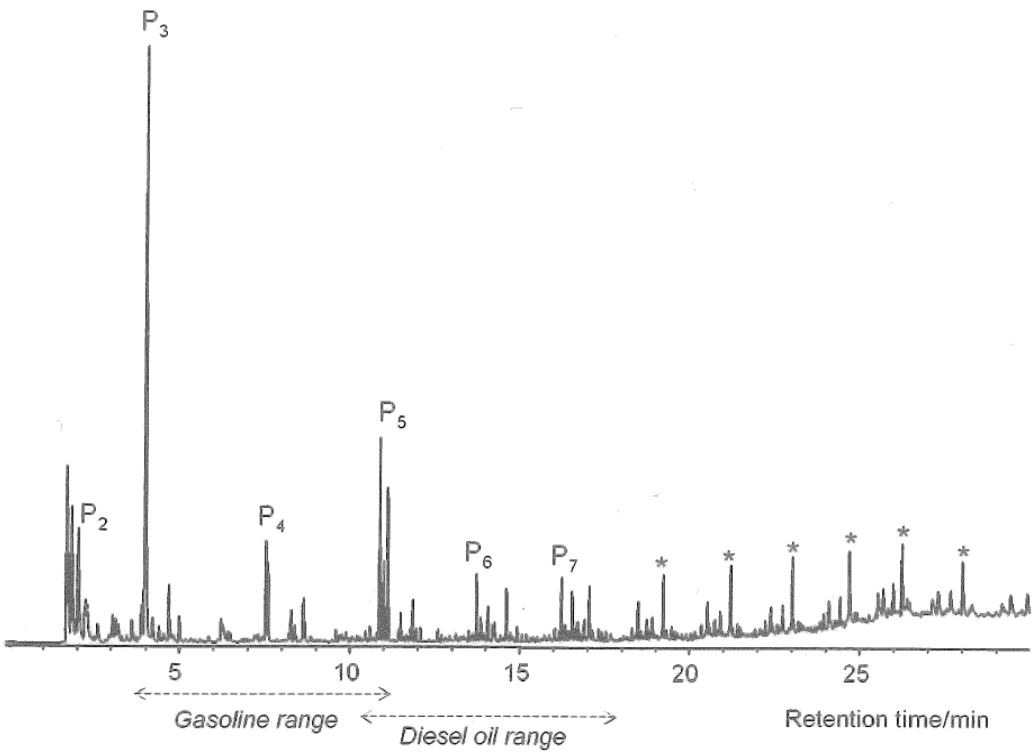


**Figure 6-7 Py-GC-MS chromatogram of isotactic PP at 500 ºC [68]**

Note that: $P_n$ in the GC chromatograph denotes oligomers of n propene unites. Peaks labelled * are dialkenes.

The isoalkanoic structure of PP is retained in its pyrolysis products. Therefore, the octane number of PP pyrolysis oil might be higher than other straight chain oil products such as oils from PE pyrolysis. [86, 125]

In the PP pyrolysis, very little char was produced which was also found to be fine black powder attaching on the wall in the reactor pipe as found in the PE pyrolysis. The amount of char was insignificant thus ignored in the product analysis.

### 6.1.4. Conclusions

In the PP pyrolysis, the pyrolysis reactions started at a similar temperature as that of PE of 450 ºC. In the non-condensable gas product of PP pyrolysis, there were 96% hydrocarbons and 4% hydrogen. Propene accounted for 44% and dominated in the gases.

It is believed that the methyl side group in PP structure is the main reason for high proportion of oligomers of propene in the PP pyrolysis oil products. Based on the analysis of PP pyrolysis liquid, 99 components were found in which 1, 3, 5 - trimethyl - cyclohexane ($C_9H_{18}$), oligomers with 3 propene units, is one of the most dominant components, which accounts for 21% in the liquid products. The low molecular weight oligomers with 2 to 5 propene units (first 13 minutes in GC graph Figure 6-6) accounted for 68% of the total liquid product. The components after the $13^{th}$ minute were high molecular weight oligomers, in which series of isoalkanes, 1-isoalkenes, and α, ω-isodialkenes are the major components. However, the products from PE pyrolysis are straight chain hydrocarbons, 1-alkenes, n-alkanes, and α, ω-dialkenes. No significant amount of isomers was found in the PE product because of the difference between the chemical structure of PP and PE.

## 6.2. Pyrolysis of Polystyrene

### 6.2.1. Materials

There are many types of polystyrene (PS) materials. One of the popular types is high impact polystyrene (HIPS) and thus in this part of study, the virgin HIPS 486B was used as the pyrolysis material in order to maintain consistency. The HIPS 486B is in the form of white oval particles with dimensions of 3 mm x 2 mm (Figure 6-8) and its properties are given in Table 6-4. It is suitable for packaging as sheet application or other applications where high impact strength and rigidity are required.


**Figure 6-8 HIPS 486B sample**

**Table 6-4 The properties of HIPS 486B**

| Item | Unit | HIPS 486B | ASTM method |
|---|---|---|---|
| Melt flow index (200/5) | g/10 min | 2.5 | D1238 |
| Melting point | ºC | 200 – 220 | - |
| Density | $g/cm^3$ | 1.05 | D792 |

### 6.2.2. Experimental

The experiment apparatus used in this part of study was described in Section 5.1.1. In this experiment, 20 g HIPS 486B was placed in the reactor before the experiment started. After this, the apparatus was purged with nitrogen gas for one minute and then the M303PY Gallenkamp electronic furnace was turned on to full scale of 100 power load. As mentioned previous section, three lengths of the reactor pipe were used (200 mm, 280 mm and 380 mm), which corresponded to low, medium and high reflux rates for the distillation. The results from medium reflux rate pyrolysis will be discussed in more details in next section except that the effect of the reflux rate is discussed.

When vapour was produced, it was cooled down in the condenser from which the liquid oil and non-condensable gas were separated and collected separated. For each condition, two duplicate runs were conducted; one for measurement of gas volume production rate and one for gas collection for analysis. Once there was no further vapour coming out from the reactor, the experiment was completed when the reactor outer wall surface temperature reached above 700 ºC.

As described in previous sections, the non-condensable gas product was analyzed through 3000A Micro GC and the liquid pyrolysis product was analyzed through GC and GCMS. In the liquid analysis, pure styrene diluted into n-hexane in a ratio of 1:100 was applied as a standard to identify the produced styrene in the HIPS pyrolysis liquid. In the pyrolysis of PS, the char content was significant. The elements in the char product were analyzed through the JEOL JSM 7000F high resolution scanning electron microscope.

### 6.2.3. Result and discussion

Pyrolysis Process Analysis

The measured temperatures at the reactor outer wall surface ($T_3$) and in the reactor space ($T_1$) as well and the accumulated non-condensable gas volume are shown in Figure 6-9 during the PS pyrolysis with medium reflux rate. From the results, it was found that the non-condensable gases started to be produced at the 14$^{th}$ minute, a similar time as the pyrolysis of LDPE and PP. (Figure 6-9) At that time, the pyrolysis reactions of HIPS 486B started. The wall temperature $T_3$ at this time was 320 ºC which, unlike the pyrolysis of LDPE and PP, continued increasing although a brief plateau was noticed at the temperature of 400°C. The temperature when the gas started to be produced is close to the temperature from other studies which means that the cracking temperature of PS is lower than that of PE pyrolysis. [106] This is attributed to the side group of benzene in the polystyrene which is illustrated as follows.

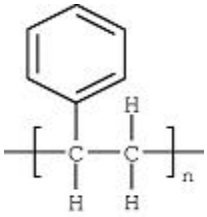

The benzene side group reduced the stability of C-C bond in the PS polymer compared with polymers with -H or -$CH_3$ side groups. Hence, the activation energy of PS pyrolysis is lower than that of PP and PE.[34]

After the start of the pyrolysis reactions at 14 minutes, more non-condensable gases were produced quickly which lasted about 17 minutes until 31 minutes and at that time the major reactions were completed. There was no secondary cracking for gas production appeared from the experimental results and this applied also to both high and low reflux rate distillation pyrolysis experiments. Therefore, in the PS pyrolysis, the primary cracking is dominant and all of the products were generated from the primary pyrolysis. Reflux rate has insignificant effect on the process and the pyrolysis products. This behaviour of the PS pyrolysis was not found in the literature review and is different from the pyrolysis of PE and PP.

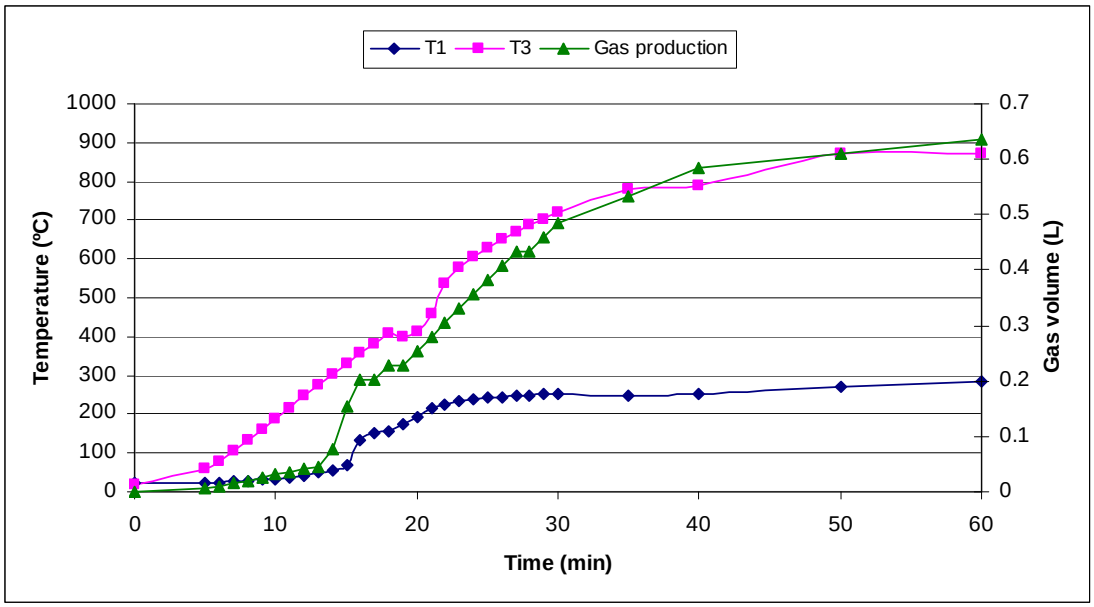


**Figure 6-9 Profiles of reactor outer wall surface temperature, space temperature in the reactor and the accumulated volume of the non-condensable gas in the PS pyrolysis with medium reflux rate**

Product distribution Analysis

In PS pyrolysis with medium reflux rate, liquid product was found to be clear red-brown oils. (Figure 6-10) It is interesting to note that the liquid oil appearance did not change much with the reflux rate. In the chemical analysis of the liquid oil, 52 components were detected which were much less than those of PE pyrolysis liquid or PP pyrolysis liquid. It was found that styrene was the dominant component in the pyrolysis liquid that accounts for 68.6% v/v of the total liquid product.(Figure 6-13) This finding was consistent with to the results of McCaffery and other researchers. [108, 117-118] In different studies, the yield of styrene varies from 50% to 79%. [11-12, 21, 24-25, 34, 37, 106, 114, 126] This variation is likely to be due to differences in pyrolysis conditions. Based on the above discussion, one of the major cracking reactions in the PS pyrolysis is the chain strip cracking in which side functional group (styrene monomer) broke off from the carbon backbone, forming the major component in the liquid product.

From previous analysis on the PE pyrolysis reactions, it has been known that products (including gas and liquid) from the random cracking should distribute continuously from low molecular weight product to high molecular weight products. However, the distribution of the PS pyrolysis products was not continuous. There were only six major components in the liquid products (over 1% v/v). Styrene is from the chain strip cracking. Others are mainly from end chain crackings but not from random crackings.[127] During the pyrolysis, polystyrene was cracked into styrene, non-condensable gases and other light aromatics in the primary cracking. From the discussion in last section, the temperature profiles and non-condensable gas production confirmed that there was no significant secondary cracking occurred on the primary pyrolysis products. Therefore, the PS pyrolysis products were mainly formed during the primary reactions. The proportions of non-condensable gases, liquid oil and char are given in Table 6-4 which shows majority of the products is liquid (93%) with much less gas (4%). However, compared to PE and PP pyrolysis, the char content in the PS pyrolysis was much higher (3%). The char was black chips accumulated on the wall of the pyrolysis zone.

**Figure 6-10 Liquid product from PS pyrolysis with medium reflux rate**

**Table 6-5 Distribution of PS pyrolysis products**

| Product | Gas ($C_1 \sim C_4$) | Liquid ($C_{5+}$) | Char |
|---|---|---|---|
| Collected value | 0.64 L | 18.59 g | 0.6 g |
| Corrected value (g) | 0.81* | 18.59 | 0.61 |
| Proportion | 4% | 93% | 3% |

Note: * The mass of non-condensable gases was calculated from the measured gas volume and the calculated average molecular weight of the gases.

Non-condensable gas product

The volume of non-condensable gas from the PS pyrolysis PS was much less than that of the pyrolysis of HDPE, LDPE and PP as shown in Figure 6-11. The total non-condensable gas from the high reflux rate pyrolysis of 20g PE and 20g PP was 2L which accounted for 16.7% for PE (Table 5-9) and 15.7% for PP (Table 6-2) in the total products. However, for the same material (20g) in the PS pyrolysis, only 0.64L gas was collected and this accounted for 4% of the total products. (Table 6-5) Williams also reported similar findings in his research. [24] Theses differences in the gas production between different types of plastics are the results of different primary cracking process. [83, 94, 97, 106]

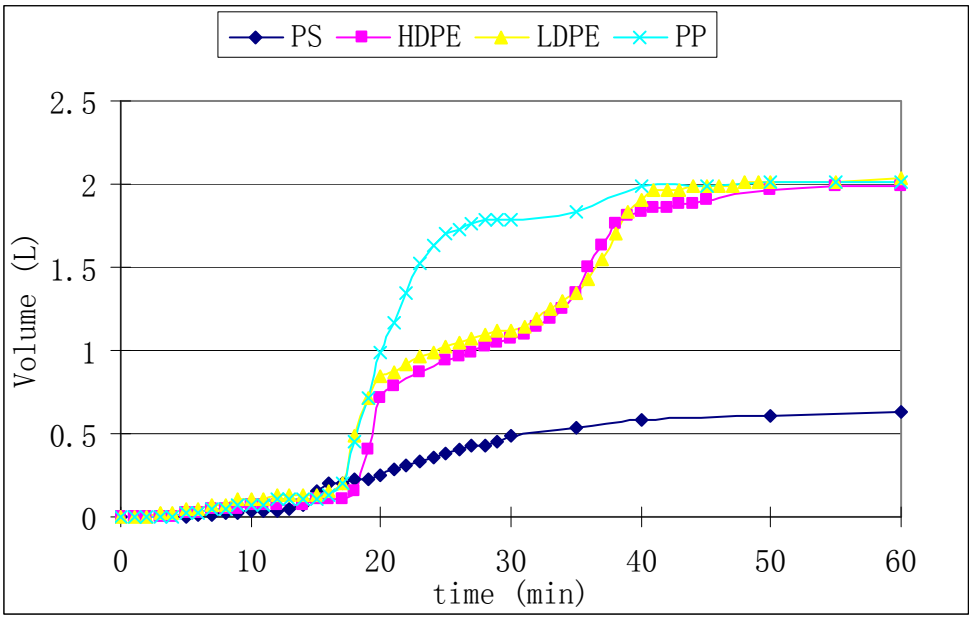


**Figure 6-11 Non-condensable gas production from pyrolysis of of PS, HDPE, LDPE, and PP at medium reflux rate**

The results from the GC analysis of PS pyrolysis gas are presented in Figure 6-12 which shows six major components with corresponding proportion greater than 5%. (The

highest concentration gas component was methane (21%) followed by hydrogen (19%), ethene (17%), propene (16%), unidentified component at peak 13 (13.5%) and ethane (6%). The concentration of the hydrogen gas was the highest in all investigated plastic types. It was also found the concentration of the alkenes was higher than that of the alkanes. Ethene was 3 times as much as ethane. Propene was 11 times as much as propane. Peak 13 was one of the unidentified components. According to its retention time, it could be butene or butane isomer. The overall low proportion of the non-condensable gas and the gas component concentration could be attributed to the operation temperature and the structure of the PS. The results found from this study are similar to those reported by other studies although there are some variations among the reported values. [21, 84, 117-119]

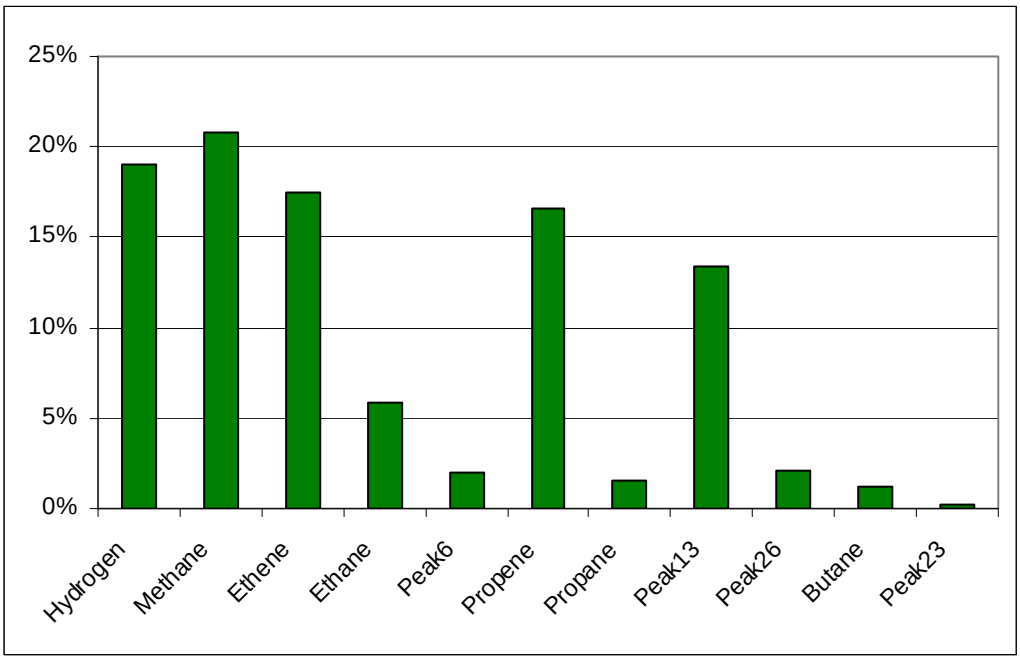


**Figure 6-12 Composition of PS pyrolysis gases with medium reflux rate**

Liquid product

As discussed earlier, the liquid product from PS pyrolysis was the highest (93%) in all of the three types of plastics (PE, PP and PS). (Table 6-5) The GC chromatograph of the PS pyrolysis oil is shown in Figure 6-13 from which it can be seen that there were much less components in the liquid than in the liquids produced from PE pyrolysis and PP pyrolysis. Styrene is a dominant peak that accounts for 68.9% of the liquid. Kaminsky *et al.* reported that in the liquid product from PS pyrolysis in a fluidised bed reactor,

styrene concentration was 64.9% of the feedstock mass..[20] Because the breaking off of the styrene side groups from the carbon backbone of the polystyrene is the major reaction in the PS pyrolysis, it is not surprising that the styrene is the main component in the product. [35, 96, 108, 117-119, 121] In order to confirm this hypothesis and findings in previous studies, a styrene standard was used in this study to identify this outstanding peak in the GC analysis graph following the same procedure as discussed in identifying liquid component in PE pyrolysis liquid. (see Section 5.1.4) This is illustrated in Figure 6-14.

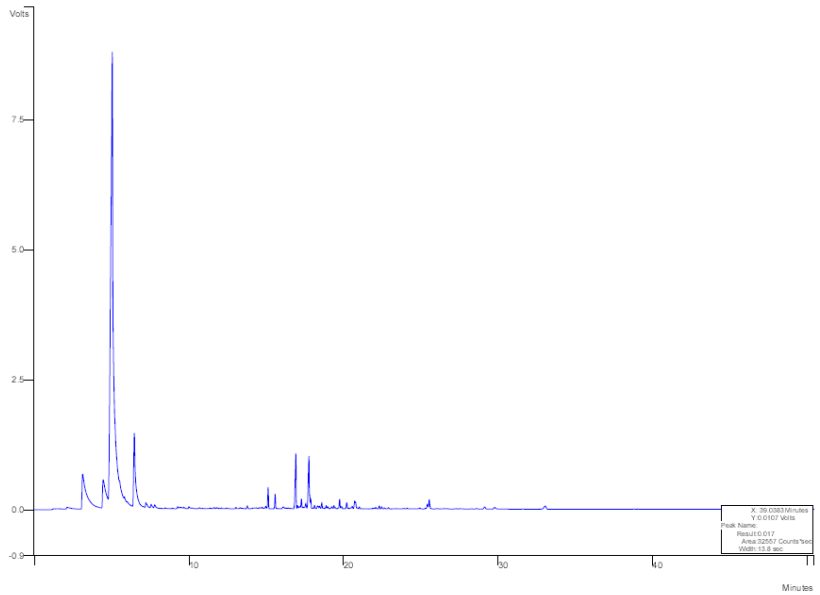


**Figure 6-13 GC chromatograph in analysis of PS liquid pyrolysis product**

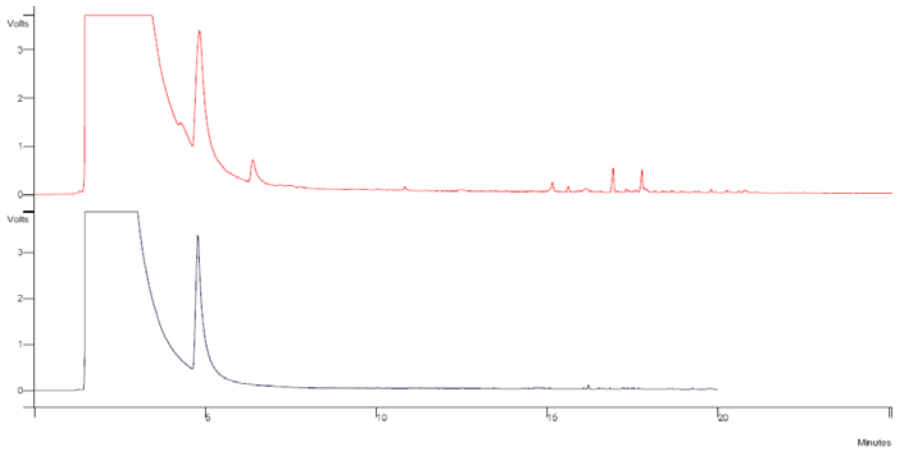


**Figure 6-14 Comparison of styrene standard (bottom graph) and polystyrene liquid product (top graph)**

Note: Top graph: polystyrene pyrolysis liquid in n-hexane with concentration of 1:100 ; bottom graph: styrene in n-hexane with concentration of 1:100.

Based on the comparison of the styrene standard and PS pyrolysis liquid as shown in Figure 6-14, it is further confirmed that the highest concentration component in the PS pyrolysis liquid was indeed the styrene. A similar GC analysis result was reported with all six major components identified by William. [25] Other major five components with concentration over 1% in this research, which were assumed to be the same components as William's GC analysis results. (Table 6-6) The main components in the PS pyrolysis liquid are styrene and other aromatics.

**Table 6-6 Major components in the PS pyrolysis liquid**

| Peak number | Component | Concentration % | Time (Peak on GC chromatograph) (min) |
|---|---|---|---|
| 2 | Benzene | 8.24% | 3.157 |
| 3 | Toluene | 2.93% | 4.487 |
| 4 | Styrene | 68.59% | 5.011 |
| 5 | Trimethlybenzene | 7.51% | 6.475 |
| 21 | Styrene dimer | 2.77% | 16.912 |
| 26 | Phenanthrene | 1.98% | 17.765 |
| Total | | 92.02% | |

Char product

The char was found at the bottom and on the wall in the pyrolysis zone in the reactor where the pyrolysis reaction occurred. No char was found in the transition area between distillation zone and pyrolysis zone which further confirmed that the PS reflux products

would not be further cracked in the distillation like PE or PP. The proportion of char from PS pyrolysis was 3%, which is much higher than that from PE and PP pyrolysis (less than 0.5%). The appearance of the char from PS pyrolysis was also different from that in the PE or PP pyrolysis. The char from the PS pyrolysis was 1 mm x 1 mm black chips with metallic shine on their smooth surfaces. The element in the char was analyzed with a scanning electron microscope (SEM) as shown in Figure 6-15. The analysis results based on ZAF standard are given in Table 6-7. The PS pyrolysis char consisted of only carbon (96.61%) and oxygen (3.39%).

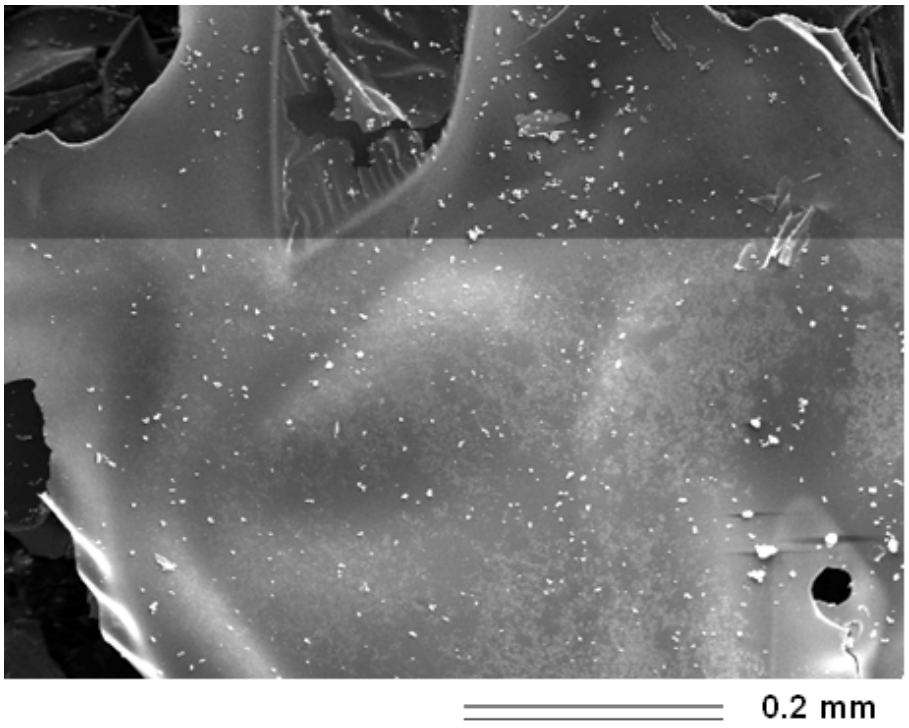


**Figure 6-15 SEM image of the surfaces of PS pyrolysis char**

**Table 6-7 ZAF Method Standard less Quantitative Analysis**

| Element | (keV) | Mass (%) | Error (%) |
|---|---|---|---|
| C | 0.277 | 96.61 | 0.18 |
| O | 0.525 | 3.39 | 2.80 |
| Total | | 100.00 | |

### 6.2.4. Conclusions

In the PS pyrolysis, the side group of polystyrene has very significant effects on the pyrolysis process and the products. The side group, styrene monomer, reduces the cracking temperature at the start point to about 320 ºC. Chain strip cracking is the main reaction in the initial reactions. As a result, the yield of styrene is 63.8 % w/w of the total feedstock. Different from PE and PP pyrolysis, reflux distillation has insignificant effect on the PS product distribution because the molecular weight of the primary products is relatively light. The percentage of non-condensable gases, oils and char is 4%, 93% and 3%; respectively. The composition of the gases consisted of 19% hydrogen, and other hydrocarbon gases. The liquid contained 68.6% styrene, and other aromatics. The elements found in the char are mainly pure carbon with a small amount of oxygen.

## 6.3. Pyrolysis of the virgin and the post-consumed plastic mixture

### 6.3.1. Materials and apparatus

This part of the study aimed at the conversion of waste plastic into diesel or other fuels through pyrolysis. Thus, pyrolysis experiments of post-consumed plastics were conducted using post-consumed plastics provided by Green Fuel Technologies Ltd. (Figure 6-16) The post-consumed plastics were plastic chips with a mixture of 50% PE, 25% PP, and 25% PS. The plastic chips were pre-washed but tags and labels were not removed from the plastics, which would have some influence on the pyrolysis process and the products.


**Figure 6-16 Post-consumer plastic mixture of PE, PP, and PS**

For comparison purposes, mixed virgin plastics with 25% of HDPE, LDPE, PP, and PS each were also pyrolyzed using the same apparatus as used in the post-consumer plastics. The properties of the virgin plastics were illustrated in the previous sections. Thus, the interaction between PE, PP, and PS in the pyrolysis reactions can be revealed. The effect of the contamination of post-consumer plastics was also investigated.

The pyrolysis apparatus used were the same one used in the previous experiments. (Figure 5-2) In this part of study, the longest reactor pipe (380 mm) was applied in order to achieve the best quality of liquid oil due to the secondary cracking of the PE and PP primary products. The Micro GC and the GC CP-3800 with the same analysis program were used to analyze non-condensable gases and liquid oils.

### 6.3.2. Experimental

There were two runs of the experiments, one for post-consumer plastic mixture and one for virgin plastic mixture. Both of the virgin and the post-consumer plastic went through the same pyrolysis process. In each run, 20 gram samples were placed in the 380 mm long reactor pipe first before the experiment started. Then the system was purged by nitrogen gas. After that, the furnace was turned on at full power load at scale of 100 which was equivalent to 881 W. During the experiment, the temperature of the reactor outer wall surface ($T_3$) and the temperature in the reactor space ($T_1$) as well as the non-condensable gas volume were recorded every one minute since the power was on. The experiment was stopped 60 minutes after the start, at which time no further products came out and $T_3$ was above 800 ºC.

The non-condensable gas and the liquid products were collected and analyzed separately. The liquid was analyzed using GC and GC-MS to investigate the components.

### 6.3.3. Result and discussion

From analysis of the experimental results, it was found that the temperature profiles and the gas production curve in the pyrolysis of the mixed post-consumer plastics were similar to those of the pyrolysis of mixed virgin plastics due to the dominant PE (50%) in both cased. This can clearly be seen from the comparison of the experimental results of pyrolysis of virgin LDPE (Figure 5-8) and those of pyrolysis of mixed post-consumer plastics. (Figure 6-17) It can be observed that in both cases, the gas production had two

fast production stages, one after about 18mintes and one after 32 minutes. The first one corresponded the primary cracking and the second one corresponded to the secondary cracking of the dominant feedstock, PE. However, in pyrolysis of mixed post-consumer plastics, there was another small peak in the gas production at about 18 minutes which was the gas production from PS pyrolysis. It is most interesting to note from the pyrolysis of mixed plastics that there was a reduction in reactor wall surface temperature ($T_3$) after the small peak in the gas production. This is the evidence that the primary cracking temperature of the PS is lower than that of PE and PP.

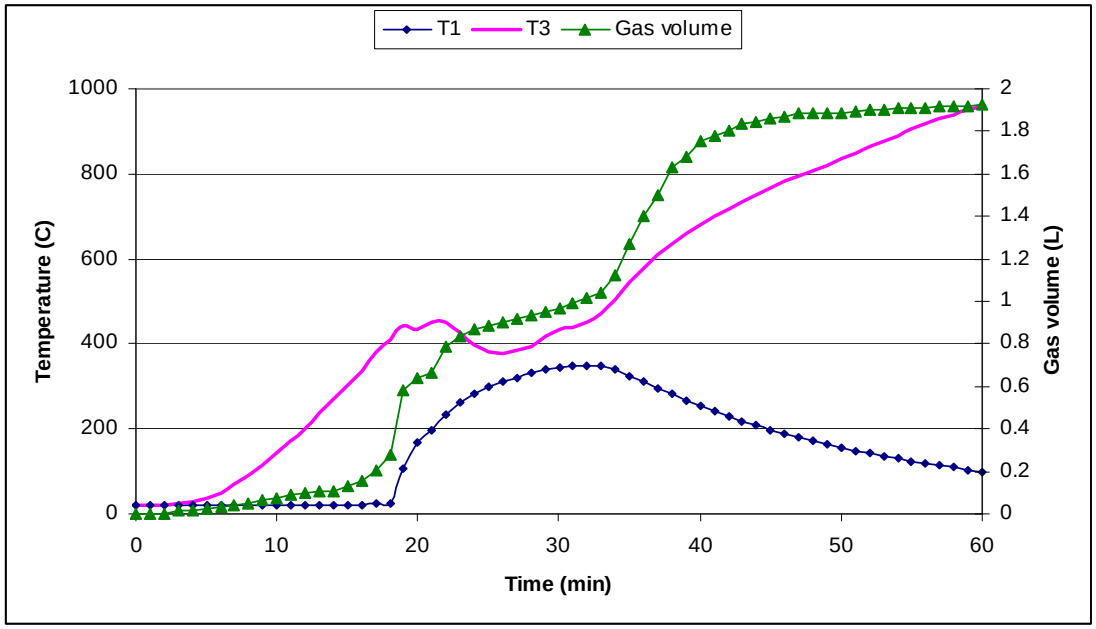


**Figure 6-17 Profiles of $T_1$, $T_3$, and non-condensable gas production in the pyrolysis of post-consumer plastic mixture**

The liquid product from pyrolysis of mixed plastic mixture was analyzed through GC and the results are shown in Figure 6-18. Although the composition of the product from the pyrolysis of mixed plastics is complex, it was found that most of the peaks present in the mixture product could be identified form the individual plastic pyrolysis products. (Figure 6-18) However, the peaks in the pyrolysis of mixed plastics are more plat without any single outstanding peak observed. The major components from individual plastic pyrolysis like 1-alkene and n-alkane groups from PE pyrolysis and aromatics from PS still remained high concentration in the mixture product.

The components in the liquid product from post-consumer and virgin plastic mixtures were very similar as shown in the bottom two graphs in Figure 6-18. The percentage of each component varied slightly but not significantly. In both cases (mixed post-consumer plastics and mixed virgin plastics) styrene was identified as the dominant component in the liquid products with corresponding concentration of the styrene being 23.5% and 45.9%, respectively. The difference could be due to the difference of the PS proportion in the post-consumer plastic mixture as this was supplied from industry. Although the PS proportion was 25% in the bag supplied, there could be a higher percentage of PS in the tested samples for the post-consumer plastic mixture. The proportion of PS in the mixed virgin plastics was more reliable as the test mixture was prepared by mixing required masses from each type, 25% PS in the tested virgin plastic mixture.

Based on the results from the pyrolysis of mixed virgin plastics, the percentage of styrene in the total product was 19.3%, which was derived from the chain strip reaction of PS. This was calculated from GC analysis result (23.5% of the liquid product from virgin plastic mixture) and the final product distribution (82% liquid product in Table 6-8). The conversion was then calculated to be 77.1%, which is higher than that in pyrolysis of pure PS (63.8%). Therefore, the interaction among the different type of plastics promoted the conversion of styrene in the PS pyrolysis.

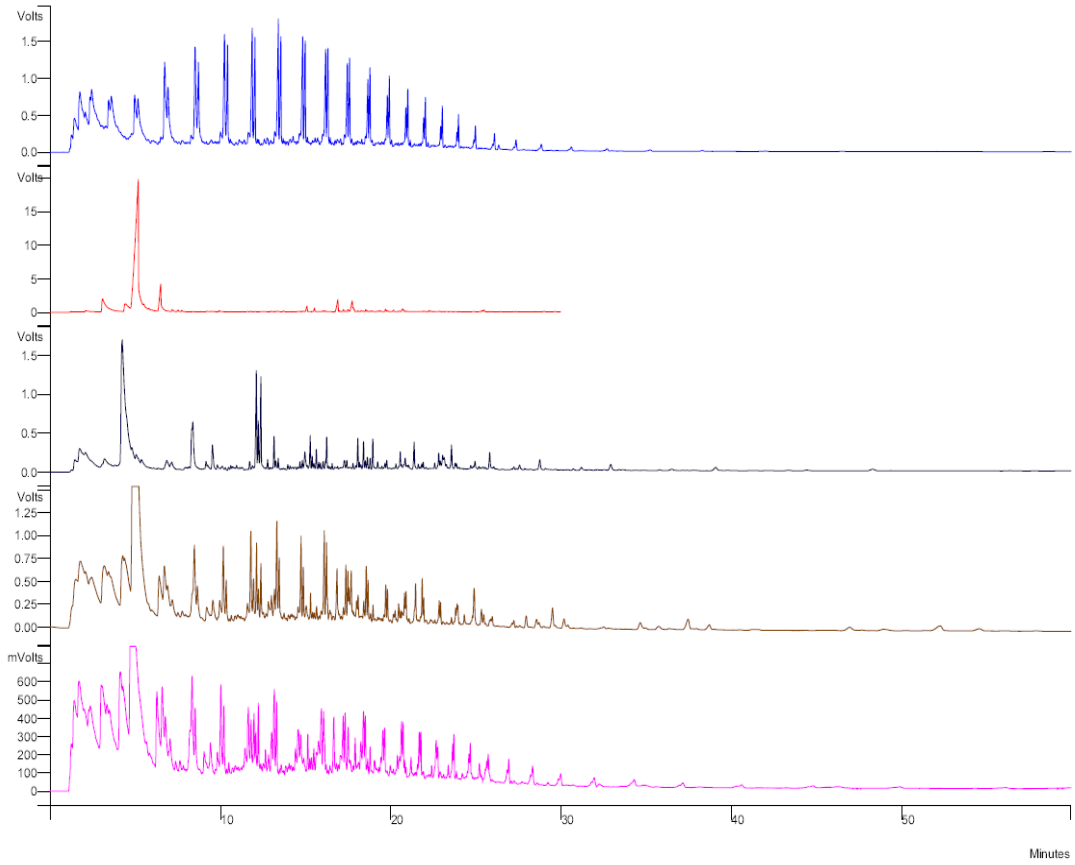


**Figure 6-18 Liquid products from individual and mixture of plastics pyrolysis**

In the figure, the top graphs are for virgin PE, virgin PS and virgin PP. The bottom two are for mixed post-consumer plastics (second from bottom) and mixed virgin plastics (bottom).

From the gas production in pyrolysis of individual plastics (Figure 6-11), the expected gas volume was calculated to be 1.65L from the 20g mixed virgin plastics if there were no interaction among the plastics. However, the volume of the collected non-condensable gases from the pyrolysis of mixed virgin and post-consumer plastics was 2.13L and 1.92L, respectively. The gas volume of both plastic mixtures is higher than the expected gas volume, 1.65L. Therefore, the interaction promoted the gas production. It was reported that the increased proportion of gas product could be taken as an indicator for the interaction of various plastic. [21, 24, 108] However, the effect of mixed plastic interaction in this study was not as significant as reported by Williams. [21, 24] This is likely to be due to the higher PS composition in the post-consumer

plastic mixture in this study than that in William's study. In high reflux rate pyrolysis, the percentage of non-condensable gas from pyrolysis of individual plastics was 4% for PS, 18.3% for LDPE and 15.7% for PP. (Table 6-8) As a result, higher PS content led to a lower proportion of non-condensable gases in the mixture of PP, PE and PS.

There was a small quantity of char found at the bottom of the reactor in the pyrolysis of mixed plastics. Most of the char was black carbon chips with metal shine. This char was mainly generated from pyrolysis of PS as the char content from the PS pyrolysis was much higher than other plastics. The char content in the post-consumer plastic product was three times as much as that in the virgin plastic product, again likely due to the higher PS content in the mixture and the paper contamination on the post-consumer plastics.

**Table 6-8 Product distribution from pyrolysis of individual virgin plastics, and pyrolysis of mixed virgin plastics and mixed post-consumer plastics**

| Product distribution | Gas | Liquid | Char |
|---|---|---|---|
| LDPE | 18.3%* | 81.7% | - |
| PP | 15.7%* | 84.2% | - |
| PS | 4.0%* | 93.0% | 3.0% |
| Virgin mixture* | 17.5%** | 82.0% | 0.5% |
| Post-consumer mixture** | 7.2%** | 92.3% | 1.5% |

* The value is calculated from molecular weight and the volume of collected gases.

** The value is calculated by the difference of material and the other two products.

### 6.3.4. Conclusions

The product from pyrolysis of the mixed PE, PP and PS is very complex. However, most of the major components are also present in the products from pyrolysis of individual plastics. The effect of the interaction among the plastics during the pyrolysis on the distribution of liquid product is not significant. However, the interaction promotes the production of non-condensable gases during the pyrolysis.

Styrene is the dominant component in the product, which is promoted by the interaction. The char content in the plastic mixture is small, and is mainly determined by the content of PS in the mixture. Contamination of paper labels on the post-consumer plastics may result more char content in the product.

# 7. Study on Semi-scale Pyrolysis Plant

## *7.1. Introduction*

Pyrolysis of waste plastic has been intensively investigated in recent years because of the concerns for the solid waste disposal and the crisis of future energy. There are a number of pyrolysis plants in the world to convert waste plastic to energy and liquid fuels. [18] In Europe, 22% of the post-consumer plastics have been treated for energy recovery. A Japanese pyrolysis plant was recently built in Niigata city with an official annual capacity of 6000 tons and this process is shown in Figure 7-1. [89] Another pyrolysis plant was recently constructed in Sapporo which has a capacity of 40 tons municipal waste plastic per day. However, there is no commercial plant built in New Zealand for the pyrolysis of waste plastic. [7]

Due to the lack of understanding of the pyrolysis conditions on the products, the products are only used as boiler fuel or for power generator. In addition, there are some issues and concerns in the waste plastic pyrolysis which limit the commercialisation of the technology. In the municipal waste plastic stream, there is a certain amount of PVC and PET. The major products from pyrolysis of PET and PVC contain benzoic acid and hydrogen chloride which are not desirable in the transport fuels. Therefore, the current pyrolysis plants for treating municipal waste plastic normally have to apply a dechlorination and HCl removal treatment. [17-18]

In this part of research, the aims were to design and build a semi-scale continuous pyrolyzer to experimentally investigate the pyrolysis products using virgin and post-consumer PE. Previous investigation in this study has found that the three types of plastics have similar cracking temperature and the pyrolysis products are mainly hydrocarbon products. Therefore, the effect of semi-scale plant on the product of PE pyrolysis was experimentally investigated in this part of study. The difference of batch and continuous processes was also investigated. The actual energy consumption of the process can be measured on this semi-scale plant.

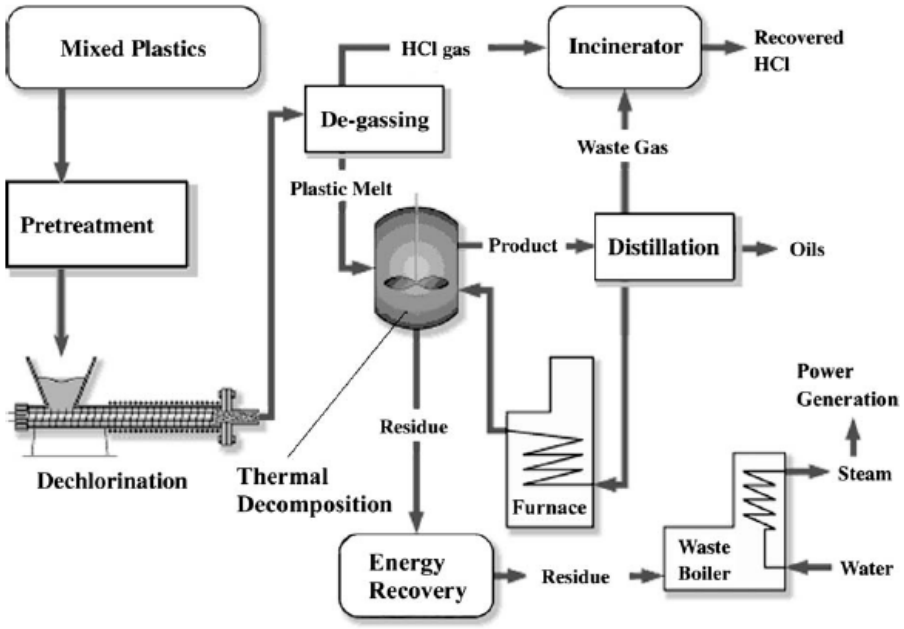


**Figure 7-1 Scheme of the Niigata pyrolysis plant [89]**

Most of the current commercial pyrolysis plants are using continuous pyrolysis process while plants applied for research purposes are normally laboratory scale, batch process apparatuses. This part of the study will use the semi-scale continuous pyrolysis system to develop optimal design and operation conditions thus to maximise desired diesel range products. A typical continuous pyrolysis plant consists of three sections: feeding system, pyrolysis section, and product separation, therefore, each part of the system will be analysed and its design will be determined based on the follow analysis.

Pyrolysis reactions occur in oxygen free or inert environment. Therefore, the feeding system has two major functions: prevent the air flowing into pyrolyzer and control the feeding rate. In practical operation, the feeding system also needs to be able to prevent pyrolysis vapour escaping from the reactor. A popular feeding system applied in the continuous reaction is to pre-melt the plastic into liquid and send the melted plastic into the reactor. The air is removed from the melted plastic by this way. Due to the poor heat conductivity and the high viscosity, plastic can hardly be heated evenly. Some types of plastic may start cracking before others melt because of the temperature gradient within

the melting chamber. Another popular system is to use inert gas to purge the air off from the feedstock and feed the plastic into the reactor with an extruder. The advantage of using an extruder is that the feeding rate can be precisely controlled.

In the pyrolysis section, reactor type is a key factor that determines the retention time, product distribution and separation under given operation conditions. In the literature review, fixed-bed, fluidized bed, and rotary kiln type of reactors have been reported. [21-22, 24, 29, 44-46, 61, 69, 87-88, 111, 115, 128-129] Each type of the reactor has different features and advantages.

Fixed bed reactor is relatively simple in design and construction, and normally used in batch process. It can achieve very high conversion efficiency with proper control. The quality of the oil product can be equivalent to the mixed conventional fuels. [61] However, large temperature gradients exist in the reactor, which cause difficulties of temperature control and scale-up problems. The heat transfer is not efficient for a fixed bed reactor; therefore, it requires large surface of heat exchanger. The size of feedstock particles should be very small and uniform in order to improve the heat transfer. Due to the above features, fixed bed reactor is normally applied in research but not for large commercial use. An example of the fixed bed reactor is shown in Figure 7-2. [24]

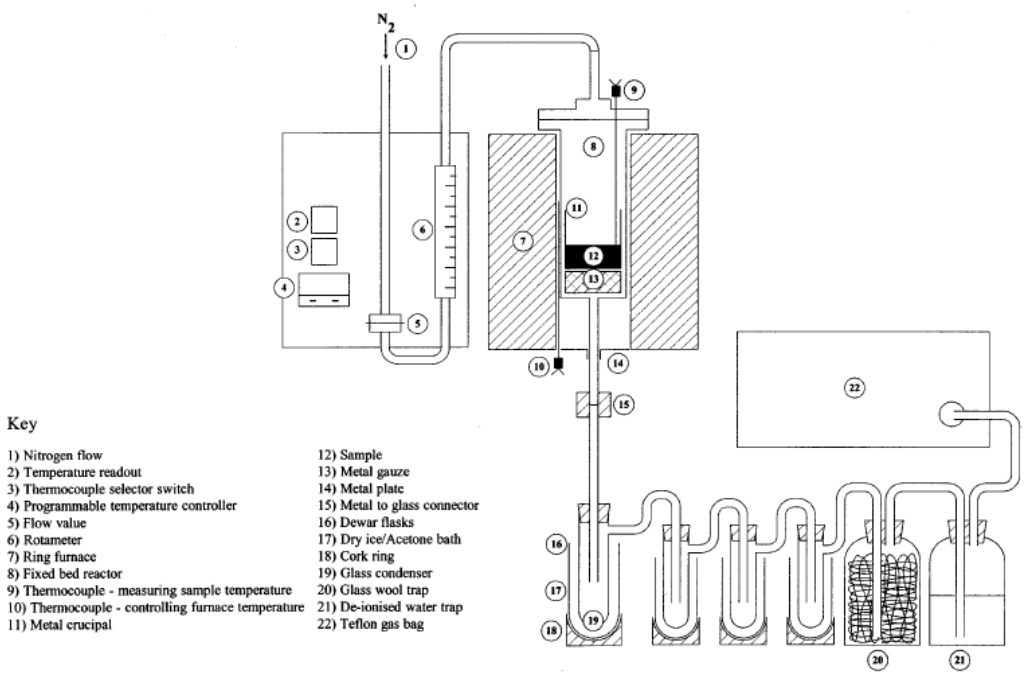


**Figure 7-2 Scheme of a fixed bed apparatus [24]**

Fluidized bed reactor has been commonly used in large scale pyrolysis plants as it can provide very efficient heat transfer and much less temperature gradient than those of a fixed bed reactor. The efficient heat transfer is due to the uniform turbulent mixing between carrier gas and solid particles in the reactor. (Figure 7-3) [88] However, the use of bed material and separation of the carrier gas may be disadvantageous which can reduce the conversion efficiency and the quality of the products compared to the fixed bed reactor Fluidized bed reactor is suitable for continuous operations which produces pyrolysis product with consistent quality. The small temperature gradient and good temperature control in the fluidised bed reactor allow it to be used in large scale operations. Additional advantages of the fluidized bed reactor include flexibility of using catalyst and varying retention time by changing the carrier gas velocity.

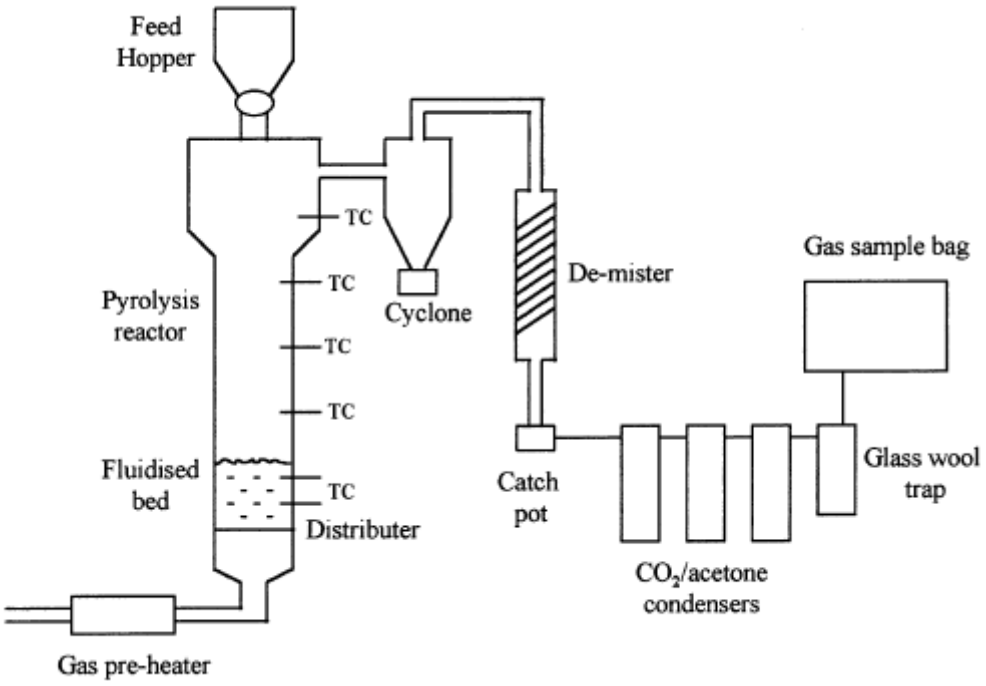


**Figure 7-3 Scheme of a fluidized bed apparatus [88]**

Rotary kiln reactor is another popular type for commercial applications. The rotary kiln reactor is a horizontal cylinder in which the feed plastic is moved from one end to the other by a screw. The heat is provided by the heating source in the cylinder shell jacket through the wall to the moving plastics inside. The heat transfer in the rotary kiln reactor is not as good as in the fluidised bed reactor thus long cylinder kiln is normally required for long retention time. [61] There is a high longitudinal temperature gradient along the length of the rotary kiln reactor. The cylinder kiln has different functions along the process as shown in Figure 7-4 for pyrolysis of LDPE. [45, 60] In the figure, the first section of the screw under the hopper of LDPE-oil mixture moves the feedstock into the pyrolysis section. The temperature in the pyrolysis section is above the cracking point of LDPE thus the LDPE is pyrolyzed in this section. The products are then removed to the next section for product collection and separation. The rotary kiln reactor has the primary pyrolysis reactions only so that there are less non-condensable gases and more heavy hydrocarbons produced during the process with regard to conventional fixed-bed reactors. [29-30] This type of reactor is relatively easy to operate for plastic feeding and product removal. Particularly, the char generated from the plastics can be removed from the pyrolysis section.

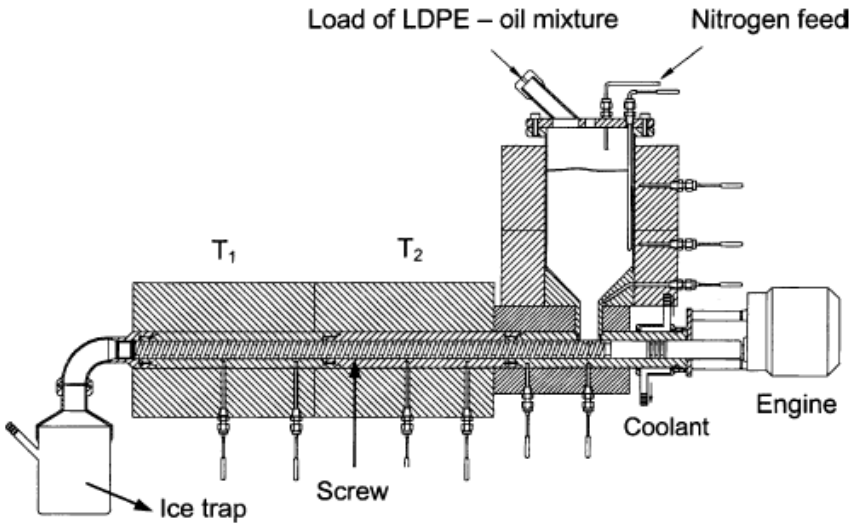


**Figure 7-4 Scheme of a rotary kiln apparatus [45, 60]**

## 7.2. Design and construction of the continuous waste plastic pyrolysis system

In this part of the study, a continuous pyrolysis apparatus was designed and built for investigating and optimisation of the waste plastic pyrolysis process in a large scale reactor. The apparatus was designed for pyrolysis of PE, PP, and PS and their mixture. The differences between virgin and post-consumer plastics in the continuous process were investigated as well. The products were separated by its boiling points and collected as wax, diesel, petrol, and non-condensable gases. The continuous process can then be controlled by altering operation conditions and system configuration to achieve the optimized product distribution. As one of the major objectives for this study was to maximize the diesel range product, the process will be optimized towards high diesel range distribution. The diesel range product produced from normal pyrolysis systems cannot meet New Zealand diesel regulation requirements as outlined in Table 7-1. [130] However, it was hoped that the products from this continuous process apparatus designed in this study would be able to meet these regulation requirements. The diesel derived from plastic has some advantages compared with the retailed diesel derived from cruel oil.

**Table 7-1 New Zealand requirements for diesel regulation [130]**

| Property | Limits | Test method |
|---|---|---|
| Fatty acid methyl esters (% volume) | 5 maximum | EN 14078 |
| Density at 15°C (kg/m$^3$) | 820 minimum<br>850 maximum | ASTM D1298 |
| Distillation—95% volume recovered at (°C) (T95) | 360 maximum | ASTM D86 |
| Cetane | 51 minimum cetane index, or 51 minimum cetane number and 47 minimum cetane index | Cetane number: ASTM D613 or ASTM D6890<br>Cetane index: ASTM D976 |
| Water content (mg/kg) | 200 maximum | IP 438 |

| Property | Limits | Test method |
|---|---|---|
| Total contamination (mg/kg) | 24 maximum | IP 440 |
| Colour (ASTM colour) | 3.0 maximum | ASTM D1500 |
| Cloud point (°C) and cold filter plugging point (°C) | Summer maxima: Auckland and Northland: +6 cloud point; rest of New Zealand: +4 cloud point. Winter maxima: +2 cloud point and –6 cold filter plugging point | Cloud point: ASTM D5773 cold filter plugging point: IP 309 |
| Sulphur(mg/kg) | 50 maximum<br>10 maximum on and from 1 January 2009 | IP 497 or ASTM D5453 |
| Polycyclic aromatic hydrocarbons (% mass) | 11 maximum | IP 391 |
| Filter blocking tendency | 2.5 maximum; fuel must be of acceptable filterability so that it is fit for common purposes | IP 387 or ASTM D2068 |
| Lubricity—HFRR wear scar diameter at 60°C (μm) | 460 maximum | IP 450 |
| Viscosity at 40°C $mm^2$ per second | 2.0 minimum<br>4.5 maximum | ASTM D445 |
| Oxidation stability (g/m3) | 25 maximum | ASTM D2274 |
| Carbon residue (on 10% distillation residue) (% mass) | 0.2 maximum | ASTM D4530 |
| Copper strip corrosion (3 hours at 50°C) | Class 1 maximum | ASTM D130 |
| Ash (% mass) | 0.01 maximum | ASTM D482 |
| Flash point (°C) | 61 minimum | ASTM D93 |

Table 7-1 New Zealand requirements for diesel regulation (Continued)

### 7.2.1. Determination of apparatus functional sections

The continuous process requires a system that can feed the material continuously. In order to control the feeding rate, an auger with a rotation speed controller was applied to feed the plastic particles into the pyrolyzer. Another requirement of the feeding system is to prevent the air contamination into the reactor or to prevent the pyrolysis vapour leaking from the reactor into the ambient atmosphere. An auger with sufficient length and relatively small feedstock dimensions can prevent the pyrolysis vapour leaking from the reactor. (Figure 7-6, Figure 7-8)

The batch reactor that used previously was a relatively slow pyrolysis process based on the heating rate and the cracking temperature achieved. The power input in the batch reactor was not sufficient to pyrolyze the plastic and to vaporize the products in a few seconds. Therefore, the temperature remained at the plastic pyrolysis point for several minutes during the pyrolysis. In this part of the study, a fixed-bed reactor was selected based on scale of the system and the results from the previous experiment using the batch reactor. Based on the previous experiments, char accumulated at the surface where the reactions occurred. Therefore if this occurs in the fixed bed reactor, the char can not be removed easily. The present of char affects the heat exchange and limits the maximum process running time. The maximum capacity of the slow pyrolysis plant was also limited by the input power and the feeding rate. In normal operation in the continuous fixed bed pyrolysis reactor, the energy transferred to the plastics is equal to the energy requirement for the pyrolysis and the vaporization. In the mean time, the mass of the plastic fed in is the same as that of the plastic vaporized; therefore, the liquid level should remain constant in the reactor. The temperature of the melted plastics also remains constant close to the cracking temperature.

From the previous experiments of batch pyrolysis of the plastic, the liquid is a mixture of hydrocarbons with various molecular weights. This mixture needs to be separated through distillation into different fractions in order to obtain liquid products which match the current retail liquid fuels. The function of the separation section on the apparatus is to separate hydrocarbons into different ranges which correspond to retails

products such as diesel, petrol, wax and LPG. According to the boiling points of the products obtained from previous experiments, the products can be separated into four groups: hydrocarbons heavier than diesel (wax), hydrocarbons in the range of diesel, hydrocarbons lighter than the diesel; and non-condensable gases (LPG). Conventional diesel is a mixture of hydrocarbons from $C_{10}$ to $C_{25}$ with a normal distribution as shown in Figure 7-5 in which the liquid products from previous batch pyrolysis of LDPE are also illustrated. To separate the LDPE pyrolysis products, two re-boilers (Pot 1 and Pot 2) are designed to control the boiling points of the liquid products. Two corresponding distillation columns are also designed, each being mounted above the corresponding reboiler to control the desired fractions of the liquids.

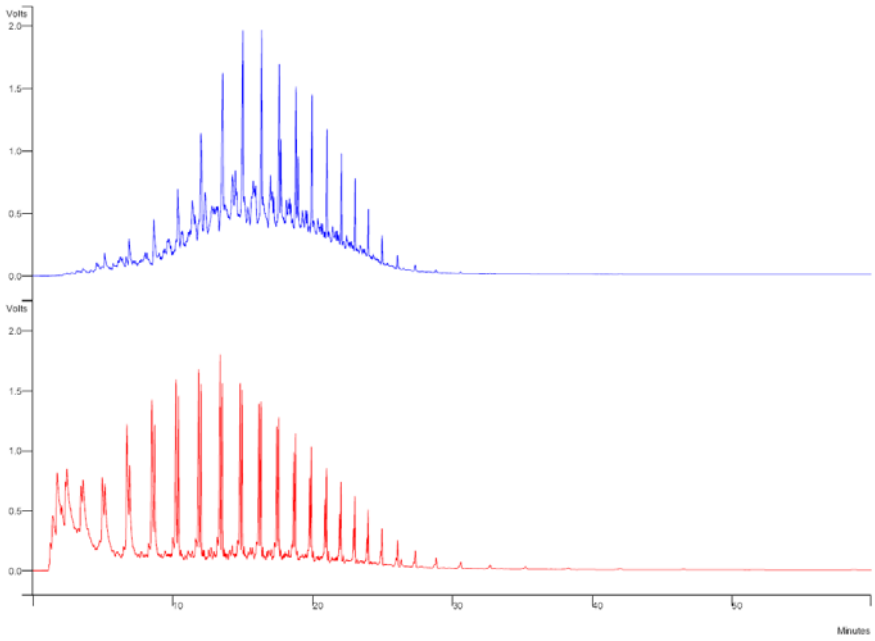


**Figure 7-5 GC results of diesel (top) and PE condensable products (bottom)**

The designed continuous pyrolysis apparatus is shown in Figure 7-7. Figure 7-7 is for the actual system and Figure 7-8 is for the flow sheet diagram. This system can produce four groups of products: wax, high quality diesel, petrol range product, and non-condensable hydrocarbon gases. The pyrolysis system also includes safety guard devices to prevent potential hazards, failure of electrical parts, or other accidental leaking and breakage.

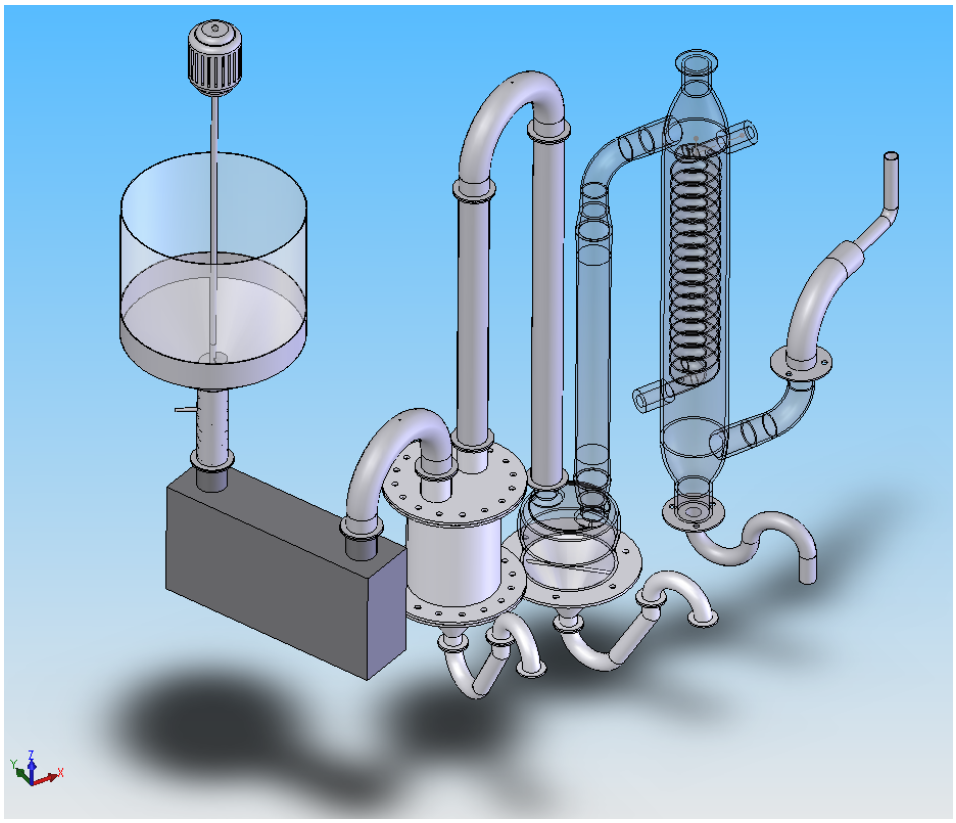

Figure 7-6 Engineering scheme of the apparatus


**Figure 7-7 Photo of the apparatus**

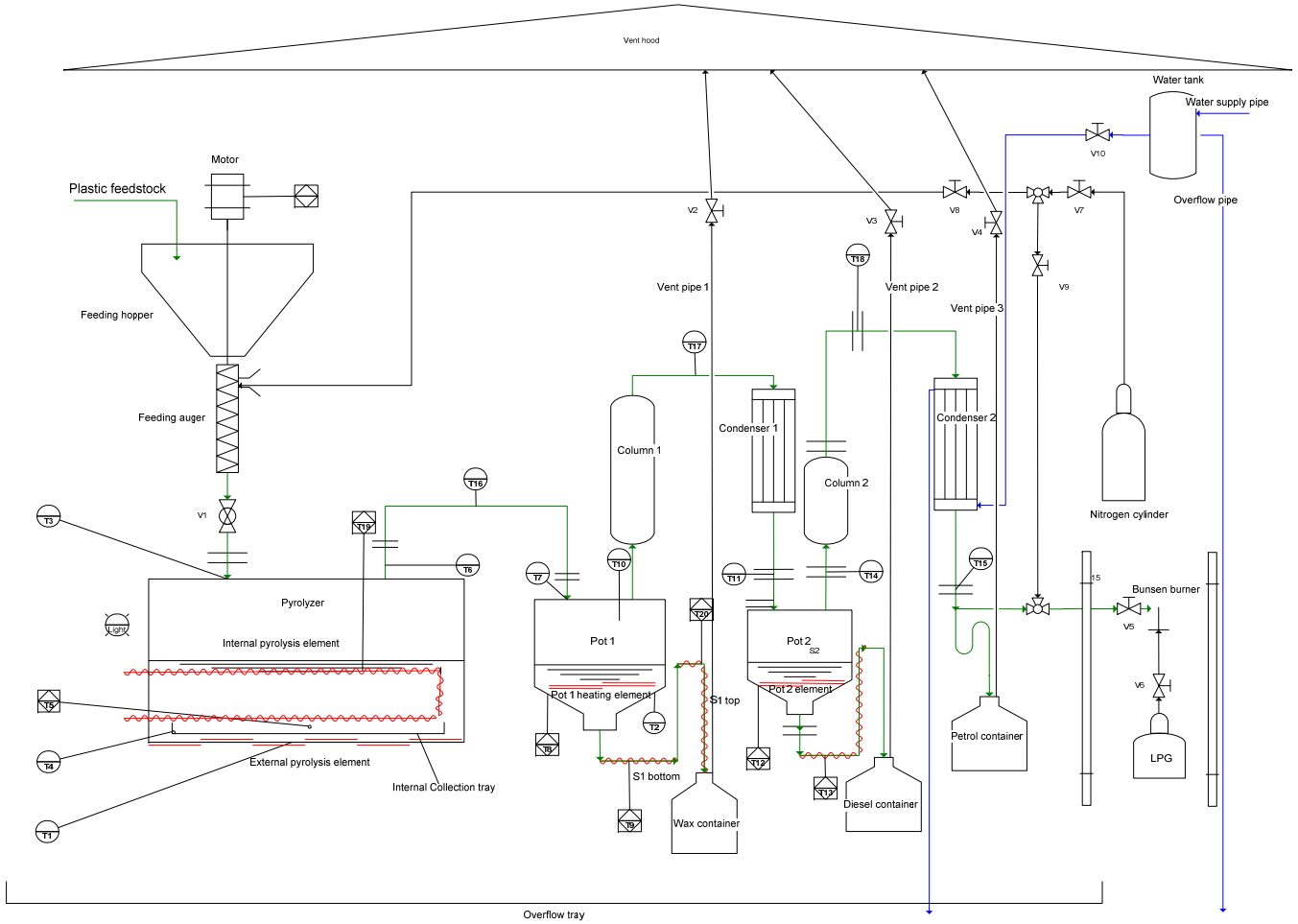


**Figure 7-8 Scheme of continuous pyrolysis apparatus**

### 7.2.2. Design calculations of the pyrolysis apparatus

According to the energy balance calculation described in Section 3.2.2, the theoretical energy demand for pyrolysis of 1 kg PE is 1048 kJ to generate a product of10% w/w $C_3H_6$, 30% $C_8H_{16}$, 40% $C_{16}H_{32}$ and 20% $C_{28}H_{56}$. The further calculations for energy demand feeding rate in the designed system are based on this product distribution. However, in practical pyrolysis, other factors affecting the energy requirements should be considered for the design which include heat loss, reflux rate and retention time.

The feeding rate of the waste plastic (kg/min) to the pyrolysis system is mainly determined by the performance of the pyrolysis reactor section. Therefore, the calculations of energy demand and feeding rate begin with the pyrolyzer. There is a total 10 kW energy supply to the pyrolyzer, 6 kW element installed on the bottom (inside) of the pyrolyzer and a 4 kW element installed on the pyrolyzer wall. (Figure 7-9) The total 10 kW power supply is equivalent to 36MJ energy input in one hour. This amount of energy can theoretically convert 34.4 kg/h PE into pyrolysis products based on the theoretical energy requirement, 1048 kJ/kg. Assuming that 30% of the energy is lost during the pyrolysis process, the estimated maximum capacity of the pyrolyzer is then estimated to be 24 kg/h PE into the hydrocarbons with the distribution given early.

The designed pyrolyzer system is operated in slow pyrolysis. The element on the reactor wall is folded within 100 mm from the reactor bottom and the power output is adjusted by the level of the melted plastics in the reactor. The maximum capacity can only be achieved when the internal element is completely immersed in the melted plastics, which means that level of the melt plastics is higher than 100 mm from the bottom. When the pyrolyzer is operated with the level of the melted plastic less than the 100 mm mark, the power to the elements is turned off thus the level of the melted plastic will increase. Alternatively, when the melt plastic level in the reactor is 100 mm or higher, both of the internal and the external elements are turned on, thus

providing a higher pyrolysis production. When the feeding rate is lower than the maximum capacity of the reactor, the power will automatically turned off till the temperature drops below the pre-set cracking temperature by the feedstock or heat loss. The feedstock was heated from under cracking temperature to the cracking temperature until all feedstock was completely cracked and vaporized. Therefore, there is not significant effect of the batch and the continuous processes on the cracking reactions because both feedstocks were cracked as slow process. The only difference is that the feeding and the cracking are continuous in the continuous process while the feedstock is fed as a batch before the cracking in the batch process.

The pyrolyzer is shown in Figure 7-8. The main part of the pyrolyzer is a chamber with dimensions of 100 mm (width) x 400 mm (length) x 200 mm (height). The wall of the chamber is made of stainless steel. On the two 100 mm x 200 mm sides, two pieces of glass are installed as windows that can continuously work under 720 ºC.

**Figure 7-9 Photo of pyrolyzer**

As shown in Figures 7-7 and 7-8, there are a series of separation devices following the pyrolyzer which can separate the pyrolysis products into wax, diesel, petrol and non-condensable gases, by controlling the boiling temperatures. These can be achieved by a temperature controlled connection pipe, two distillation columns with reboilers followed by a condenser. The connection pipe and the first reboiler (Pot 1) are used to condense and collect the wax from the products. After this, the hydrocarbons in the diesel range are separated in the first distillation column (Column 1) and are collected from the second reboiler (Pot 2). Then the hydrocarbons lighter than the diesel range (petrol) are separated in the second distillation column and condensed in the downstream cooler. Once the petrol range hydrocarbons are condensed, they are collected in the petrol tank installed beneath the cooler. After the cooler, the remaining non-condensable gases flow out of the system and flared off with the Bunsen burner.

The separation of the diesel range product requires the adjustment of the highest and lowest boiling points, and the level of separation. To achieve the boiling temperature required, the power input into the two reboilers can be adjusted based on the required boiling points of the liquid products to be collected. Two packing columns are designed to control the level of the hydrocarbon separation. The dimensions including height and the packing materials of the columns can be changed based on the separation requirements. The actual maximum production rate must not exceed the theoretical capacity of the pyrolyzer because other factors like heat loss will significantly reduce the actual maximum capacity of the production. Therefore, the theoretical maximum production rate, 34.4 kg/hr (9.56 g/s), was accepted for the calculation of the dimensions of the separation pipeline. According to the maximum production rate, the maximum volume of the product and the volume at different temperature can be calculated. (Table 7-2)

**Table 7-2 Expected value of products**

| Product | Expected proportion | mass flow (g/s) | MW (g/mol) | mol | Expected volume flow at 400ºC (L/s) |
|---|---|---|---|---|---|
| C3H6 | 10% | 0.96 | 30 | 0.0319 | 1.76 |
| C8H16 | 30% | 2.87 | 112 | 0.0256 | 1.41 |
| C16H32 | 40% | 3.82 | 224 | 0.0171 | 0.94 |
| C28H56 | 20% | 1.91 | 392 | 0.0049 | 0.27 |
| Total | 100% | 9.56 | 189.5 | 0.0794 | 4.38 |

The pipe connecting the pyrolyzer and the first reboiler (Pot 1) is 316L stainless steel pipe with 48.4 mm inner diameter and 1.2 mm wall thickness. The cross section area of the pipe is 0.002 $m^2$ which allows a maximum vapour velocity of the product at 2.3 m/s. Because some products are condensed in the pipe, the linear velocity of the vapour in the following devices will gradually be decrease and will be less than 2.3 m/s. The temperature of the non-condensable gases is designed to be at about 30 ºC with a volumetric flow rate of approximately 0.73 L/s. The non-condensable gases are flared off by using Bunsen burner with a LPG ignition source. The pipe from the separation section to the Bunsen burner non-condensable gases is 20 mm inner diameter PVC pipe which allows a maximum gas linear velocity of 2.3 m/s with pressure drop less than 45 Pa in total.

In the designed of system, the two re-boilers have the same shape and the same dimensions, each consisting of a cone-shape section and a cylinder section above the cone. (Figure 7-10) In the cone section, a set of 1 kW elements are installed on the outside wall for heating. The temperature of the liquid inside each reboiler is measured with two pairs of thermocouples. One pair of thermocouples is used for temperature recording and the other pair for temperature control. The cylinder above

the cone is made of QVF glass that makes the visual observation possible. (Figure 7-11)

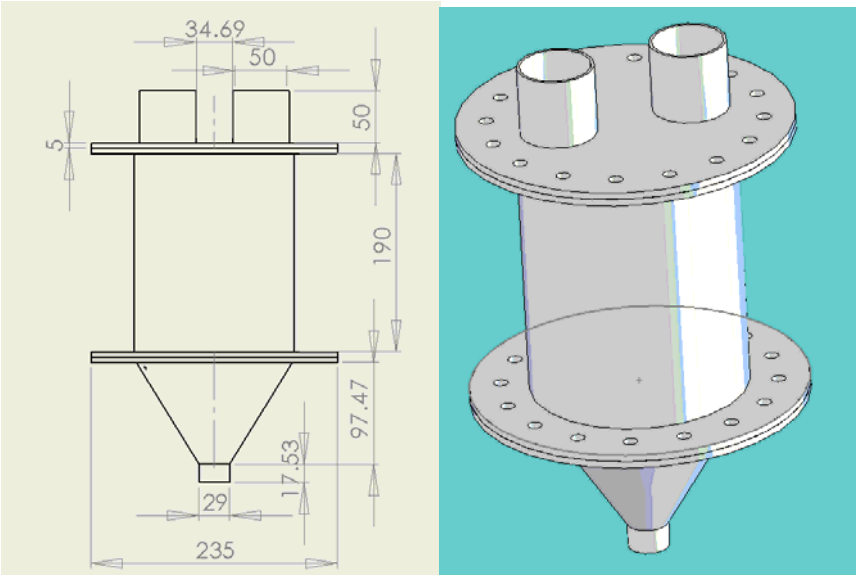


**Figure 7-10 Scheme and dimensions of Pot 1**

**Figure 7-11 Pot 2 of the pyrolysis plant**

As discussed previously, there are two packing distillation columns in the system for separation of the hydrocarbons. Column 1 is made of 1.5 mm thick, 316L stainless steel pipe with 50.4 mm outer diameter. The packing are copper rings with 5 mm high, 5 mm in diameter, and 1 mm wall thickness. The copper rings were piled for 400 mm high in the column. Column 2 is a standard QVF glass pipe, which is 500 mm long and 51 mm in inner diameter. The packings in the Column 2 are 1 mm thick, 7 mm x 7 mm glass rings.

This pyrolysis system is monitored and controlled by a Shimaden SR92 digital controller. (Figure 7-12) The temperatures in 20 locations are monitored or controlled in the system and these locations are illustrated in Figure 7-8. In the 20 pairs of thermocouples used, 8 are used for temperature control and 12 for temperature recording.


**Figure 7-12 Control panel of the apparatus**

In the commissioning tests, significant reflux occurred in the feeding pipeline between the feeding hopper and the pyrolyzer. Reflux was also found in the U shape

connection pipe between the pyrolyzer and the Pot 1. Therefore, the maximum actual productivity achieved, 27.11kg/hr was less than the maximum theoretical production rate 34.4kg/hr because of significant heat loss and reflux in the pyrolysis system.

## 7.3. Experimental

In the experiments, both virgin PE and post-consumer PE were tested on this semi-scale continuous plant. The products were then compared with each other to find out the effect of use, recycling and contamination. The virgin PE was 3 mm long and 3 mm wide white ovals. Its properties were described in Section 5.1.1 and Table 5-1. Virgin plastic was tested on the continuous plant for comparison with the batch process experiments. The whole system was purged with nitrogen gas for two minutes. During the purging time, nitrogen gas was fed from the feeing port but the plastic feeding valve, $V_1$, as well as the exits of Pot 1 and Pot 2 were all closed. In this way, the remaining air in the system was pushed out of the system from the outlet of the non-condensable gas. After that, the internal element was set and hold at 550 ºC; and the external element was set and hold at 500 ºC, at which the actual reaction surface temperature was tested just over the PE cracking temperature. Once the temperature of the reactor was hold steady, 1kg virgin plastic was fed into the reactor with feeding rate at 1kg/hr. The power on Pot 1 and Pot 2 was turned of for a complete separation of liquid and gaseous products. The one kg virgin plastic was evenly fed into the reactor in one hour, then, $V_1$ was closed. The power of the reactor was switched off at 10 minutes after $V_1$ was closed. At the time, no more products were produced from the reactor. No flame came out of the Bunsen burner. After the experiment, the liquid product was analyzed through GC with the same method as used in Section 5.

The post-consumer PE used in the experiments was in the form of small chips provided by a local waste recycling company near Christchurch, New Zealand. In the recycling process, the waste plastics were crashed to 15 x 10 x 2 mm chips as shown in Figure 7-13. However, some of the chips are too large to feed through the auger.

**Figure 7-13 Pre-treated post-consumer PE used in the experiment.**

Due to the feeding problems, the system was run as batch and in each run, 2.5kg of post-consumer plastics were fed into the pyrolyzer at the beginning. Then, the continuous plant was purged with nitrogen gas for two minutes. After the purging process was completed, the reactor was heated up to 420 ºC. At this point, it is assumed that the pyrolysis was about to start based on the previous lab scale test results. Then the reactor was held at 420 ºC for 15 minutes to ensure the temperature was uniform within the reactor and the plastics were melted. After this, the heating elements both on the wall and at the reactor bottom were turned on at full capacity and the target temperature was set at 550 ºC in order to generate fast pyrolysis conditions. The start of the pyrolysis process was indicated by the temperature in the U-shape connection pipe between the pyrolyzer and Pot 1. During the pyrolysis, part of the vapour generated from the pyrolyzer started to condense first in the U-shape connection pipe and collected in Pot 1. Then the remaining vapour flew further into Column 1 from which some fraction of the vapour was condensed and flew back to Pot 1 and the rest moved further to the downstream cooler. The condensed liquid from this cooler and from Column 2 was collected in Pot 2 which the non-condensable gases exited from the outlet of the system and flared off.

After about 6 minutes, the temperature in the U-shape connection pipe between the pyrolyzer and Pot 1, $T_6$, started decreasing indicating that the end of primary cracking

was completed. The power was then switched off when the temperature in the U pipe dropped for ten minutes. After the experiment, the liquid products in Pot 1 and Pot 2 were collected and mixed together in an 80ºC water bath for GC analysis.

### 7.3.1. Results and discussion

Condensed product analysis

The condensed product from pyrolysis of the virgin plastic was analysed with GC. (Figure 7-14) The hydrocarbons detected in both of the products are mainly straight chain hydrocarbons ranging from $C_5$ to $C_{42.}$ The peaks of the straight chain hydrocarbons with the same carbon chain number were grouped together on the GC graphs. As defined in Chapter 5, the three dominant peaks in each group are α, ω-dialkene, 1-alkene, and n-alkane from left to right in the GC graphs.

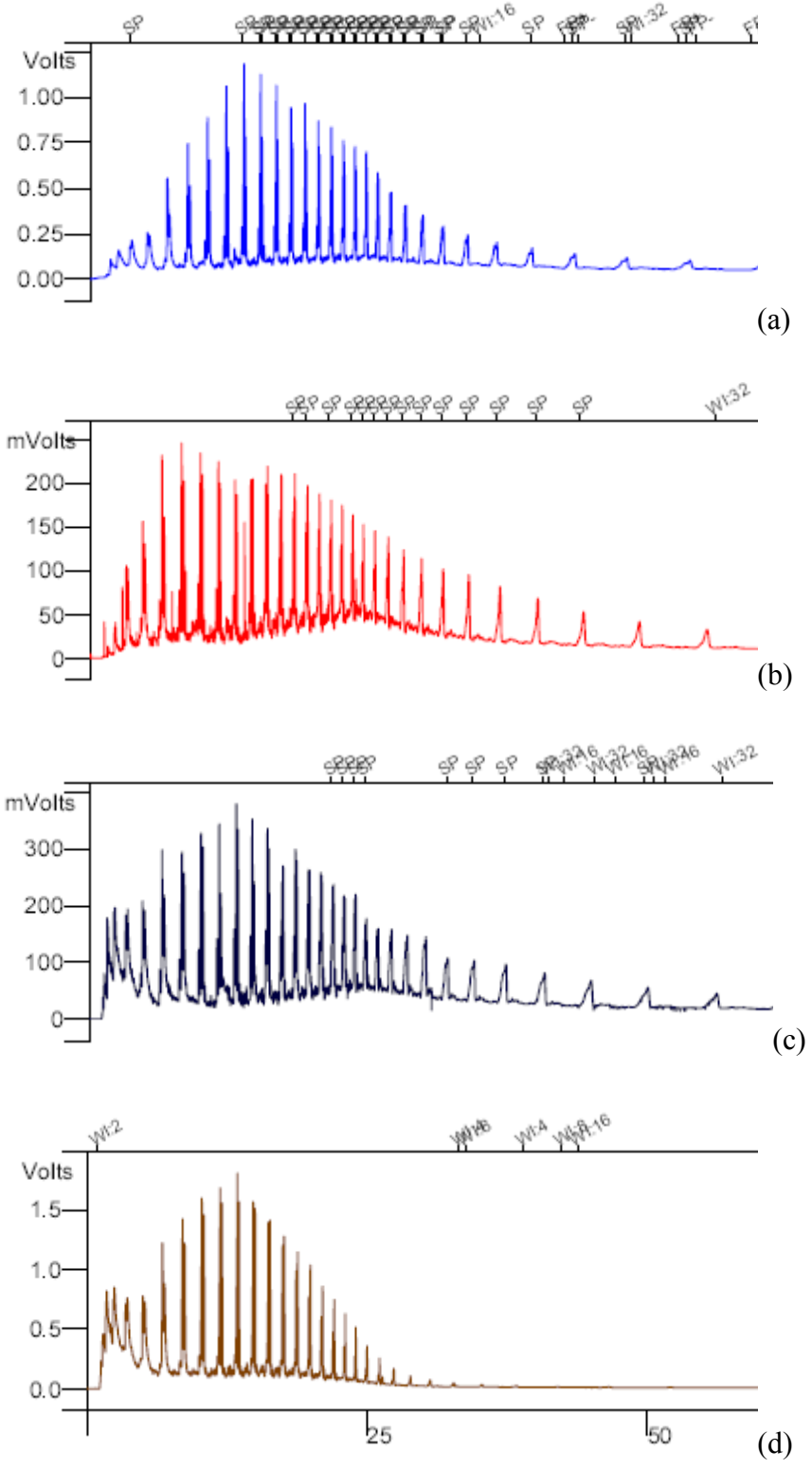


**Figure 7-14 GC graphs of analysis results**

Note:

Virgin PE pyrolysis product, low reflux rate, batch process, lab-scale reactor (a)

Post-consumer PE pyrolysis product, batch process, semi-scale reactor (b)

Virgin PE pyrolysis product, continuous process, semi-scale reactor (c)

Virgin PE pyrolysis product, high reflux rate, batch process, lab-scale reactor (d)

By examining the GC graphs, it is apparent that the concentration of the light hydrocarbons appearing in the first five minutes on the GC graphs is lower in (a) and (b) than in (c) and (d). This is due to the volatiles loss in the hot water bath process. There are 10% w/w and 13% w/w loss in (a) and (b); respectively. (c) and (d) were analyzed straight after collection in order to prevent any product loss. It can be observed that the product from continuous process, (c), has a very similar distribution as that of product from high reflux rate batch process, (b), except for the high proportion of the heavy hydrocarbons which came out after 25 minutes from the beginning. The reduction of heavy hydrocarbons in the high reflux rate process products has been identified as the effect of the secondary cracking reactions. Hence, the product from the continuous process is more like the low reflux rate product, (a), rather than the high reflux rate product. It can also be found in Figure 7-14. The difference in the light hydrocarbons is due to the hot water bath process. (b) has also got similar distribution as (a). However, the proportion of $C_{12}$ to $C_{16}$ is lower in (b) than that in (a).

The distribution of the product from the semi-scale and the lab-scale plants has been compared in Table 7-3. From the pyrolysis of virgin PE, 89.03% w/w of the total feedstock was condensed and less than 0.1% solid mixture of char and small quantity of wax was found being left in the reactor. The rest of the feedstock, 10.87 % w/w, is believed to be the non-condensable gases. (Table 7-3) The proportion of char in both continuous and batch processes with the semi-scale plant was insignificant, which was similar to the batch pyrolysis of the PE. However, the char content in post-consumer PE pyrolysis is higher than that in virgin PE pyrolysis.

**Table 7-3 Comparison of product distribution of different plants**

| | PE product | Gas* | Condensed product | Char | Total |
|---|---|---|---|---|---|
| Semi-scale plant | Virgin | 10.87% | 89.03% | <0.1% | 100% |
| | Post-consumer | 11.56% | 88.24% | <0.2% | 100% |
| Lab-scale plant | Low reflux rate | 6.9% | 93.1% | - | 100% |
| | Medium reflux rate | 16.7% | 83.3% | - | 100% |
| | High reflux rate | 18.3% | 81.7% | - | 100% |

*The weight of gas product is a calculated value from the total feedstock and the collected product.

According to the proportion of the gaseous product, the product from continuous process was equivalent to the product from the lab-scale plant with a reflux rate between low and medium reflux rate. (Table 7-3) However, there is no reflux effect in the semi-scale plant because of the design. The semi-scale plant should perform like a low or no reflux rate process. By comparing the distribution of the condensed products, it was found that the distribution of product from semi-scale plant is very close to that from lab-scale plant. (Table 7-4) The proportion of heavy molecular weight hydrocarbons, wax, in the semi-scale plant product is even more than in the lab-scale plant product. This high proportion of heavy hydrocarbons indicates that no reflux effect in the semi-scale plant, which match the design of the plant and performed with no reflux process. Therefore, the non-condensable gases are totally from the primary cracking in the semi-scale plant. However, there is significant difference in the proportion of the non-condensable gasses between the two reactors, 11.56% for semi-scale reactor and 6.9% for lab-scale reactor operating at low reflux rate. This is caused by the different cracking temperature. By comparing with the

temperature at cracking surface, it was found that the reaction surface temperature in semi-scale reactor (500ºC) is about 50 ºC higher than that in lab-scale reactor (450ºC). According to other references, higher reaction temperature leads to higher gas proportion in the products. [42], [44]

**Table 7-4 hydrocarbon distribution in the condensed product**

| Product | Petrol $C_5$-$C_{12}$ | Diesel $C_{13}$ –$C_{20}$ | Wax $C_{21+}$ | Total |
|---|---|---|---|---|
| Virgin continuous semi-scale (c) | 33.42% | 30.32% | 36.26% | 100% |
| Post-consumer, batch semi-scale (b)* | 33.22% | 29.83% | 36.95% | 100% |
| Virgin high reflux rate lab-scale (d) | 36.16% | 51.35% | 12.49% | 100% |
| Virgin low reflux rate lab-scale (a)* | 34.07% | 30.85% | 35.08% | 100% |

Note:

* The compensation has been added for the petrol loss.

(a), (b), (c), (d) refer to Figure 7-14.

Based on the GC analysis, although the hydrocarbons with carbon chain number from 5 to 12 accounts for 33.42% in the virgin PE pyrolysis product, which is much higher than that of post-consumer PE pyrolysis (23.24%) due to the volatile loss as mentioned before. The difference of the proportion of the other two groups would be less than 1% when the volatile loss in the post-consumer PE pyrolysis product is compensated to the petrol range product in Table 7-4. Therefore, the distribution of

the product from post-consumer PE pyrolysis is virtually the same as that in the product of virgin PE pyrolysis.

The components in products from both plants are almost the same although the concentration may vary within a relatively small range. (Figure 7-14) There were 196 and 204 peaks found, respectively, in the products of post-consumer PE and virgin PE. Heavier molecular weight components are found compared to that in the product from the high reflux rate lab-scale process. (Section 5.1.4) As the concentration of each peak is the area covered by the peak thus it is proportional to both the width and the height of the peak. 1-alkenes and n-alkanes are the most important peaks in all groups of both virgin and post-consumer PE products. However, the concentration of 1-alkenes is lower in the post-consumer PE product than in the virgin PE product. Similarly, the concentration of α, ω-dialkenes is also lower in the post-consumer PE products than in the virgin PE product. This could be caused by the difference of the feedstock. The contamination on the post-consumer PE is mainly paper tags attached on the plastic chips, which are mainly cellulose and hemicelluloses. Hydrogen is a main product from cracking of wood or paper. [131-132] Under the pyrolysis conditions, there could be hydrogenation reactions in the processes. [2, 38, 93] The hydrogen produced from cracking of the contaminants could saturate the double bond and formed more n-alkanes in the final products. As the products in both the post-consumer PE pyrolysis and the virgin PE pyrolysis were from the primary cracking because they were immediately removed after produced. Therefore, heavy hydrocarbons, up to $C_{42,}$ and unsaturated hydrocarbons are rich in the products.

Pyrolysis process analysis

In the continuous process, the power of each element on the plant is self-controlled by the digital program controller. However, the temperature was strongly related to the power on/off status rather than the reactions in the plant. Therefore, the temperature profile of the continuous process can not provide much information about the pyrolysis process. However, the temperature profiles of the batch process contained useful information because the power was not switch on and off that often. The

temperature profiles of the system in the pyrolysis of post-consumer PE are shown in Figure 7-15. From the temperature profiles, the process had three stages: plastic melting, cracking, and cooling. $T_4$ is the temperature at inner surface of the reactor, which shows the reaction temperature. In the first five minutes, the reactor was heated up and held at 420 ºC. There was no product coming out during this period until the internal and the external elements were switched on to the new set point of 550 ºC. Product started being produced once the element temperature started increasing again at 20 minutes from the beginning. The hot product flow affected the temperature of other thermal indicators. The temperature inside the U-shape connection pipe ($T_6$) and the temperature at the entrance of Column 1, $T_{17,}$ show the product flowing into Pot 1 and Pot 2, respectively. No product was coming out of the pyrolyzer during the melting stage, hence, $T_6$ and $T_{17}$ also remained at the room temperature. This cracking process is very similar to the low reflux rate lab-scale batch process that was described in the previous chapters.

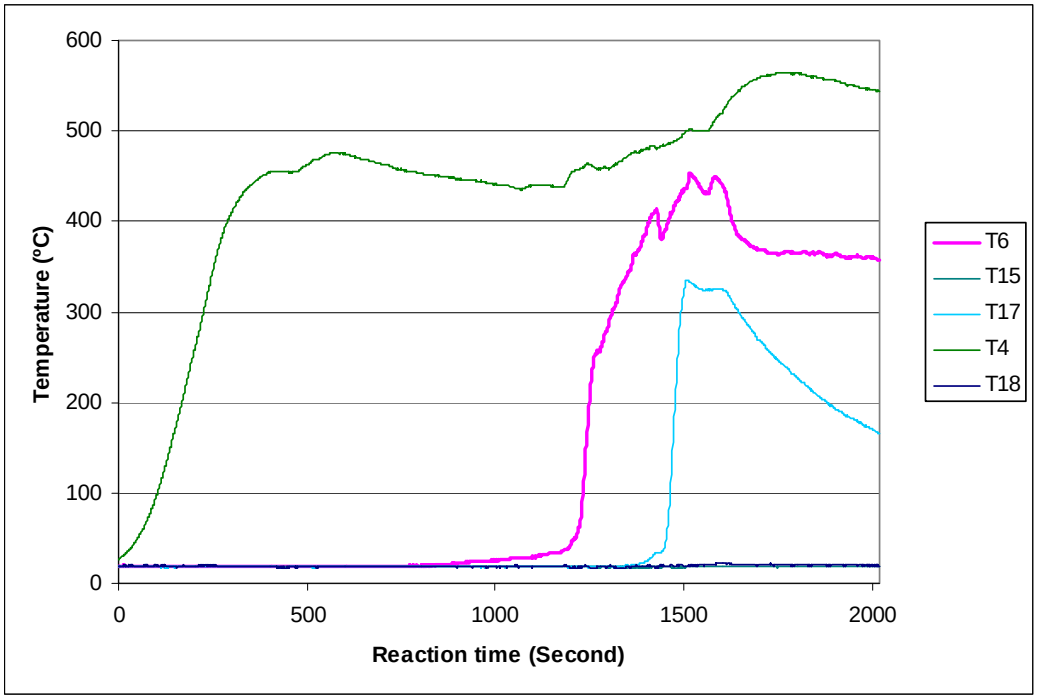


**Figure 7-15 Temperature profiles of the continuous pyrolysis process**

The cracking process occurred between 1200$^{th}$ second and the 1585$^{th}$ second in which period the temperature inside the reactor ($T_4$) increased to 500 ºC and then remained relatively constant at that temperature. During this period, $T_6$ increased rapidly to 450 ºC and then remained at that temperature very briefly before it decreased. This indicates massive products produced and flew out at 450 ºC during this period. The U-shape pipe was insulated with glass fibre rope to reduce heat loss and reflux of the condensate to the reactor. During the cracking period, it was observed that some liquid hydrocarbons were condensed and collected in Pot1, but a larger amount of liquid hydrocarbons was collected in Pot2. The flame of the non-condensable gases above the Bunsen burner was orange and was about one meter high.

The sudden increase of $T_{17}$ was noticed at the 1450$^{th}$ second, which shows the remaining vapour flowing from the Column 1 into Condenser 1. However, in the experiment of the PE pyrolysis, all of the liquids were collected only in Pot 1 and Pot 2 while no liquid was found in the petro tank which was caused by the lower temperature of the vapour from Condenser 2 even the cooling water was turned off to the Condenser 2. The temperatures after the Condenser 2 ($T_{18}$) and above the petrol tank ($T_{15}$) remained at room temperature throughout the experiment.

Towards the end of the pyrolysis at the 1585th second from the start, the temperature in the pyrolyzer ($T_4$) started increasing rapidly whereas the temperatures in the U-shape pipe ($T_6$) and above Column 1 ($T_{17}$) started decreasing. These indicate the end of the cracking stage and the start of the system cooling. The increase of $T_4$ was due to less energy requirement after the plastics had been pyrolyzed. As a consequence, no vapour was generated thus there was no vapour flow in the system and the temperature in the system dropped. After 30minutes, the experiment was completed and the power to the heating elements was switched off. Then the system was cooled down to the room temperature.

After the system was cooled down to room temperature, the liquid products collected in both Pot 1 and Pot 2 were taken out. In the pyrolysis of post-consumer PE, the condensed product from Pot1 was yellow wax at 20 ºC but it was melted into liquid when being heated to about 80 ºC. The product from Pot 2 was clear yellow liquid at 20 ºC. The two products were melted and mixed in a flask and analyzed through the GC used previously in Section 5. (Figure 7-16) The flask was put in a water bath at 80ºC for one hour to homogenize the product. However, some of the volatile hydrocarbons were vaporized due to heating in the hot water bath.

The products from virgin PE pyrolysis were only melted for GC analysis but were not heated in the hot water bath. Therefore, there was less volatile product loss in the liquid product obtained from the pyrolysis of virgin PE compared to that of pyrolysis of post-consumer PE.

**Figure 7-16 Collected liquid product from pyrolysis of post-consumer PE.**

Energy consumption

The energy required for pyrolysis of 2.5kg post-consumer PE can be calculated from the input power and the elapsed time. The total power input from the heating elements in the pyrolyzer is 10kw when these elements are switched on at full capacity. However, the elements were switched off twice during the cracking stage to control the temperature; from the 1430$^{th}$ to the 1440$^{th}$ second, and from the 1519$^{th}$ to the 1562$^{nd}$ second. The total time of the cracking stage was from the 1200$^{th}$ to the 1585$^{th}$

second except the time when the power of the elements was off. Thus, 2.5 kg PE waste requires heating from 10kw elements for 332 seconds to complete the primary cracking and vaporization, which is 3.32 MJ. Therefore, the actual maximum production rate is 27.11 kg/hr when the feedstock is pre-heated to the cracking temperature. Therefore, the energy consumed for the pyrolysis and the vaporization is 1.328 MJ/kg. Based on the pyrolysis reactions, the theoretical energy requirement for pyrolysis of the post-consumer PE is 1.033 MJ/kg based on the discussion in Chapter 3. Table 7-5 gives the detailed energy demand for production of each hydrocarbon group in which $C_3H_6$, 1-$C_8H_{16}$, 1-$C_{16}H_{32}$, 1-$C_{28}H_{56}$, respectively, represent $C_1$ to $C_4$, $C_5$-$C_{12}$, $C_{13}$ –$C_{22}$, and $C_{23+}$.

**Table 7-5 Theoretical energy consumption of PE pyrolysis**

| 1kg PE | $C_3H_6$ | 1-$C_8H_{16}$ | 1-$C_{16}H_{32}$ | 1-$C_{28}H_{56}$ | Total |
|---|---|---|---|---|---|
| w/w | 11.56% | 29.49% | 32.90% | 25.84% | 100% |
| mol | 2.75 | 2.63 | 1.47 | 0.66 | 7.51 |
| ΔHr kJ/mol | 23.00 | 23.00 | 23.00 | 23.00 | 172.81 |
| ΔH kJ/mol | 24.12 | 72.32 | 163.34 | 304.12 | 697.19 |
| ΔHv kJ/mol | | 33.76 | 50.42 | | 162.95 |
| Total Energy kJ | 129.69 | 339.87 | 347.74 | 215.63 | 1032.94 |

Where: Hr is the energy required for the cracking reaction. H is the energy required for heating the compound. Hv is the heat of vaporization for the hydrocarbons. The assumption of the calculation is under 1 atm. The pyrolysis products were at 400 ºC.

### 7.3.2. Conclusions

According to the experiment with the semi-scale apparatus, negligible difference was found between continuous pyrolysis process of virgin PE and batch pyrolysis process of post-consumer PE. The process of the pyrolysis on the semi-scale plant is very similar to the low reflux rate process on the lab-scale plant.

In the pyrolysis of PE with the semi-scale plant, the distribution of the condensed product is almost the same as that of low reflux rate process with the lab-scale plant. 10.87% w/w and 11.56% w/w of the virgin and the post-consumer PE were converted to non-condensable gases. Because of no secondary cracking reactions in the process, the non-condensable gases were produced during the primary cracking reaction. The proportion of the gaseous product is higher from the semi-scale plant than from the lab-scale plant because the semi-scale plant has higher reaction surface temperature. In both cases, negligible amount of char was found in both virgin and the post-consumer plastic products. The components in both products are also very similar. 1-alkenes, n-alkanes, and α, ω-dialkenes are the dominant hydrocarbons in the products. The proportion of dialkene in the virgin PE pyrolysis product is significantly higher than that in post-consumer PE product from the semi-scale plant. The proportion of n-alkane is higher in post-consumer PE product than that in virgin PE product. These could be affected by the contamination in the post-consumer PE.

The experimental energy consumption was measured as 1.328 MJ/kg.

# 8. Conclusions and future work

## *8.1. Conclusions*

In this PhD study, pyrolysis of the hydrocarbon polymers, PE, PP and PS was investigated both theoretically and experimentally in a lab-scale reactor for maximizing the diesel oil products. Factors which affect the pyrolysis process have been identified and quantified from the investigation. Based on the achievements, the distribution of the product and the process was optimized. A semi-scale plant was built based on the results of studies on the lab-scale reactor.

From the experiments on the PE pyrolysis, three types of products can be produced which include non-condensable gases, condensed liquid hydrocarbons and char. The distribution of the product varies greatly under different reaction conditions. For example, char content was 13%w/w under certain conditions but can be minimized to less than 0.2%w/w with the semi-scale plant. The proportion of non-condensable gases is 18.3% w/w from the experiment in pyrolysis of PE with high reflux rate as described in Chapter 4, but this is reduced to only 6.9% w/w in PE pyrolysis with low reflux rate as presented in Chapter 5. Non-condensable gases are generated from random cracking reactions. Higher reaction temperature or heating rate favours higher production of non-condensable gases. According to GC and Micro-GC analysis, the straight chain hydrocarbons are dominant in the non-condensable gases, liquid and wax. They are mainly 1-alkenes, n-alkanes, and α, ω-dialkenes with carbon number ranging from 1 to 45+.

It was found that heavy molecular weight hydrocarbons produced from primary cracking can be further cracked into light molecular weight products through a secondary cracking process. This secondary cracking process has significantly influence on the distribution of the product. This process converts heavy hydrocarbons into gas or light liquid product. At high reflux rate, 1-alkenes and α, ω-dialkenes are significantly reduced. This secondary process can be controlled by

adjusting the reflux rate of the primary product. This find is new in this field as other researches only alter the factors which only affect the primary cracking, such as temperature, pressure, catalyst, or resistance time. With the adjusting of the reflux rate in the pyrolysis, the quality of the product can be optimised which can be very useful for commercial plant to achieve target products.

The proportion of char was negligible in all experiments both with the lab-scale pyrolysis reactor and with the semi-scale pyrolysis reactor. Carbon is the dominant element in the char in the SEM-EDS analysis results.

Some zeolite catalysts were tested to reduce the heavy molecular weight wax. It was found that the catalyst of NKC-5 (ZSM-5) is the most effective catalyst among other zeolites tested.

Pyrolysis of PP was also investigated in this study. It is found that the secondary cracking also has effects on the pyrolysis product but the effect is not as significant as that on PE. The high reflux rate PP pyrolysis product consists of 15.7% non-condensable gases, 84.2% condensed liquid product, and less than 0.25% char. The conversion rate to fuel is over 99.7% which is the higher than any reported values in literature. In the PP pyrolysis, the methyl side group in PP structure breaks off through chain strip cracking reactions, therefore, the methyl-radicals are combined with other free radicals, forming propene or other oligomers. Propene is the dominant component in the gases, which accounts for 44% v/v. In the liquid product of PP pyrolysis, 1, 3, 5 - trimethyl - cyclohexane ($C_9H_{18}$) is identified to be one of the dominant components, which accounts for 21% w/w. The low molecular weight oligomers with 2 to 5 propene units accounts for 68% of the total liquid product.

The pyrolysis process of PS is different from those of PE and PP. In the pyrolysis, most PS molecules are cracked into small molecular weight hydrocarbons in the

primary cracking through chain strip reactions. In the PS pyrolysis products, there are 4% non-condensable gases, 93% liquid, and 3% char. The proportion of PS pyrolysis gases is much less than that of PE and PP. In the PS pyrolysis gas product, there is 19% v/v hydrogen which is not found in PE pyrolysis gas product. In the PS pyrolysis liquid product, 92% (w/w) is found to be five aromatic compounds and styrene is the dominant component that accounts for 68.59%, which has further confirmed the chain strip reactions in the PS pyrolysis process. The char from the PS pyrolysis is mainly pure carbon that is similar to the char from pyrolysis of PP and PE. However, the proportion of the char in the PS pyrolysis is much higher than that in the pyrolysis of PP and PE.

By comparison of the pyrolysis of individual HDPE, LDPE, PP, and PS, it is found that HDPE, LDPE, and PP have very similar cracking temperature, 450ºC. However, PS has a relatively low cracking temperature, 320ºC. Therefore, the plastic mixture of these plastics starts cracking below 450ºC due to the interactive effect of PS. The interaction among the plastics promotes the production of non-condensable gases during the pyrolysis. However, the effect of the interaction on the distribution of liquid product is not significant. Contamination of paper labels on the post-consumer plastics may result in higher char content in the product but no significant effect on the liquid and gaseous products has been found in this study.

In this study, a semi-scale continuous pyrolysis plant was built in Department of Chemical and Process Engineering, with the maximum capacity of 27.11 kg PE /hr. In the PE pyrolysis experiments on the semi-scale plant, the plastic feedstock only undergoes the primary cracking, and the pyrolysis product is removed and separated through the following separation distillation columns. It is found that the liquid products have a similar distribution as those of PE pyrolysis at the lab-scale reactor with low reflux rate. The pyrolysis process in the semi-scale plant is also similar to that in the lab-scale plant. The major components in the PE pyrolysis product from the semi-scale pyrolysis include hydrocarbons of 1-alkenes, n-alkanes, and α, ω-dialkenes which are the same as those from the PE pyrolysis at the lab-scale reactor. However,

the proportion of non-condensable gases from semi-scale plant is much higher than that from PE pyrolysis at the lab-scale reactor with low reflux rate. This is due to the high reaction temperature during the pyrolysis process in the semi-scale plant. Further analysis of the pyrolysis products has found that there is lower proportion of unsaturated hydrocarbons in the post-consumer PE than in the virgin PE. This is possibly due to the contamination in the post-consumer PE.

The energy consumption was calculated based on pyrolysis kinetic models. Theoretically, it requires 1.033 MJ to pyrolyze 1kg PE into hydrocarbons with a certain distribution. The calorific value of the hydrocarbon products is about 42.3 MJ/kg. The energy consumption for the pyrolysis and vaporization of PE was measured as 1.328 MJ/kg on the semi-scale plant experiment, which is les than 3% of the energy possessed by the pyrolysis products. Therefore, the plastic pyrolysis is an energy-efficient process. Based on the results and skilled gained from the design and operation of the semi-scale plant, a commercial plant for pyrolysis of post-consumer PE, PP, and PS could be designed. This technology can be applied to significantly reduce the conventional landfill or incineration of waste plastics.

## 8.2. Future work

In order to commercialise the pyrolysis technology to recycling of the waste plastics and to better understand the pyrolysis process, the following work is recommended for further studies:

- In the semi-scale plant, the current continuous feeding system has minor leaks and needs some modification. The feeding system should be able to control the required feeding rate and prevent back-flow of the high temperature pyrolysis vapour. On the other hand, the oxygen leaking into the feeder must be prevented. Better and effective distillation columns should be applied on the semi-scale plant for refining of the pyrolysis products.

- The effect of contamination in post-consumer plastics is still not clear due to the variation of the contamination on different post-consumer plastics. Virgin and post-consumer plastics on the process and the distribution of the product should be investigated on the semi-scale plant. The detailed interaction among different plastic materials during the cracking reactions is unknown, thus further investigation is needed to quantitatively analyse the interaction effect of different post-consumer plastics. This could be very valuable for commercialization of the technology.

- The non-condensable gases were flared off in the experiment. It would be valuable to collect some of the gases and investigate its composition. The diesel range product should be separated out of the condensed products in the semi-scale plant. The diesel range product should be tested in accordance to New Zealand diesel requirements standard for the properties of commercial uses. It is worthwhile to add hydrogen into the reaction to saturate the hydrocarbons thus to modify the product to increase the target diesel products. Hydrogenation can significantly improve the product quality towards transport use. Many oil refinery

factories apply this process to convert alkenes into alkane in order to get higher stability oil.

# Reference


1. Brydson, J.A. and ScienceDirect. *Plastics materials*. 1999 1999; Available from: http://www.sciencedirect.com/science/book/9780750641326

2. Chanda, M., *Advanced polymer chemistry : a problem solving guide*. 2000, New York [u.a.]: Marcel Dekker.

3. The Sociaty of the Plastic Industry, I. *SPI MATERIAL CONTAINER CODING SYSTEM*. 1999 15/Sep/2008]; Available from: http://www.plasticsindustry.org/outreach/recycling/resincodes.htm.

4. PlasticsEurope, *The Compelling Facts About Plastics 2007*. 2008: Brussels.

5. USEPA, *Municipal Solid Waste Generation, Recycling, and Disposal in the United States:*

*Facts and Figures for 2008*. 2008, USEPA.

6. Watch, W., *Waste Watch Information Sheet Plastics*. 2008, Waste Watch Institution.

7. Withington, N., *Sustainable End-of-Life Options for Plastics in New Zealand*. 2005, Plastics New Zealand: Manukau City.

8. Street, A. and S. Zydenbos, *Analysis of the Christchurch Mixed Municipal Waste Stream -1 July 2003 to 30 June 2004*. 2004, City Water & Waste Unit, Christchurch City Council. p. 6.

9. Regnier, N. and B. Mortaigne, *Analysis by pyrolysis/gas chromatography/mass spectrometry of glass fibre/vinylester thermal degradation products.* Polymer Degradation and Stability, 1995. **49**(3): p. 419-428.

10. Williams, E.A. and P.T. Williams, *Analysis of products derived from the fast pyrolysis of plastic waste.* Journal of Analytical and Applied Pyrolysis

Proceedings of the 1996 12th International Symposium on Analytical and Applied Pyrolysis, Oct 14-18 1996, 1997. **40-41**: p. 347-363.

11. Williams, P.T. and E. Slaney, *Analysis of products from the pyrolysis and liquefaction of single plastics and waste plastic mixtures.* Resources, Conservation and Recycling, 2007. **51**(4): p. 754-769.

12. Karaduman, A., et al., *Flash pyrolysis of polystyrene wastes in a free-fall reactor under vacuum.* Journal of Analytical and Applied Pyrolysis, 2001. **60**(2): p. 179-186.

13. Demirbas, A., *Pyrolysis of municipal plastic wastes for recovery of gasoline-range hydrocarbons.* Journal of Analytical and Applied Pyrolysis, 2004. **72**(1): p. 97-102.

14. Baines, T., *New Zealand Energy Information Handbook*, ed. J.T. Baines. 1993, Christchurch: Taylor Baines and Associates.

15. Engineering, N.Z.C.f.A., *Regional Energy Survey 2006*. 2008: Christchurch.

16. Kittle, P.A., *Alternate Daily Cover Materials And Subtitled - The Selection Technique*. 1993, Rusmar Incorporated West Chester, PA.

17. Scheirs, J., *Overview of Commercial Pyrolysis Processes for Waste Plastics*, in *Feedstock Recycling and Pyrolysis of Waste Plastics*, J.S.a.W. Kaminsky, Editor. 2006, John Wiley & Sons, Ltd: Edithvale Australia. p. 399.

18. Zadgaonkar, A., *Process and Equipment for Conversions of Waste Plastics into Fuels*, in *Feedstock Recycling and Pyrolysis of Waste Plastics*, J.S.a.W. Kaminsky, Editor. 2006, John Wiley & Sons, Ltd: Nagpur India. p. 709-728.

19. Masuda, T. and T. Tago, *Development of a Process for the Continuous Conversion of Waste Plastics Mixtures to Fuel*, in *Feedstock Recycling and Pyrolysis of Waste Plastics*, J. Scheirs and W. Kaminsky, Editors. 2006, John Wiley & Sons, Ltd: Sapporo. p. 161-192.

20. Kaminsky, W., M. Predel, and A. Sadiki, *Feedstock recycling of polymers by pyrolysis in a fluidised bed.* Polymer Degradation and Stability, 2004. **85**(3 SPEC ISS): p. 1045-1050.

21. Kaminsky, W., B. Schlesselmann, and C. Simon, *Olefins from polyolefins and mixed plastics by pyrolysis.* Journal of Analytical and Applied Pyrolysis, 1995. **32**(pt 1): p. 19-27.

22. Kaminsky, W., B. Schlesselmann, and C.M. Simon, *Thermal degradation of mixed plastic waste to aromatics and gas.* Polymer Degradation and Stability, 1996. **53**(2): p. 189-197.

23. Scheirs, J. and W. Kaminsky, *Feedstock recycling and pyrolysis of waste plastics : converting waste plastics into diesel and other fuels*. Wiley series in polymer science, ed. J. Scheirs. 2006, Austrilia: John Wiley & Sons, Ltd.

24. Williams, E.A. and P.T. Williams, *Pyrolysis of individual plastics and a plastic mixture in a fixed bed reactor.* Journal of Chemical Technology and Biotechnology, 1997. **70**(1): p. 9-20.

25. Williams, P.T., *Yield and composition of gases and oils/waxes from the feedstock recycling of waste plastic*, in *Feedstock Recycling and pyrolysis of waste plastics*, J. Scheirs and W. Kaminsky, Editors. 2006, John Wiley & Sons, Ltd: Leeds. p. 286-313.

26. Williams, P.T. and E.A. Williams, *Recycling plastic waste by pyrolysis.* Journal of the Institute of Energy, 1998. **71**(487): p. 81-93.

27. Williams, P.T. and E.A. Williams, *Interaction of plastics in mixed-plastics pyrolysis.* Energy & Fuels, 1999. **13**(1): p. 188-196.

28. Aguado, J., D.P. Serrano, and J.M. Escola, *Catalytic Upgrading of Plastic Wastes*, in *Feedstock Recycling and Pyrolysis of Waste Plastics*, J. Scheirs and W. Kaminsky, Editors. 2006, John Wiley & Sons, Ltd: Mostoles, Spain. p. 73-110.

29. Aguado, J., et al., *Catalytic conversion of low-density polyethylene using a continuous screw kiln reactor.* Catalysis Today, 2002. **75**(1-4): p. 257-262.

30. Aguado, J., et al., *Catalytic conversion of polyolefins into fuels over zeolite beta.* Polymer Degradation and Stability, 2000. **69**(1): p. 11-16.

31. Aguado, J., et al., *Enhanced production of α-olefins by thermal degradation of High-Density Polyethylene (HDPE) in decalin solvent: Effect of the reaction time and temperature.* Industrial and Engineering Chemistry Research, 2007. **46**(11): p. 3497-3504.

32. Ivanova, S.R., et al., *Selective catalytic degradation of polyolefins.* Progress in Polymer Science (Oxford), 1990. **15**(2): p. 193-215.

33. Lee, K.H., *Thermal and Catalytic Degradation of Waste HDPE*, in *Feedstock Recycling and Pyrolysis of Waste Plastics*, J. Scheirs and W. Kaminsky, Editors. 2006, John Wiley & Sons, Ltd: Korea. p. 130.

34. Arandes, J., et al., *Thermal recycling of polystyrene and polystyrene-butadiene dissolved in a light cycle oil.* Journal of Analytical and Applied Pyrolysis, 2003. **70**(2): p. 747-760.

35. Bagri, R. and P.T. Williams, *Fluidised-bed catalytic pyrolysis of polystyrene.* Journal of the Institute of Energy, 2002. **75**(505): p. 117-123.

36. Bouster, C., P. Vermande, and J. Veron, *Evolution of the product yield with temperature and molecular weight in the pyrolysis of polystyrene.* Journal of Analytical and Applied Pyrolysis, 1989. **15**: p. 249-259.

37. Karaduman, A., *Pyrolysis of polystyrene plastic wastes with some organic compounds for enhancing styrene yield.* Energy Sources, 2002. **24**(7): p. 667-674.

38. McMurry, J., *Organic Chemistry*. fifth edition ed. Vol. 5. 2000, Pacific Grove: Brooks/Cole. 172.

39. Sobko, A.A., *Generalized van der Waals-Berthelot equation of state.* Doklady Physics, 2008. **53**(8): p. 416-419.

40. Patra, C.N. and A. Yethiraj, *Generalized van der Waals density functional theory for nonuniform polymers.* The Journal of Chemical Physics, 2000. **112**(3): p. 1579-1584.

41. Ciliz, N.K., E. Ekinci, and C.E. Snape, *Pyrolysis of virgin and waste polypropylene and its mixtures with waste polyethylene and polystyrene.* Waste Management, 2004. **24**(2): p. 173-181.

42. Shah, N., J. Rockwell, and G.P. Huffman, *Conversion of waste plastic to oil: Direct liquefaction versus pyrolysis and hydroprocessing.* Energy and Fuels, 1999. **13**(4): p. 832-838.

43. Miller, S.J., N. Shah, and G.P. Huffman, *Conversion of waste plastic to lubricating base oil.* Energy and Fuels, 2005. **19**(4): p. 1580-1586.

44. Mastral, F.J., et al., *Pyrolysis of high-density polyethylene in a fluidised bed reactor. Influence of the temperature and residence time.* Journal of Analytical and Applied Pyrolysis, 2002. **63**(1): p. 1-15.

45. Serrano, D.P., et al., *Performance of a continuous screw kiln reactor for the thermal and catalytic conversion of polyethylene-lubricating oil base mixtures.* Applied Catalysis B: Environmental, 2003. **44**(2): p. 95-105.

46. Simon, C.M., W. Kaminsky, and B. Schlesselmann, *Pyrolysis of polyolefins with steam to yield olefins.* Journal of Analytical and Applied Pyrolysis, 1996. **38**: p. 75-87.

47. Jung, C.G. and A. Fontana, *Production of Gaseous and Liquid Fuels by Pyrolysis and Gasfication of Plastics: Technological Approach*, in *Feedstock Recycling and Pyrolysis of Waste Plastics*, J. Scheirs and W. Kaminsky, Editors. 2006, John Wiley & Sons, Ltd: Belgium. p. 251.

48. Uemura, Y., et al., *Flash-pyrolyzed product distribution of major plastics in a batch reactor.* Journal of Chemical Engineering of Japan, 2001. **34**(10): p. 1293-1299.

49. Miranda, R., et al., *Vacuum pyrolysis of commingled plastics containing PVC II. Product analysis.* Polymer Degradation and Stability, 2001. **73**(1): p. 47-67.

50. Lee, K.-H. and D.-H. Shin, *Characteristics of liquid product from the pyrolysis of waste plastic mixture at low and high temperatures: Influence of lapse time of reaction.* Waste Management, 2007. **27**(2): p. 168-176.

51. Saha, B. and A.K. Ghoshal, *Thermal degradation kinetics of poly(ethylene terephthalate) from waste soft drinks bottles.* Chemical Engineering Journal, 2005. **111**(1): p. 39-43.

52. Faravelli, T., et al., *Gas product distribution from polyethylene pyrolysis.* Journal of Analytical and Applied Pyrolysis, 1999. **52**(1): p. 87-103.

53. Kayacan, I. and O.M. Dogan, *Pyrolysis of low and high density polyethylene. Part I: non-isothermal pyrolysis kinetics.* Energy Sources, 2008. **30**(5-8): p. 385-91.

54. Kim, S., *Pyrolysis kinetics of waste PVC pipe.* Waste Management, 2001. **21**(7): p. 609-616.

55. Kiran, N., E. Ekinci, and C.E. Snape, *Recycling of plastic wastes via pyrolysis.* Resources, Conservation and Recycling, 2000. **29**(4): p. 273-283.

56. Marcilla, A., M.d.R. Hernandez, and A.N. Garcia, *Study of the polymer-catalyst contact effectivity and the heating rate influence on the HDPE pyrolysis.* Journal of Analytical and Applied Pyrolysis, 2007. **79**(1-2 SPEC ISS): p. 424-432.

57. Bhaskar, T., et al., *Pyrolysis studies of PP/PE/PS/PVC/HIPS-Br plastics mixed with PET and dehalogenation (Br, Cl) of the liquid products.* Journal of Analytical and Applied Pyrolysis, 2004. **72**(1): p. 27-33.

58. Horvat, N. and F.T.T. Ng, *Tertiary polymer recycling: Study of polyethylene thermolysis as a first step to synthetic diesel fuel.* Fuel, 1999. **78**(4): p. 459-470.

59. Ludlow-Palafox, C. and H.A. Chase, *Microwave-induced pyrolysis of plastic wastes.* Industrial and Engineering Chemistry Research, 2001. **40**(22): p. 4749-4756.

60. Serrano, D.P., et al., *Conversion of low density polyethylene into petrochemical feedstocks using a continuous screw kiln reactor.* Journal of Analytical and Applied Pyrolysis, 2001. **58-59**: p. 789-801.

61. Arena, U. and M.L. Mastellone, *Fluidized Bed Pyrolysis of Plastic Wastes*, in *Feedstock Recycling and Pyrolysis of Waste Plastics*, J.S.a.W. Kaminsky, Editor. 2006, John Wiley & Sons, Ltd: Caserta, Italy. p. 440.

62. Uemichi, Y., et al., *Conversion of polyethylene into gasoline-range fuels by two-stage catalytic degradation using silica-alumina and HZSM-5 zeolite.* Industrial & Engineering Chemistry Research, 1999. **38**(2): p. 385-390.

63. Bagri, R. and P.T. Williams, *Catalytic pyrolysis of polyethylene.* Journal of Analytical and Applied Pyrolysis, 2002. **63**(1): p. 29-41.

64. Songip, A.R., et al., *Kinetic studies for catalytic cracking of heavy oil from waste plastics over REY zeolite.* Energy and Fuels, 1994. **8**(1): p. 131-135.

65. Hernández, M.d.R., et al., *Effect of residence time on volatile products obtained in the HDPE pyrolysis in the presence and absence of HZSM-5.* Industrial and Engineering Chemistry Research, 2006. **45**(26): p. 8770-8778.

66. Buekens, A., *Introduction to Feedstock Recycling of Plastics*, in *Feedstock Recycling and Pyrolysis of Waste Plastics*, J. Scheirs and W. Kaminsky, Editors. 2006, John Wiley & Sons, Ltd: Brussels, Belgium. p. 3-41.

67. Hernández, M.d.R., et al., *Effect of the temperature in the nature and extension of the primary and secondary reactions in the thermal and HZSM-5*

*catalytic pyrolysis of HDPE.* Applied Catalysis A: General, 2007. **317**(2): p. 183-194.

68. Blazso, M., *Composition of Liquid Fuels Derived from the Pyrolysis of Plastics*, in *Feedstock Recycling and Pyrolysis of Waste Plastics*, J.S.a.W. Kaminsky, Editor. 2006, John Wiley & Sons, Ltd: Budapest, Hungary. p. 315-344.

69. Garforth, A.A., et al., *Production of hydrocarbons by catalytic degradation of high density polyethylene in a laboratory fluidised-bed reactor.* Applied Catalysis A: General, 1998. **169**(2): p. 331-342.

70. Maesen, T., *The Zeolite Scene - An Overview*. 3rd Revised Edition ed. Introduction to Zeolite Science and Practice, ed. G. Centi. Vol. 1. 2007, Richmond, CA, USA: Elsevier B.V. 1-12.

71. McCusker, L.B. and C. Baerlocher, *Zeolite Structures*. 3rd Revised Edition ed. Introduction to Zeolite Science and Practice, ed. G. Centi. Vol. 2. 2007, Zurich, Switzerland: Elsevier B.V. 13-38.

72. McCusker, L.B., F. Liebau, and G. Englehardt, *Nomenclature of structural and compositional characteristics of ordered microporous and mesoporous materials with inorganic hosts (IUPAC recommendations 2001): Physical chemistry Division commision on colloid and surface chemistry including catalysis.* Microporous and Mesoporous Materials, 2003. **58**(1): p. 3-13.

73. Barrer, R.M. *SYNTHESIS OF ZEOLITES*. 1985. Portoroz, Yugosl: Elsevier.

74. Yang, J., et al., *Location, acid strength, and mobility of the acidic protons in Keggin 12-H3PW12O40: A combined solid-state NMR spectroscopy and DFT quantum chemical calculation study.* Journal of the American Chemical Society, 2005. **127**(51): p. 18274-18280.

75. Janik, M.J., R.J. Davis, and M. Neurock, *The relationship between adsorption and solid acidity of heteropolyacids.* Catalysis Today, 2005. **105**(1 SPEC. ISS.): p. 134-143.

76. Benito, P.L., et al., *Effect of Si/Al ratio and of acidity of H-ZSM5 zeolites on the primary products of methanol to gasoline conversion.* Journal of Chemical Technology and Biotechnology, 1996. **66**(2): p. 183-191.

77. Murata, K., K. Sato, and Y. Sakata, *Effect of pressure on thermal degradation of polyethylene.* Journal of Analytical and Applied Pyrolysis, 2004. **71**(2): p. 569-589.

78. Murty, M.V.S., et al., *Thermal degradation/hydrogenation of commodity plastics and characterization of their liquefaction products.* Fuel Processing Technology, 1996. **49**(1-3): p. 75-90.

79. Miranda, R., et al., *Vacuum pyrolysis of commingled plastics containing PVC. I. Kinetic study.* Polymer Degradation and Stability, 2001. **72**(3): p. 469-491.

80. Uemura, Y., et al. *Products from flash pyrolysis of plastics*. 1999. Philadelphia, PA, USA: Widener Univ School Eng, Chester, PA, USA.

81. Lovett, S., F. Berruti, and L.A. Behie, *Ultrapyrolytic upgrading of plastic wastes and plastics/heavy oil mixtures to valuable light gas products.* Industrial & Engineering Chemistry Research, 1997. **36**(11): p. 4436-4444.

82. The Ministry of Economic Development, N.Z., *Petroleum Products Specifications Amendment Regulations 2007*. 2007, The Ministry of Economic Development, New Zealand.

83. Mehl, M., et al., *A kinetic modeling study of the thermal degradation of halogenated polymers.* Journal of Analytical and Applied Pyrolysis, 2004. **72**(2): p. 253-272.

84. Gerpen, J.V., *Diesel Combustion and Fuels*. second edition ed. Diesel Engine Reference Book, ed. B. Challen and R. Baranescu. 1999, Warrendale, USA: Society of Automotive Engineers, Inc.

85. Bains, M., et al., *The compatibility of linear low density polyethylene-polypropylene blends: Viscosity ratio plots.* Polymer Engineering and Science, 1994. **34**(16): p. 1260-8.

86. Walendziewski, J., *Continuous flow cracking of waste plastics.* Fuel Processing Technology, 2005. **86**(12-13): p. 1265-1278.

87. Mastral, J.F., C. Berrueco, and J. Ceamanos, *Pyrolysis of high-density polyethylene in free-fall reactors in series.* Energy and Fuels, 2006. **20**(4): p. 1365-1371.

88. Williams, P.T. and E.A. Williams, *Fluidised bed pyrolysis of low density polyethylene to produce petrochemical feedstock.* Journal of Analytical and Applied Pyrolysis, 1999. **51**(1-2): p. 107-126.

89. Okuwaki, A., *Feedstock recycling of plastics in Japan.* Polymer Degradation and Stability, 2004. **85**(3 SPEC. ISS.): p. 981-988.

90. Miller, E., *Introduction to Plastics and Composites*. A Series of Textbooks and Reference Books, ed. L.L. Faulkner. 1996, Long Beach, California: Marcel Dekker.

91. Wunderlich, B., *Thermal analysis of Polymeric Materials*. 2005, Berlin: Springer.

92. Baker, A.-M.M. and J. Mead, *Thermoplastics*, in *Modern Plastics Handbook*, C.A. Harper, Editor. 2000, McGraw-Hill: Lutherville.

93. Wade, L.G., *Organic chemistry*. 3rd edition ed. The study of chemical reactions. 1995, Upper Saddle River, New Jersey 07458: Prentice Hall.

94. Levine, S.E. and L.J. Broadbelt, *Detailed mechanistic modeling of high-density polyethylene pyrolysis: Low molecular weight product evolution.* Polymer Degradation and Stability, 2009. **94**(5): p. 810-822.

95. Marongiu, A., T. Faravelli, and E. Ranzi, *Detailed kinetic modeling of the thermal degradation of vinyl polymers.* Journal of Analytical and Applied Pyrolysis, 2007. **78**(2): p. 343-362.

96. Miskolczi, N., *Kinetic Model of the Chemical and Catalytic Recycling of Waste Polyethylene into Fuels*, in *Feedstock Recycling and Pyrolysis of Waste Plastics*, J.S.a.W. Kaminsky, Editor. 2006, John Wiley & Sons, Ltd: Veszprem. p. 228.

97. Ranzi, E., et al., *Kinetic modeling of polyethylene and polypropylene thermal degradation.* Journal of Analytical and Applied Pyrolysis, 1997. **40-41**: p. 305-319.

98. Kodera, Y. and B.J. McCoy, *Distribution kinetics of polymer thermogravimetric analysis: A model for chain-end and random scission.* Energy and Fuels, 2002. **16**(1): p. 119-126.

99. Sezgi, N.A., et al., *Polyethylene pyrolysis: Theory and experiments for molecular-weight-distribution kinetics.* Industrial and Engineering Chemistry Research, 1998. **37**(7): p. 2582-2591.

100. Staggs, J.E.J., *A continuous model for vapourisation of linear polymers by random scission and recombination.* Fire Safety Journal, 2005. **40**(7): p. 610-627.

101. Wallis, M.D. and S.K. Bhatia, *Thermal degradation of high density polyethylene in a reactive extruder.* Polymer Degradation and Stability, 2007. **92**(9): p. 1721-1729.

102. Yuan, X., *Converting Waste Plastics into Liquid Fuel by Pyrolysis : Developments in China*, in *Feedstock Recycling and Pyrolysis of Waste Plastics*, J. Scheirs and W. Kaminsky, Editors. 2006, John Wiley & Sons, Ltd: Changsha, P.R. China. p. 729-755.

103. Mascia, L., ed. *Thermalplastics: Materials Engineering*. 2nd ed. 1982, Elsevier Science Publishers Ltd.: New York.

104. Wilhoit, R.C. and B.J. Zwolinski, *Handbook of vapor pressures and heats of vaporization of hydrocarbons and related compounds*. Publication No. 101. 1971, United States: Thermodynamics Research Center,College Station, TX. Pages: 337.

105. Poling, B.E., J.M. Prausnitz, and J.P. O'Connell, eds. *The Properties of Gases and Liquids*. 5th ed. 2000, McGraw-Hill.

106. Bockhorn, H., A. Hornung, and U. Hornung, *Stepwise pyrolysis for raw material recovery from plastic waste.* Journal of Analytical and Applied Pyrolysis, 1998. **46**(1): p. 1-13.

107. Demirbas, A., *Recovery of chemicals and gasoline-range fuels from plastic wastes via pyrolysis.* Energy Sources, 2005. **27**(14): p. 1313-1319.

108. Shah, J., M.R. Jan, and Z. Hussain, *Catalytic pyrolysis of low-density polyethylene with lead sulfide into fuel oil.* Polymer Degradation and Stability, 2005. **87**(2): p. 329-333.

109. Koptelov, A.A., Y.M. Milekhin, and O.F. Shlenskii, *Heat effects in thermal degradation of polymers.* Vysokomolekularnye Soedineniya. Ser.A Ser.B Ser.C - Kratkie Soobshcheniya, 2005. **47**(9): p. 1634.

110. Echlin, P., *Scanning electron microscopy X-ray microanalysis.* . 2009, New York Springer

111. Ballice, L. and R. Reimert, *Classification of volatile products from the temperature-programmed pyrolysis of polypropylene (PP), atactic-polypropylene (APP) and thermogravimetrically derived kinetics of pyrolysis.* Chemical Engineering and Processing, 2002. **41**(4): p. 289-296.

112. McCaffrey, W.C., M.R. Kamal, and D.G. Cooper, *Thermolysis of polyethylene.* Polymer Degradation and Stability, 1995. **47**(1): p. 133-139.

113. McCaffrey, W.C., D.G. Cooper, and M.R. Kamal, *Tertiary recycling of polyethylene: Mechanism of liquid production from polyethylene by thermolysis/reactive distillation.* Polymer Degradation and Stability, 1998. **62**(3): p. 513-521.

114. McCaffrey, W.C., et al., *Thermolysis of polyethylene/polystyrene mixtures.* Journal of Applied Polymer Science, 1996. **60**(12): p. 2133-2140.

115. Ballice, L. and R. Reimert, *Temperature-programmed co-pyrolysis of Turkish lignite with polypropylene.* Journal of Analytical and Applied Pyrolysis, 2002. **65**(2): p. 207-219.

116. Doruker, P., Y. Wang, and W.L. Mattice, *Simulation of the random scission of C-C bonds in the initial stage of the thermal degradation of polyethylene.* Computational and Theoretical Polymer Science, 2000. **11**(2): p. 155-166.

117. Gao, Z., I. Amasaki, and M. Nakada, *A thermogravimetric study on thermal degradation of polyethylene.* Journal of Analytical and Applied Pyrolysis, 2003. **67**(1): p. 1-9.

118. Ji, X., et al., *Study on the controlled unsequential pyrolysis of polyethylene to polyethylene wax with desired molecular weight range.* Energy Sources, 2003. **25**(3): p. 217-222.

119. Saha, B. and A.K. Ghoshal, *Model-free kinetics analysis of ZSM-5 catalyzed pyrolysis of waste LDPE.* Thermochimica Acta, 2007. **453**(2): p. 120-127.

120. University, N. *Product Information of 3A*. 2007 [cited 2009 02/01/2009]; Available from: http://www.nkcatalyst.com/en/ht_world/chanpin2/main.asp?id=463.

121. University, N. *Product Information of NKC5*. 2007 [cited 2009 02/01/2009]; Available from: http://www.nkcatalyst.com/en/ht_world/chanpin2/main.asp?id=468.

122. University, N. *Product Information of NKC7*. 2007 [cited 2009 02/01/2009]; Available from: http://www.nkcatalyst.com/en/ht_world/chanpin2/main.asp?id=465.

123. Kiang, J.K.Y., P.C. Uden, and J.C.W. Chien, *POLYMER REACTIONS - 7: THERMAL PYROLYSIS OF POLYPROPYLENE.* Polymer Degradation and Stability, 1980. **2**(2): p. 113-127.

124. Seth, D. and A. Sarkar, *Thermal pyrolysis of polypropylene: Effect of reflux-condenser on the molecular weight distribution of products.* Chemical Engineering Science, 2004. **59**(12): p. 2433-2445.

125. Walendziewski, J., *Engine fuel derived from waste plastics by thermal treatment.* Fuel, 2002. **81**(4): p. 473-481.

126. Kaminsky, W. and J.-S. Kim, *Pyrolysis of mixed plastics into aromatics.* Journal of Analytical and Applied Pyrolysis, 1999. **51**(1): p. 127-134.

127. Kaminsky, W. and J.-S. Kim, *Pyrolysis of mixed plastics into aromatics.* Journal of Analytical and Applied Pyrolysis, 1999. **51**(1-2): p. 127-134.

128. Westerhout, R.W.J., et al., *Techno-economic evaluation of high temperature pyrolysis processes for mixed plastic waste.* Chemical Engineering Research & Design, Transactions of the Institute of Chemical Engineers, Part A, 1998. **76**(A3): p. 427-439.

129. Scott, D.S., et al., *Fast pyrolysis of plastic wastes.* Energy & Fuels, 1990. **4**(4): p. 407-411.

130. Development, t.M.o.E., *Petroleum Products Specifications Amendment Regulations 2007*, t.M.o.E. Development, Editor. 1 July 2008.

131. Bhattacharya, S.C., A.H.M. Mizanur Rahman Siddique, and H.-L. Pham, *A study on wood gasification for low-tar gas production.* Energy, 1999. **24**(4): p. 285-296.

132. Bridgwater, A.V., *The technical and economic feasibility of biomass gasification for power generation.* Fuel, 1995. **74**(5): p. 631-653.